RECEIVED
LAWRENCE
RADIATION LABORATORY

FEB 9 1971

LIBRARY AND
DOCUMENTS SECTION

UCRL-20412

c.2

DECAY STUDIES OF NEUTRON-DEFICIENT ISOTOPES OF ASTATINE, POLONIUM, AND BISMUTH

Janis M. Dairiki
(Ph.D. Thesis)

November 1970

AEC Contract No. W-7405-eng-48

TWO-WEEK LOAN COPY

This is a Library Circulating Copy which may be borrowed for two weeks. For a personal retention copy, call Tech. Info. Division, Ext. 5545

LAWRENCE RADIATION LABORATORY
UNIVERSITY of CALIFORNIA BERKELEY

UCRL-20412 c.2

DISCLAIMER

This document was prepared as an account of work sponsored by the United States Government. While this document is believed to contain correct information, neither the United States Government nor any agency thereof, nor the Regents of the University of California, nor any of their employees, makes any warranty, express or implied, or assumes any legal responsibility for the accuracy, completeness, or usefulness of any information, apparatus, product, or process disclosed, or represents that its use would not infringe privately owned rights. Reference herein to any specific commercial product, process, or service by its trade name, trademark, manufacturer, or otherwise, does not necessarily constitute or imply its endorsement, recommendation, or favoring by the United States Government or any agency thereof, or the Regents of the University of California. The views and opinions of authors expressed herein do not necessarily state or reflect those of the United States Government or any agency thereof or the Regents of the University of California.

DECAY STUDIES OF NEUTRON-DEFICIENT ISOTOPES OF ASTATINE, POLONIUM, AND BISMUTH

Contents

Abstract vi

I. Introduction 1

II. Alpha Measurements 5

A. Source Preparation 7

1. Recoil Collection 10

2. Chemistry 12

B. Results and Discussion 17

III. Gamma Measurements 31

A. Experimental 33

1. Gamma Ray Singles 33

2. Gamma Ray Coincidence Measurements . . . 34

B. Data Analysis 45

1. General Considerations 45

2. Peak Fitting--MAGIC 50

3. Half-Life Determination 56

4. Coincidence Sorting--POLLY 65

IV. Results: Decay of Astatine Isotopes 68

A. Even Mass Isotopes 68

1. ^{206}At 68

2. ^{204}At 76

3. ^{202}At 80

4. Discussion 83

B. Odd Mass Isotopes 86

1. ^{205}At 86

2. ^{203}At 95

3. Discussion 98

C. Lower Mass Isotopes 100

V. Results: Decay of Polonium Isotopes 101
A. Odd Mass Isotopes 101
1. ^{205}Po 101
2. ^{203}Po 109
3. Lower Mass Isotopes 115
4. Discussion 117
B. Even Mass Isotopes 120
1. ^{204}Po 120
2. ^{202}Po 126
3. ^{200}Po 126

VI. Results: Decay of Bismuth Isotopes 128
A. Even Mass Isotopes 128
1. ^{204}Bi 128
2. ^{202}Bi 134
3. ^{200}Bi 139
4. ^{198}Bi 140
5. Discussion 142
B. ^{201}Bi 146

VII. Conclusions 148

Acknowledgments 151

References 153

DECAY STUDIES OF NEUTRON-DEFICIENT ISOTOPES OF ASTATINE, POLONIUM, AND BISMUTH

Janis M. Dairiki
(Ph. D. Thesis)

Lawrence Radiation Laboratory
University of California
Berkeley, California 94720

November 1970

ABSTRACT

Alpha particle and gamma ray studies were made of the decay of neutron-deficient isotopes of astatine, polonium, and bismuth. Astatine isotopes were produced in Au(^{12}C, xn) reactions at the Berkeley Heavy Ion Linear Accelerator (HILAC). Polonium and bismuth sources were obtained as products of astatine decay.

Three kinds of experiments were performed: 1) alpha particle energies and branching ratios, 2) high resolution gamma-ray singles studies, and 3) gamma-gamma coincidence measurements. In the gamma ray studies measurements were made on a source containing a mixture of isotopes with no previous chemical separation, primarily due to the short half-lives involved. Computer codes were developed to analyze the resulting complex multicomponent gamma spectra.

Decay schemes were constructed for even-mass At isotopes, A = 202-206. Confirming evidence was obtained in alpha measurements for an isomeric state of ^{202}At. Partial decay schemes were

deduced for ^{205}At and ^{203}At, characterized by intense direct population of a 9/2- excited level in the Po daughters followed by a gamma transition to the 5/2- ground states. For ^{202}Po-^{205}Po tentative decay schemes were proposed. The odd-mass polonium nuclei exhibit substantial decay to positive parity states in their Bi daughters. In addition, an alpha group at 5.37 ± 0.15 MeV was attributed to ^{203}Po. Finally, a systematic series of energy levels (0+, 4+, 4+, and 5-) were observed in the even-even Pb nuclei produced in the electron capture decay of ^{198}Bi-^{204}Bi.

I. INTRODUCTION

During the past seven years the development of high-resolution solid state detectors has led to the accumulation of huge quantities of experimental data in the field of nuclear spectroscopy, providing many advances toward a fuller understanding of nuclear structure. The shell model, in particular, has been very successful in explaining and predicting much of the experimental information. Its successes lead us to hope to understand the nature of the effective nuclear force inside finite nuclei from a detailed theoretical analysis of experimental spectra. As theoretical calculations have become more refined, detailed experimental information has become more important as a test of theory.

The greatest successes of the nuclear shell model have been in explaining low-energy properties of nuclei near the doubly closed shells. This group of nuclei is an important and suitable subject for obtaining information on the nature of the effective nuclear force inside nuclei. The low-energy properties of these nuclei ostensibly involve only a few nucleons outside an inert core which is assumed to give rise to a central field in which the extra nucleons move. Since the shell model description near closed shells is in its simplest and most basic form, detailed experimental information for these nuclei is extremely important in providing a check for theory.

Due to their proximity to the doubly magic nucleus ^{208}Pb, bismuth, polonium, and astatine isotopes with 83, 84, and 85 protons,

respectively, present a particularly interesting and important region for study. The higher-mass isotopes situated only one to four nucleons away from the doubly closed shells have been the subjects of much study.(Pry52, Ers62, Kim63, Per62, Gle62, Pru67, Tre68) In general, good agreement has been obtained between the experimental data and theoretical calculations.

One of the most striking examples of the interplay of experiment and theory is seen in the assignment of spin values to the observed energy levels in the ^{210}Bi nucleus. The nucleus has one proton and one neutron beyond the ^{208}Pb core. The lowest proton orbital is $h_{9/2}$ and the lowest neutron orbital $g_{9/2}$. One thus expects a low-lying multiplet of 10 levels with spins from 0 to 9 for ^{210}Bi. Simple shell model calculations with any reasonable attractive central force mixture acting between the two odd nucleons predicted that the 0^- level would lie lowest. With the experimental determination (Ers62) that ^{210}Bi has a 1^- ground state and a 0^- first excited level, a difficult problem was posed for shell model theory. Kim(Kim63) explained this troubling inversion by including a tensor force with a range of ~2 Fm.

However, until just recently, very little was known about the nuclear energy levels of the more neutron-deficient isotopes of bismuth, polonium, and astatine in the mass region A = 198-205. True, the results would be harder to interpret theoretically since the nuclei are further removed from the neutron closed shell, but one would expect their low-lying nuclear levels could be described in terms of

coupling between the proton(s) outside the Z = 82 closed shell and the holes in the N = 126 neutron shell.

This study was undertaken to add information about the decay schemes of some of these low-mass nuclei. Previous information about most of these isotopes had resulted from alpha decay studies. Hoff et al.[Hof63] and Forsling et al.[For61] systematically determined the half-lives and alpha decay energies of the astatine isotopes in the mass range 200-207 produced by heavy ion reactions. This study was extended in 1966 down to mass number 196 by Tretyl and co-workers[Tre66] and isomerism was found in the odd-neutron isotopes below 118 neutrons.

Several investigations of the nuclear properties of neutron-deficient polonium isotopes--especially their alpha decays--have been carried out since 1947.[Tem47, Att59a] However, the data published up until 1964 show many inconsistencies in the mass assignments of alpha lines. Recently, three independent systematic studies of the alpha decay properties of these polonium nuclides in the mass range 193-208[Tie67, Sii67, LeB67], carried on simultaneously with this work, have resulted in definite mass assignments. The earlier discrepancies can be explained by the occurrence of alpha-active isomers in odd-mass polonium isotopes below ^{202}Po (118 neutrons).

Some early gamma studies had been carried out. The electron capture of bismuth isotopes in the mass region 202-205 was studied to give information about the nuclear levels of the

corresponding lead daughters.[Nov58, Sto58, Sto60a, McD57] Early gamma measurements exist also for the decay of ^{205}Po and ^{207}Po short-lived isomeric states [Lin57, Har62] and for the excited levels in ^{206}Bi from the decay of ^{206}Po.[Arb57, Wah57]

In just the past two years, during the course of the present investigation, there has been an added wealth of information. The electron capture decay of odd-mass polonium isotopes to levels in ^{203}Bi, ^{205}Bi, and ^{207}Bi has been studied in some detail [Hop69, Alp69, Ast70] and theoretical explanations of the observed states have been advanced.[Alp69, Ber69, Bra70] Yamasaki[Yam70] has made a systematic study of isomeric states of polonium isotopes in the nanosecond range populated by Pb(α, xn) reactions. Results of these recent investigations will be discussed more fully and compared with the decay information gained in this study.

II. ALPHA MEASUREMENTS

Although the scope of this study is broad we began initially with a very specific problem--the investigation of the alpha decay of $^{198}_{83}Bi$.

The mass assignment of ^{198}Bi is uncertain; it is labeled class D in the Table of Isotopes.[Led67] Evidence for its existence was first presented in 1950 by H. Neumann and I. Perlman[Neu50] who found a 5.81-MeV alpha activity that decayed with a half-life of about 7 min in their bombardment of lead targets with protons. They assigned its mass number on the basis of excitation functions and parent-daughter relationships. The thallium fraction was milked from the bismuth at intervals and found to contain a small amount of activity with a half-life shorter than 7 hr and consistent with 1.8-hr ^{198m}Tl (although not completely ruling out 2.84-hr ^{197}Tl and 1.84-hr ^{196}Tl).

During the course of this investigation, Siivola et al.[Sii64] reported a 5.81-MeV activity with a half-life of 8.0 ± 0.5 min in their work with alpha-active isomers of ^{201}Bi and ^{199}Bi. They definitely confirmed the element assignment of this 8-min activity to bismuth but could not definitely determine its mass number. However, they did find an isomeric state of ^{201}Bi that decays with a half-life of 52 ± 2 min by emitting a 5.27-MeV alpha particle, and also found evidence for a similar alpha-decaying isomer of ^{199}Bi with a half-life of 24.4 ± 0.5 min. Thus these results suggest that the 8-min alpha activity could belong to an excited state in ^{197}Bi.

^{198}Bi is the alpha decay daughter of ^{202}At. The alpha decay of ^{202}At has been studied by several investigators. Forsling et al. (For61) used mass separation to show that the two alpha peaks at 6.23 MeV (36%) and 6.13 MeV (64%) belong to ^{202}At. Latimer et al. (Lat60) measured the alpha branching ratio to be 0.12 for ^{202}At. Hoff and co-workers (Hof63) studied these peaks by alpha-gamma coincidence techniques. The failure to observe any gamma rays in coincidence with the 6.13-MeV alpha group suggested that the transition(s) de-exciting the ^{198}Bi state populated by this alpha are highly converted or delayed. The subsequent observation of the coincidence between L x rays and the 6.13-MeV alpha group indicated that less than 25% of the 6.13-MeV group is followed by a prompt converted transition, so the transition is probably delayed.

This leads to the possibility of isomers. Since no clear difference in the half-lives of the alpha peaks was observed, it appeared that isomerism was more likely to occur in the daughter, ^{198}Bi, than in ^{202}At. More recently, however, this supposition of ^{198}Bi isomerism was questioned by Tretyl and Valli (Tre66) in their study of the alpha decay of astatine isotopes lighter than mass 205 made by bombardment of ^{185}Re and ^{187}Re with ^{20}Ne atoms at the Berkeley Heavy Ion Linear Accelerator (HILAC). Their measurements indicated that the 6.13-MeV peak may have a somewhat longer half-life than the 6.23-MeV peak (3.0 ± 0.3 min compared to 2.6 ± 0.3 min). This fact plus the mass-energy systematics and a systematic occurrence of isomerism in neighboring isotopes led them to conclude that

the isomerism is in ^{202}At, not its ^{198}Bi daughter. Accordingly, they assigned the 6.13-MeV peak to the ground state and the 6.23-MeV peak to an isomeric state in ^{202}At. They also reported isomers in ^{200}At and ^{198}At. Their mass assignments were based on excitation functions and genetic relationships with polonium electron capture daughters.

The ^{198}Bi for our present study was obtained by collecting alpha recoils from ^{202}At. Fast-chemistry methods were utilized to identify the alpha groups present in the resulting spectra. The majority of these were assigned to polonium isotopes. No alpha groups belonging to ^{198}Bi were observed, and hence a limiting value for the alpha branching ratio was determined. Subsequent investigation of the decay of the polonium isotopes, using methods of gamma spectroscopy, immediately reopened the broad study to include the entire mass region 198-205.

A. Source Preparation

All the astatine isotopes used in this study were produced by irradiation of gold targets with carbon ions in the HILAC. Aluminum degrader foils were placed in front of the target in order to control the beam energy. There are many difficulties in this method. Among them is the fact that the astatine nuclides cannot be produced singly and the half-lives are rather short to allow rigorous chemistry. These astatine nuclides of mass 200-205 all decay by both alpha emission and electron capture, giving rise to a multitude of daughter activities.

The ratios of the various astatine isotopes produced can be changed by using different thicknesses of aluminum and gold in order to control the energy band to which the target atoms are exposed. To produce primarily ^{201}At, the full-energy beam (10.4 MeV/nucleon) was used, i.e., no Al degrader foil, whereas the ^{205}At concentration was maximized at a beam energy of 74 MeV, which required 5.25 mils of Al absorber. The desired thicknesses of absorber and target foils were determined from experimental excitation functions (Tho62) and from available energy-loss curves for carbon ions in aluminum. (Nor60) Crude excitation functions obtained by varying the ratios of the various astatine isotopes in different bombardments were helpful in assigning mass numbers to the observed radiations.

This production by heavy-ion projectiles is advantageous since it favors formation of the lower-mass isotopes ($A < 207$). The compound nucleus for carbon ion bombardment of gold is ^{209}At* as opposed to ^{213}At* for helium bombardments of bismuth for example. The high Coulomb barrier for carbon ions eliminates low nuclear excitations of the compound nucleus, even when thick targets are employed.

The ^{198}Bi for this study was prepared by collecting alpha recoils from ^{202}At. The production of ^{202}At was maximized by using a 0.5-mil Au target with 1 mil of Al absorber. There was still considerable contamination from neighboring nuclei (ratio ^{203}At: ^{202}At: ^{201}At = 1:1:0.25 after a 3-min bombardment). In order to assign mass numbers to the alpha activities seen, it was found useful to

maximize the amount of ^{201}At present by decreasing the gold thickness to 0.25 mil and using the full-energy beam. Under these conditions the ratio of ^{203}At: ^{202}At: ^{201}At was 1:3:20 after a 3-min bombardment.

The HILAC ^{12}C beam intensities were usually in the range of 1-2 μA, although in some bombardments beams as high as 7 μA were used. The target and absorber foils were mounted on a standard copper tag target holder and were water-cooled during irradiation. The entire target assembly served as a Faraday cup for monitoring the beam. The bombardment time varied; generally it was equal to the half-life of the desired astatine isotope, e.g., 3 min for ^{202}At.

After bombardment, the target holder was disassembled in a hood. The gold foil was removed and placed inside a small quartz cup, which was heated with an oxygen-acetylene torch. The gold was melted and the volatile species--At, Po, and certain fission products--were collected on a water-cooled plate, either platinum or molybdenum, held in a cold finger. The activity on this plate served as a source for alpha spectra, for recoil collections and, later on, for gamma spectroscopy. In some cases further chemistry was done on this source plate when the half-lives would permit it. Particularly when working with the lower-mass isotopes with short half-lives the above "blow torch chemistry" was carried out as quickly as possible. The time elapsed between the end of bombardment and the start of recoil collection was typically ~2 min.

The alpha spectra were obtained by using a gridded ion chamber with a gas mixture of 93% argon and 7% methane in conjunction with a RIDL 400-channel pulse-height analyzer. Alpha particles had a counting efficiency of 42% and a resolution of 30 keV when counted in this system. Alpha sources used for energy calibration were ^{252}Cf (6.118 ± 0.005 MeV), ^{244}Cm (5.805 ± 0.001 MeV), and ^{210}Po (5.305 ± 0.001 MeV). The 5.58-MeV alpha of ^{202}Po present in most of the spectra served as an internal standard as did the 6.085-MeV alpha group of ^{203}At whenever it was present.

1. Recoil Collection

One can allow the astatine on the Pt source plate to decay for an appropriate time (depending on half-life), heat the plate to remove any remaining astatine, and then measure the alpha spectrum of the daughters. This is fine in principle except that the dominant mode of decay of the astatine isotopes is by electron capture ($\geq$ 85%). The consequent polonium isotopes which grow in are therefore present in much greater abundance than the bismuth alpha decay daughters, and their alpha energies are similar. Hence the Bi alpha groups may well be masked.

In order to separate the polonium isotopes, a method of milking alpha recoils (Bi daughters) from the astatine source plate was tried. The source plate was positioned in a desiccator, which was then evacuated, and recoils were stopped on a platinum collector plate. The gap between the collector and source plates changed from 3/8 in. at

the outset to 1/8 in. in order to increase the yield. A positive potential of +300 volts was applied to the collector in order to inhibit the accumulation of Po daughters that were positively charged as a result of their formation by electron capture. The recoil efficiency with a 1/8-in. gap was ~20% and essentially uniform over the area of the collector plate. The collector plate was then removed and counted in the grid chamber arrangement.

Early spectra indicated that considerable astatine was reaching the collector plate. One explanation for this could be that the astatine formed a loose crust on the surface of the plate which was swept over onto the collector when the chamber was being evacuated. If this were so, subsequent recoil collections from the same source should contain substantially less astatine. This, however, was not found to be the case. It could still be possible that the astatine was being deposited onto the collector during evacuation, however. To test if that were so, a shield was placed between the source and collector plates during evacuation and rotated out of the way before the recoil collection began. This procedure somewhat reduced the amount of astatine detected on the collector plate, but did not remove it entirely.

This remaining astatine activity was probably vaporized over onto the collector by the radioactivity of the source itself. The same effect was observed by Thoresen.[Tho63] Much of this astatine was removed by heating the recoil plates on a 450° C hotplate before counting them; hence, astatine did not constitute a problem in the

alpha spectra.

This recoil collection technique was useful in yielding evidence for isotopic assignments on the basis of genetic relationships. Three consecutive recoil collections from a given astatine source were made and their alpha decay followed. The activity of each alpha group was extrapolated back to the time corresponding to the end of recoil collection and plotted versus that time to produce a decay curve for the parent (see Fig. II-1).

Recoils were also collected with a negative voltage on the collector plate and with no voltage. As expected, these plates showed more polonium (2-3 times as much).

Recoil collection with a 4.5 $\mu g/cm^2$ Zapon film between the source and collector plates was also attempted. This should stop the polonium nuclides (electron capture recoil energy ~ 150 eV) but allow the more energetic bismuth isotopes (alpha recoil energy ~ 122 keV) to penetrate through. No activity was found on the collector plate, however.

2. Chemistry

Considerable effort was spent trying to separate polonium from bismuth by methods based on their evaporation properties. This worked well for the removal of astatine. It can be evaporated at 450°C and, although the yield is not quantitative, that which volatilizes is quite free of polonium.[Tho63] However, when the temperature is hot enough to evaporate a sufficient amount of polonium (> 50%) some

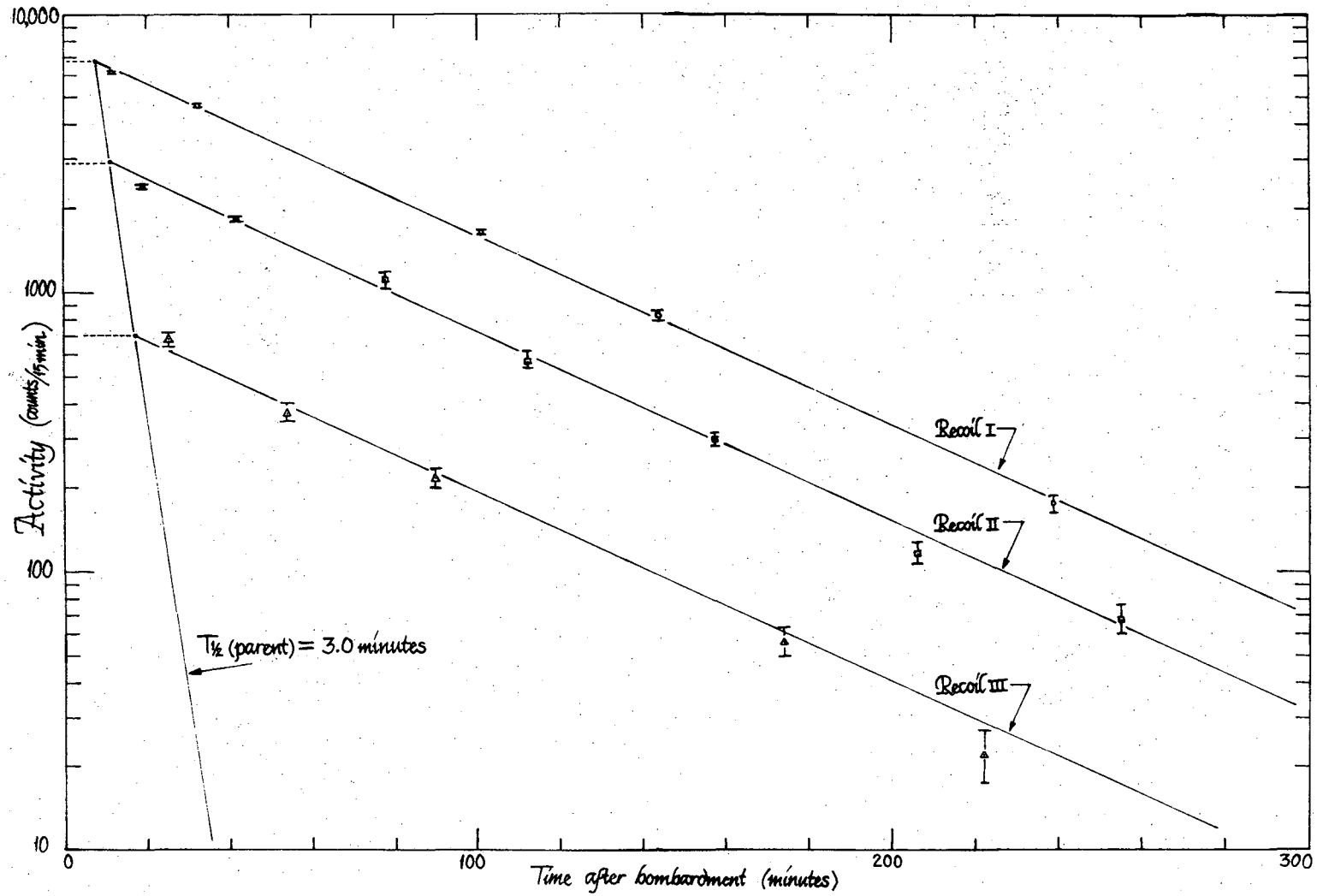

XBL 7011-7096

Fig. II-1. Illustration of the use of successive recoils to determine the half-life of the parent of the ^{202}Po 5.58-MeV alpha--3-min ^{202}At.

bismuth also evaporates. Thus the results were not reliable or even reproducible. Similar inconsistent results were found by An.[An65]

Plates made of metals other than platinum were then used. It was found that molybdenum would preferentially hold the bismuth while the polonium and astatine evaporated, but even here the results were not consistent. Astatine was easily removed but again the polonium evaporation was incomplete. The whole subject of vaporization properties is, in itself, worthy of more intense investigation.

Clearly, a better method of separation was needed. Two wet-chemistry methods were adapted for quick performance. The first of these was developed by Kimura and co-workers.[Kim58] Since polonium forms a number of complex halides in solution it was expected that some of these compounds could be extracted into organic solvents. Kimura et al. found that polonium was extracted with isopropyl ether or methyl isobutyl ketone from HCl solutions containing KI.

The platinum source plate containing the astatine from the melted gold target was allowed to decay and was then heated to remove the bulk of the remaining astatine. The plate was washed with 1 ml of a solution containing 0.25M KI and 3N HCl. This solution was then added to 4 ml isopropyl ether. The polonium was extracted into the organic phase with gentle swirling while bismuth and lead remained in the aqueous phase. The two phases were separated and the polonium was subsequently removed from the organic phase by shaking with two 1-ml portions of 3N HCl. The bismuth was washed with 1 ml ether to remove any remaining polonium. The two solutions were then

evaporated to dryness and their alpha spectra measured.

^{212}Bi obtained by collecting recoils from ^{224}Ra, ^{210}Po, and ^{202}Po were used to test the method. The whole procedure required about 10 min and effected a good separation. However, the KI tended to leave a residue on the plates, which resulted in thick samples and distorted alpha spectra. No bismuth alphas were observed in any of the actual At runs after the chemical separation.

Another chemical separation which resulted in essentially mass-free samples was then used. It was first employed by Brun and Lefort(Bru64) in their work with the low-mass polonium isotopes. The Pt source plate obtained after melting the gold target was again heated to remove the excess astatine after allowing for some decay. The polonium and bismuth were dissolved off the plate with 0.5 ml HNO_3 which was then extended to 25 ml with 0.5N HCl saturated with hydrazine. The solution was maintained with stirring at 96° C and the polonium deposited spontaneously onto a 1-in.-diameter silver disk. In effect the hydrazine prevents any oxidation of the silver while the deposition is proceeding and the rate of deposition is accelerated at the elevated temperature.

The yield depends on the length of plating time, being 10.5% in 5 min and ~16% in 10 min (Fig. II-2) with no bismuth contamination ($\leq$ 0.5% for any time less than 25 min). In later gamma experiments the total volume of the solution was kept to 10 ml. This was a great improvement since the yield depends not only on the length of the deposition time but also depends considerably on the ratio of the surface

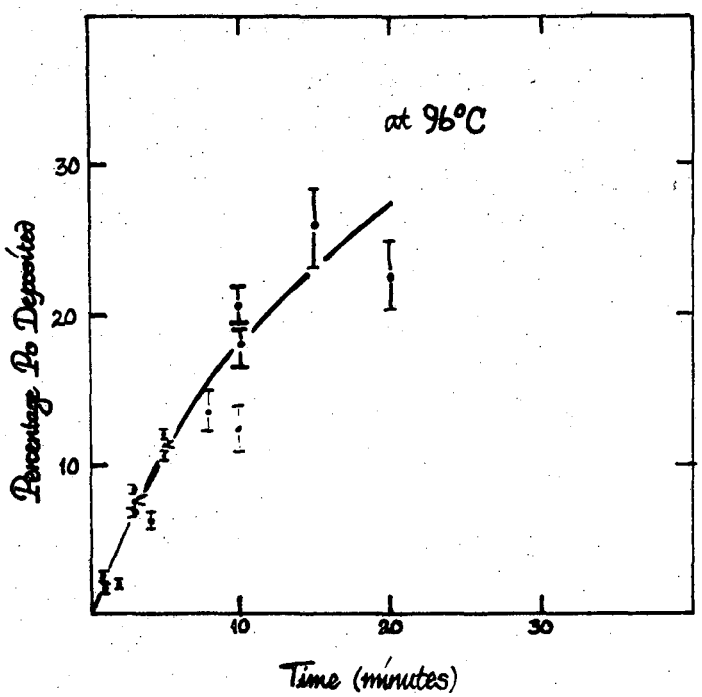

XBL 7011-7115

Fig. II-2. Percentage of polonium spontaneously deposited onto silver at 96° C as a function of plating time.

of the plate to the volume of the solution.

B. Results and Discussion

Table II-1 presents the data obtained for all the observed alpha activities. For ^{202}Po, ^{204}Po, and for the astatine and bismuth isotopes, there is excellent agreement with previous investigations. (Hof63, Att59a) The data on ^{200}Po to ^{203}Po agree well with the recent results of Brun, Le Beyec, and Lefort(Bru67a, b) and those of Tielsch-Cassel(Tie67) and Siivola(Sii67) but differ from some previous assignments. (Tem47, Att59a)

A representative alpha spectrum of ^{200}Po-^{202}Po is shown in Fig. II-3. This was obtained from the original At source plate containing all the irradiation products evaporated from the gold target. The astatine was allowed to decay 3 min. The plate was then heated to remove the remaining astatine and the alpha activity was measured. The resulting decay curves for each of the alpha groups is seen in Fig. II-4.

Mass assignments were based on 1) the parent half-lives measured by means of successive recoil collections and 2) the excitation functions, i.e., the change in peak intensity as a function of bombarding energy.

The assignment of the 5.78-MeV activity to an isomeric state in ^{201}Po required not only a mass determination but also positive identification of the element itself, which necessitated chemistry. Prior to this work Hoff, Asaro, and Perlman(Hof63) found that 1.5-min

Table II-1. Summary of data obtained for all alpha activities observed in this work.

	Results of this work			
	Alpha energy (MeV)	Half-life (min)	Alpha branching (%) This work	Alpha branching (%) Literature[a]
^{200}Po	5.86 ±0.01	11.5 ±0.5		12
^{201m}Po	5.78 ±0.01	8.9 ±0.8		3
^{201}Po	5.68 ±0.01	15.5 ±0.6		1.1
^{202}Po	5.58 ±0.01	43.8 ±1.5	1.90 ±0.11	2.0
^{203}Po	5.37 ±0.015	36.0 ±2.5	0.18 ±0.021	0.02, 0.11[b]
^{204}Po	5.375±0.005	213.0 ±9.0		0.75[b]
^{205}At	5.91 ±0.02	25.0 ±1.6		18
^{204}At	5.96 ±0.01	9.2 ±0.2		4.5
^{203}At	6.085±0.005	7.3 ±0.2		14
^{202}At	6.13 ±0.01	2.9 ±0.2		12
^{202m}At(?)[d]	6.23 ±0.01	2.6 ±0.2		
^{201}At	6.34 ±0.01	1.45±0.1		
^{200}At	6.41 ±0.02	0.93±0.15		
	6.46 ±0.01			
^{199}Bi	5.49 ±0.02	24.5 ±0.4	2.75 ±0.29	0.01[b, c]
^{201}Bi	5.25 ±0.01	57±5		0.02[b, c]
^{198}Bi		11.1 ±0.4[e]	≤0.20	0.05

[a] All values not marked are from Table of Isotopes. (Led67)

[b] Ref. (LeB67b).

[c] This is a ratio of α/K x rays.

[d] The mass number is definite. The slightly different half-lives of the 6.13-MeV and 6.23-MeV ^{202}At alpha groups support assignment of the 6.23-MeV group to an isomeric state.

[e] Half-life value obtained from the gamma measurements (Chapter VI).

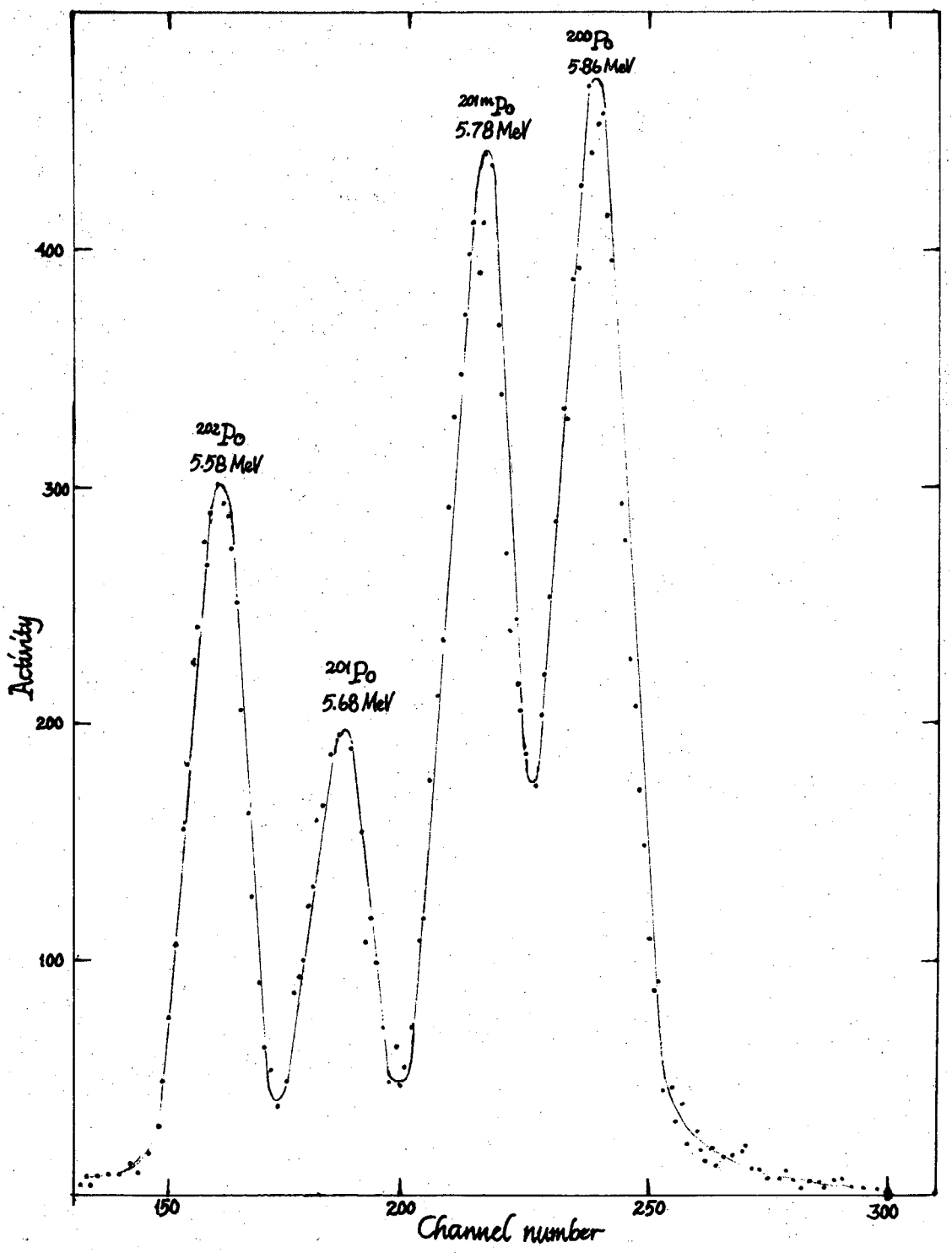

XBL 7011-7116

Fig. III-3. Alpha spectrum of ^{200}Po-^{202}Po measured 17 min after end of bombardment.

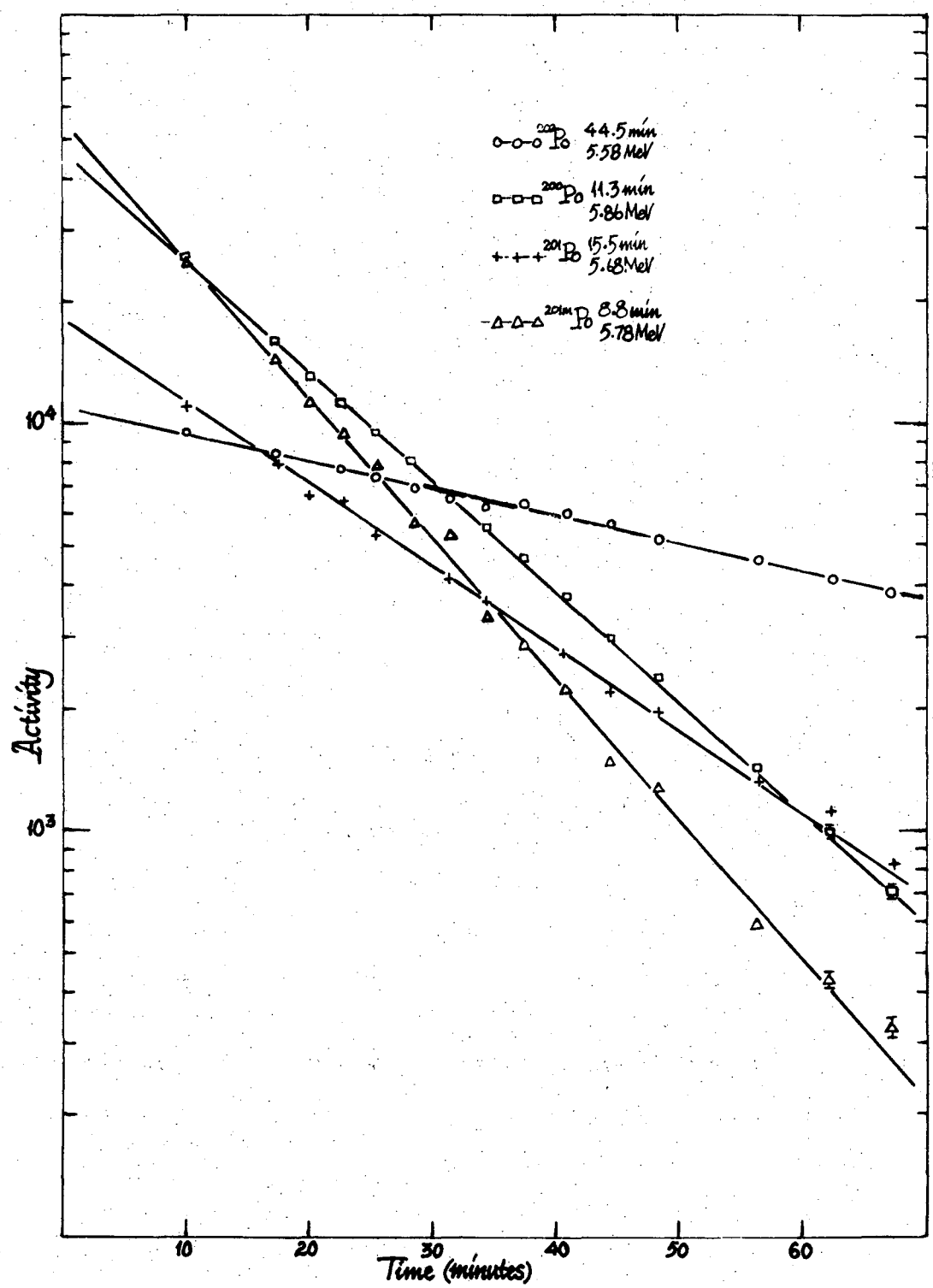

XBL 7011-7117

Fig. II-4. Decay curves of ^{200}Po-^{202}Po alpha groups.

^{201}At was the parent of both the 5.78- and 5.68-MeV activities. This result was confirmed in the current work when successive recoil collections indicated that both alpha groups had a 1.5-min parent (Table II-2). Furthermore, the ratio of the intensities of these two peaks at 5.68 and 5.78 MeV remained constant when the bombarding energy was varied--see Table II-3. This also suggested that both alpha groups have the same astatine parent. However, since the two alpha groups have different half-lives this means that either the 5.78-MeV activity is due to an isomer of ^{201}Po or to ^{197}Bi--the ^{201}At alpha decay daughter. In order to resolve this ambiguity, wet chemistry was used--spontaneous deposition of polonium onto silver.

Table II-2. Parent half-lives determined from successive recoil collections.

Observed daughter activity	E_α (MeV)	Parent half-life (min)	Parent identity
^{204}Po	5.375	9.0 ± 0.3	^{204}At
^{203}Po	5.37	6.8 ± 0.4 normalized to	^{203}At
^{202}Po	5.58	3.0	^{202}At
^{201}Po	5.68	1.6 ± 0.2	^{201}At
^{201m}Po	5.78	1.8 ± 0.3	^{201}At
^{200}Po	5.86	0.8 ± 0.2	^{200}At

The astatine evaporated from the gold target was collected onto a platinum plate, allowed to decay 3 min and then removed by heating. An alpha spectrum was obtained to determine the exact amounts

Table II-3. Relative amounts* of ^{200}Po-^{202}Po when bombarding energy is changed.

Au thickness (mil)	Al thickness (mil)	Energy range (MeV)	Relative abundance of alpha activities				
			5.86 MeV ^{200}Po	5.78 MeV ^{201m}Po	5.68 MeV ^{201}Po	5.58 MeV ^{202}Po	5.68/5.78
0.5	0	126-108	0.03	0.17	0.45	1.0	0.37
0.5	1	118-97	---	0.12	0.29	1.0	0.38
0.25	0.2	123-120	2.17	0.97	3.0	1.0	0.33

* Relative rates at end of 7 minute bombardments--not saturation amounts.

of each isotope present. The activity was then dissolved off the source plate with concentrated HNO_3; the solution was diluted to 25 ml with 0.5N HCl saturated with hydrazine, and the polonium spontaneously deposited onto silver for 5 min while the solution was stirred and maintained at 96° C. The original source plate was again counted and when decay corrections were made the exact amount of each activity going into solution was derived. The alpha activities on the silver plate were measured; the percentage of each activity which actually plated out was calculated, again including decay corrections. A 10-min deposition was also made onto a second silver plate. The results are shown in Table II-4. There is no doubt that all five alpha groups belong to polonium isotopes. Bismuth does not plate out ($\leq 0.5\%$) under these experimental conditions. Thus the 5.78-MeV activity must be assigned to an isomeric state of ^{201}Po.

In contradiction to other reports,[Att59a, 59b] no 5.48 MeV alpha group could be assigned to ^{203}Po. However, an alpha radiation of energy 5.37 MeV and half-life 36 ± 2.5 min was attributed to ^{203}Po. This line is degenerate in energy with a significant ^{204}Po contamination but it could be identified in the decay curve (Figs. II-5 and II-6). Successive recoil collections showed that this 5.37-MeV activity was genetically related to a 7-min parent--^{203}At (Table II-2). In addition, the 5.37-MeV activity followed polonium chemistry in depositing on silver (Table II-4). The 36-min half-life was later verified by following the gamma rays emitted in the ^{203}Po electron capture decay. A half-life of 36.7 ± 0.5 min was found. This agrees with the

Table II-4. The percentages of the observed alpha activities that spontaneously deposit onto silver.

E_α(MeV)	% activity remaining on source plate	% plated onto Ag in 5 min	% plated onto Ag in 10 min
5.37[a]	37.1 ± 7.4	11.9 ± 4.1	11.6 ± 4.6
5.58	55.5 ± 0.8	9.8 ± 0.6	12.0 ± 0.7
5.68	58.1 ± 1.7	9.2 ± 1.9	12.9 ± 1.6
5.78	53.8 ± 3.2	11.1 ± 2.3	16.4 ± 3.2
5.86	48.1 ± 1.9	9.0 ± 1.4	10.3 ± 1.7
^{210}Po		10.7 ± 0.6	18 ± 4
^{212}Bi		0.15 ± 0.02	0.18 ± 0.03

[a]This line is due primarily to ^{203}Po but contains a small admixture of ^{204}Po; it is about one-tenth as intense as the other lines.

recent result of Tielsch-Cassel(Tie67) but is less than the 45 min quoted previously. (Att59a, 59b, Kar51)

The weak 5.49-MeV line seen in the present spectra was found to have a half-life of ~24 min and was ascribed to ^{199}Bi on the basis of previous information. (Neu50, Sii64)

Using the measured activities of ^{203}At and ^{203}Po and the alpha branching ratio of ^{203}At listed in Table II-1, a value for the alpha branching ratio of ^{203}Po was determined:

$$\alpha/\text{total} = 0.00184 \pm 0.00021.$$

The discrepancy between the present value and the alpha branching ratio listed in the Table of Isotopes is not surprising--the published value refers to the 5.48-MeV alpha previously assigned to ^{203}Po.

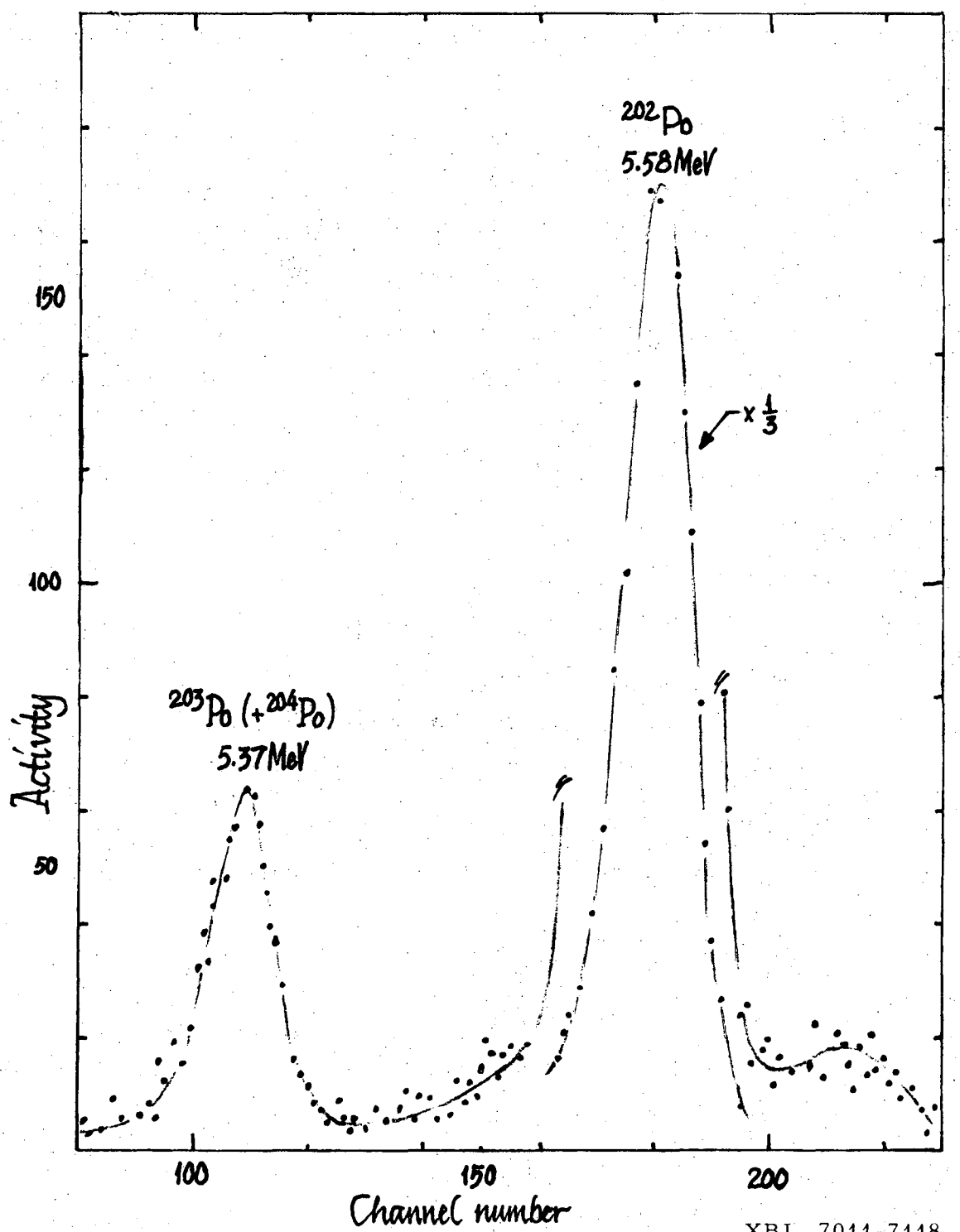

XBL 7011-7118

Fig. II-5. Alpha spectrum of ^{203}Po (+ ^{204}Po contamination) counted 24 min after the end of bombardment. The target was 0.5-mil Au with 1-mil Al absorber bombarded for 10 min. These conditions maximize the production of ^{202}At and produce sufficient ^{203}Po activity while keeping the ^{204}At and hence the ^{204}Po contamination at a minimum.

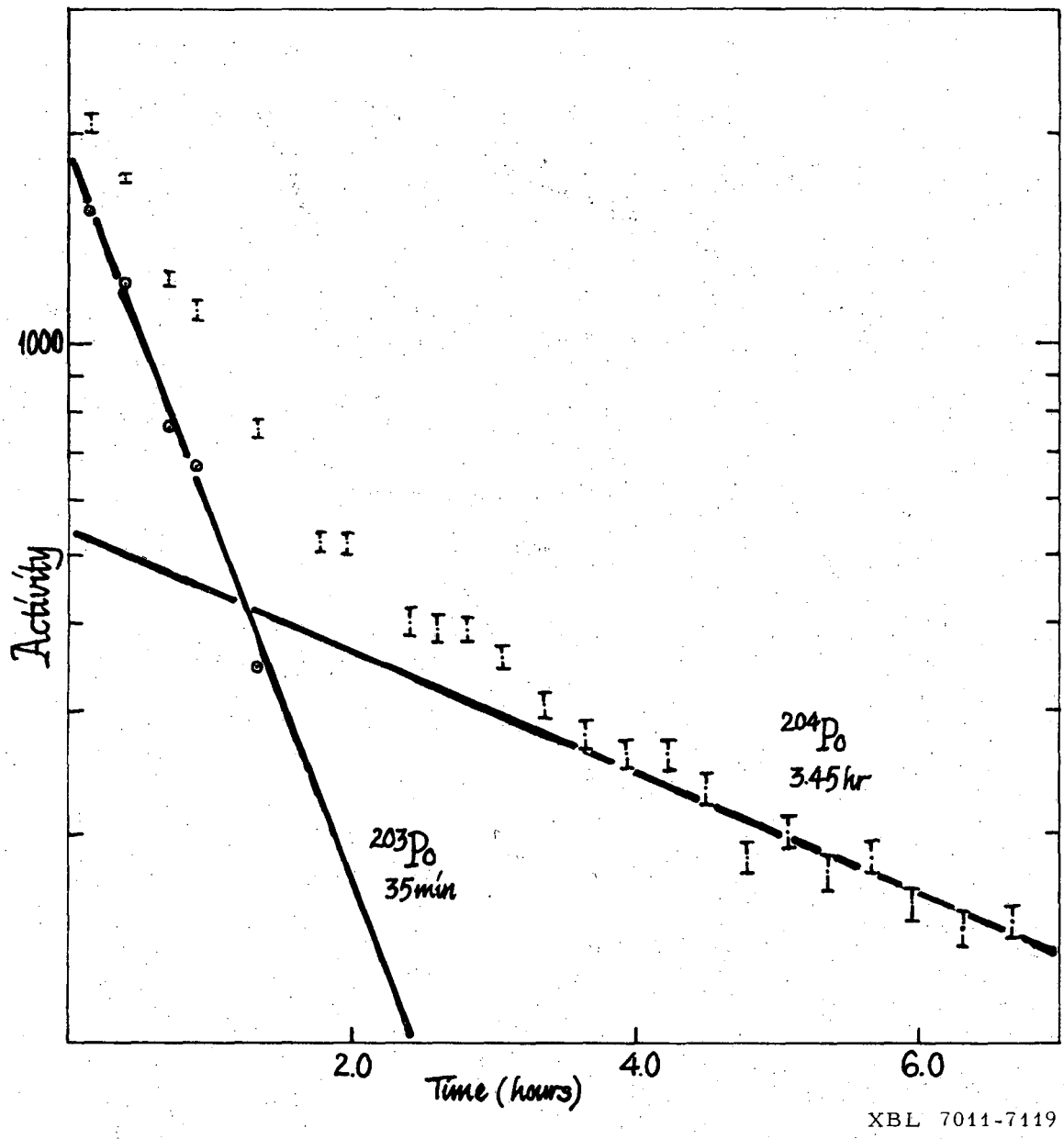

Fig. II-6. Resolved decay curve of ^{203}Po (35 min) and ^{204}Po (3.45 hr).

In the same run the alpha branching of ^{199}Bi was determined to be 2.75 ± 0.25%, which assumes all the ^{203}At undergoing alpha decay leads to the ^{199}Bi state emitting the 5.49-MeV alpha. However, there are some indications (Sii64) that the 5.49-MeV alpha belongs to the isomeric state ^{199m}Bi and that the ^{199}Bi ground state decays only by electron capture. If this is so the calculated branching ratio must be regarded as an upper limit for the true value.

Figure II-7 shows the alpha spectrum of the lighter astatine isotopes. The decay of the two ^{202}At alpha groups is shown in Fig. II-8. The half-life of the 6.13-MeV alpha was found to be slightly longer than that of the 6.23-MeV alpha group (2.9 ± 0.2 min opposed to 2.6 ± 0.2 min, respectively). This would indicate that the 6.23-MeV alpha belongs to an isomeric state, but the experimental errors do not definitely exclude the possibility of identical half-lives. Hence the question mark in Table II-1. The tentative assignment of the 6.23-MeV alpha line to ^{202m}At is consistent with the results of Tretyl and Valli. (Tre66)

No alpha groups could be assigned to ^{198}Bi. Consequently only a limiting value for the alpha branching ratio was determined by using the half-life obtained from gamma measurements--11.1 ± 0.4 min (see Chapter VI):

$$\alpha/\text{total} \leq 0.002.$$

In the same runs a branching ratio of 1.90 ± 0.11% was found for the alpha decay of ^{202}Po. This is in excellent agreement with the previously published values. (LeB67b, Led67)

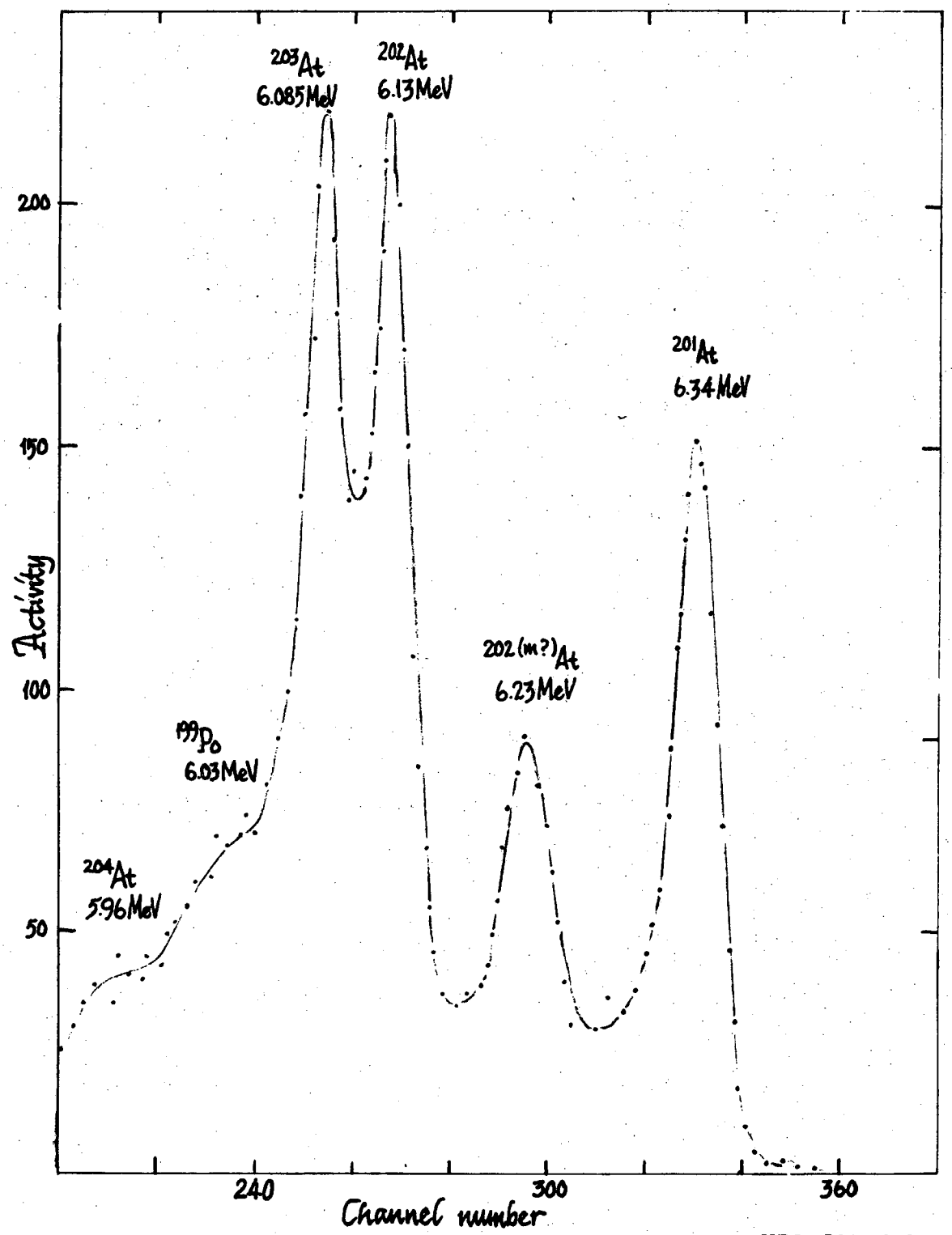

XBL 7011-7120

Fig. II-7. Alpha spectrum of light astatine isotopes, mass 201-203, obtained 5.5 min after the end of bombardment.

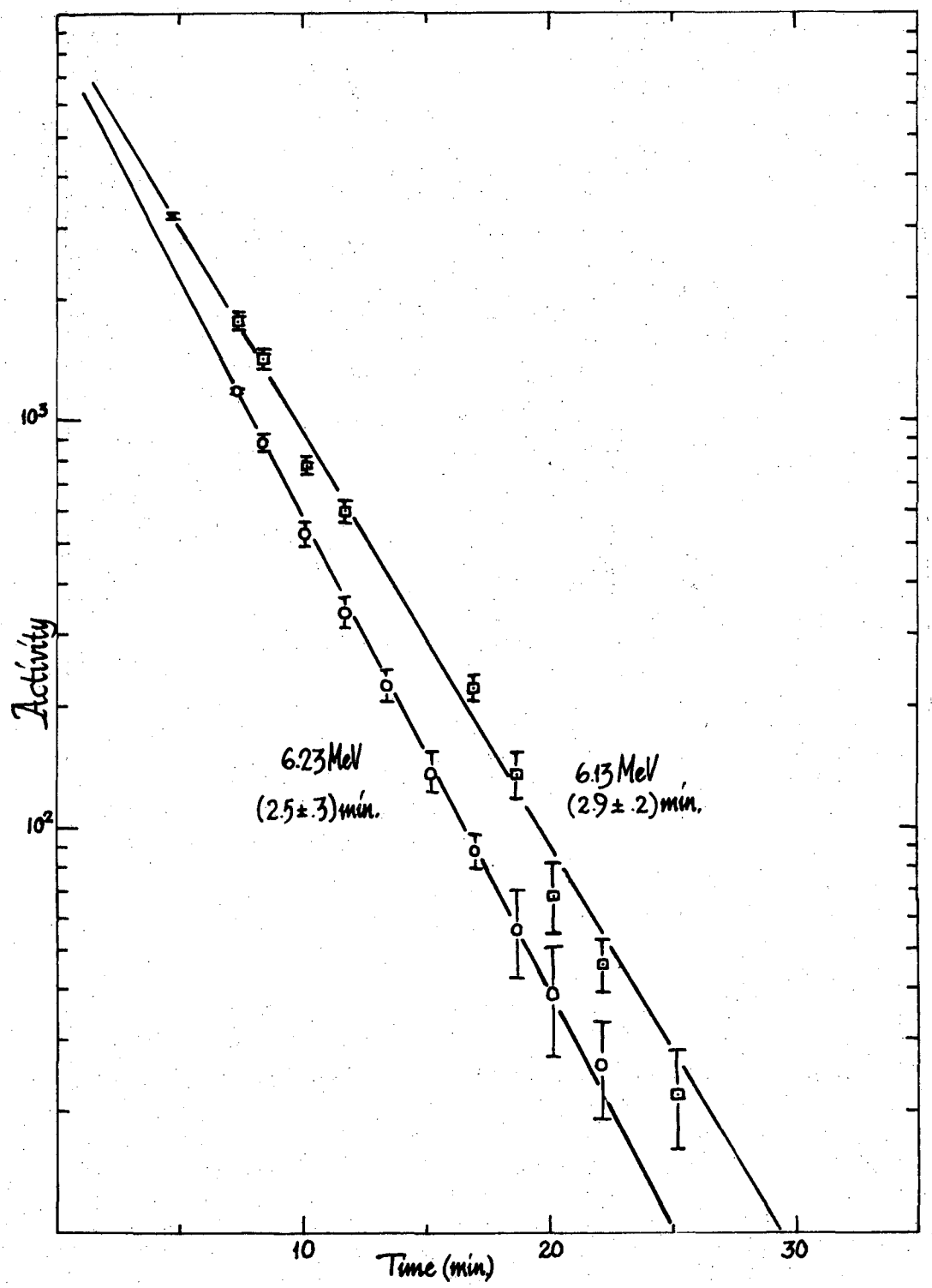

XBL 7011-7121

Fig. II-8. Decay of 6.13- and 6.23-MeV astatine alpha groups assigned to mass number 202.

No information was gained about the nuclear levels of ^{198}Bi. The polonium isotopes in the mass region 200-203 were definitely identified and were present in substantial quantities. Thus attention was turned to these polonium isotopes and to the measurement of the gamma rays emitted in their decay.

III. GAMMA RAY MEASUREMENTS

In order to gain more information about the polonium isotopes observed in the alpha spectra and to obtain some knowledge about the electron capture decay of ^{198}Bi, gamma measurements were made on a source containing the daughter activities of ^{202}At. The ^{202}At parent was prepared as previously described and allowed to decay for 3 min to enable the bismuth and polonium daughters to grow in. The source plate was then heated for 15 sec on a 450°C hot plate to remove the remaining astatine.

A gamma spectrum was obtained with a 5 cm^3 Ge(Li) detector and we found we had opened a veritable Pandora's box (Fig. III-1). Subsequent gamma spectra were obtained to follow the decay of the source and many of the gamma lines could be identified by their half-lives. However, there were many uncertainties and the possibility of many isotopes being present. Comparison of the ratios of the activities produced under various bombarding conditions provided another means of identification. Each new bombardment answered some questions, identified some gamma transitions, introduced more unknowns, and broadened out the mass region of interest.

At the higher end of the mass scale, A = 204 and 205, where the half-lives are longer (e.g., 1.8 hr and 3.5 hr for ^{205}Po and ^{204}Po, respectively, and ~27 min for ^{205}At), there was much less interference from undesired transitions. The spectra were much cleaner and meaningful gamma-gamma coincidence measurements could be made.

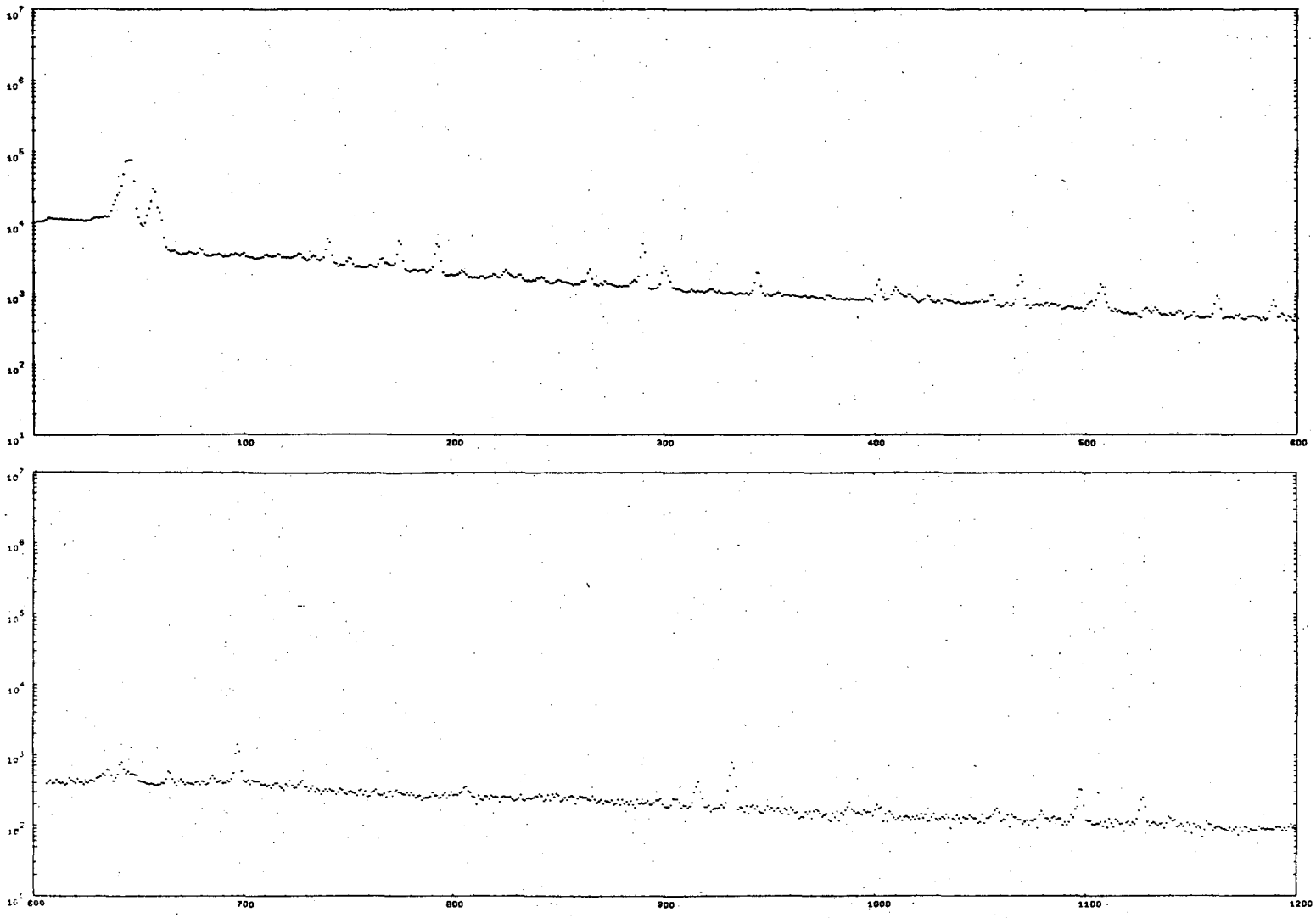

XBL 7011-7107

Fig. III-1. Gamma singles spectrum obtained from a source containing daughters of ^{202}At.

Consequently the most detailed decay data were obtained in this higher-mass region.

It is worthwhile to look first at the experimental arrangements, particularly the setup used for the coincidence measurements, and at the computer codes developed to analyze the resulting spectra.

A. Experimental

Isotopes of astatine were again prepared by carbon ion bombardments of gold targets. The astatine was evaporated onto a molybdenum or platinum plate. The activity on this plate was then used immediately as a gamma source to obtain the astatine spectra. In separate runs the astatine on this source plate was allowed to decay for an appropriate length of time (one or two half-lives) and the remaining astatine was then removed by heating. The gamma spectra of the polonium and bismuth (and lead) daughters were then measured.

1. Gamma Ray Singles

In the course of the singles experiments two very similar Ge(Li) detectors were used. Most of the gamma singles measurements were made with a ~5 cm^3 Ge(Li) crystal capable of a resolution of ~2.1 keV (FWHM) under ideal conditions. The resolution was actually 2.3 keV (FWHM) for gamma rays of 122 keV, and 2.9 keV(FWHM) for gamma rays of 1332 keV, owing to compression of the spectrum to about 0.9 keV/channel and operation at fairly high counting rates (~8000 counts/sec). The data were accumulated in a SCIPP 1600-channel pulse-

height analyzer and read out onto magnetic tape for subsequent computer analysis. The other Ge(Li) crystal used for the singles spectra was also ~5 cm^3, but had a slightly better resolution of 2.0 keV (FWHM) at 122 keV and 2.7 keV(FWHM) at 1332 keV under the actual operating conditions. It was used with a SCIPP 4096-channel pulse-height analyzer and again the spectra were read out onto magnetic tape.

Absolute photopeak efficiency curves were obtained for both detectors at the experimental geometry through the use of primary gamma standards obtained from the International Atomic Energy Agency in Vienna (Figs. III-2 and III-3).

A high-resolution Si(Li) detector--0.7 keV (FWHM)--was used to obtain the low-energy portion (< 100 keV) of the ^{205}Po spectrum.

2. Gamma-Gamma Coincidence Measurements

Gamma-gamma coincidence measurements were made on the mass 204-206 isomers with Ge(Li) detectors by using a bi-dimensional coincidence setup of 1600 × 1600 channels. The electronics arrangement used for performing and recording the coincidence measurements is shown schematically in Fig. III-4.

A leading-edge discriminator was employed to extract timing information from the detector pulses. A coincidence was then performed between these signals with a resolving time for the two detectors of 0.5 μsec. If the fast-coincidence requirement was met a signal was sent to the linear gates, allowing the two analog signals containing the energy information to pass. These signals were then

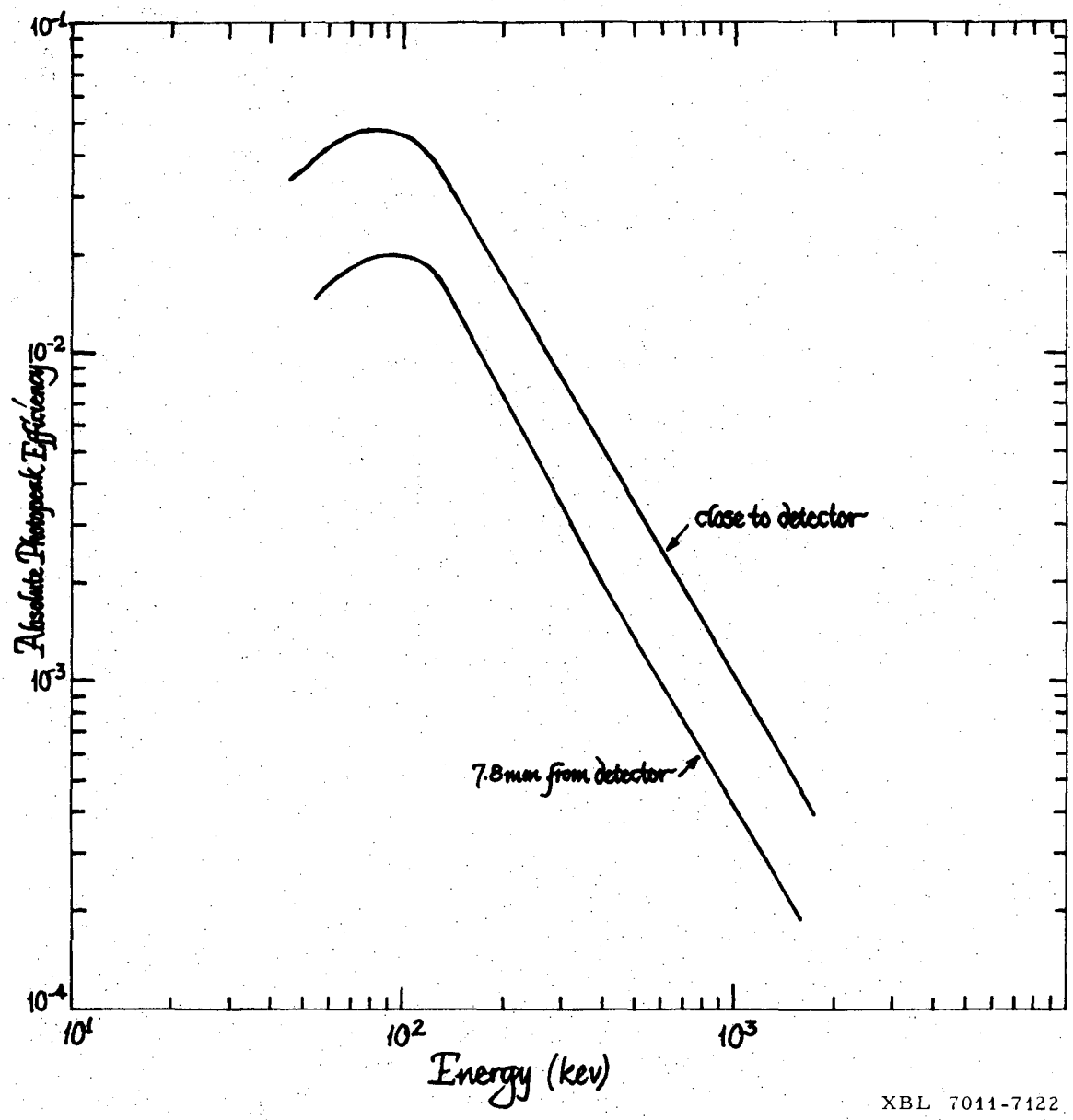

XBL 7011-7122

Fig. III-2. Absolute photopeak efficiency determined at the experimental geometries for the ~5 cm^3 Ge(Li)-I detector used in the gamma ray singles measurements.

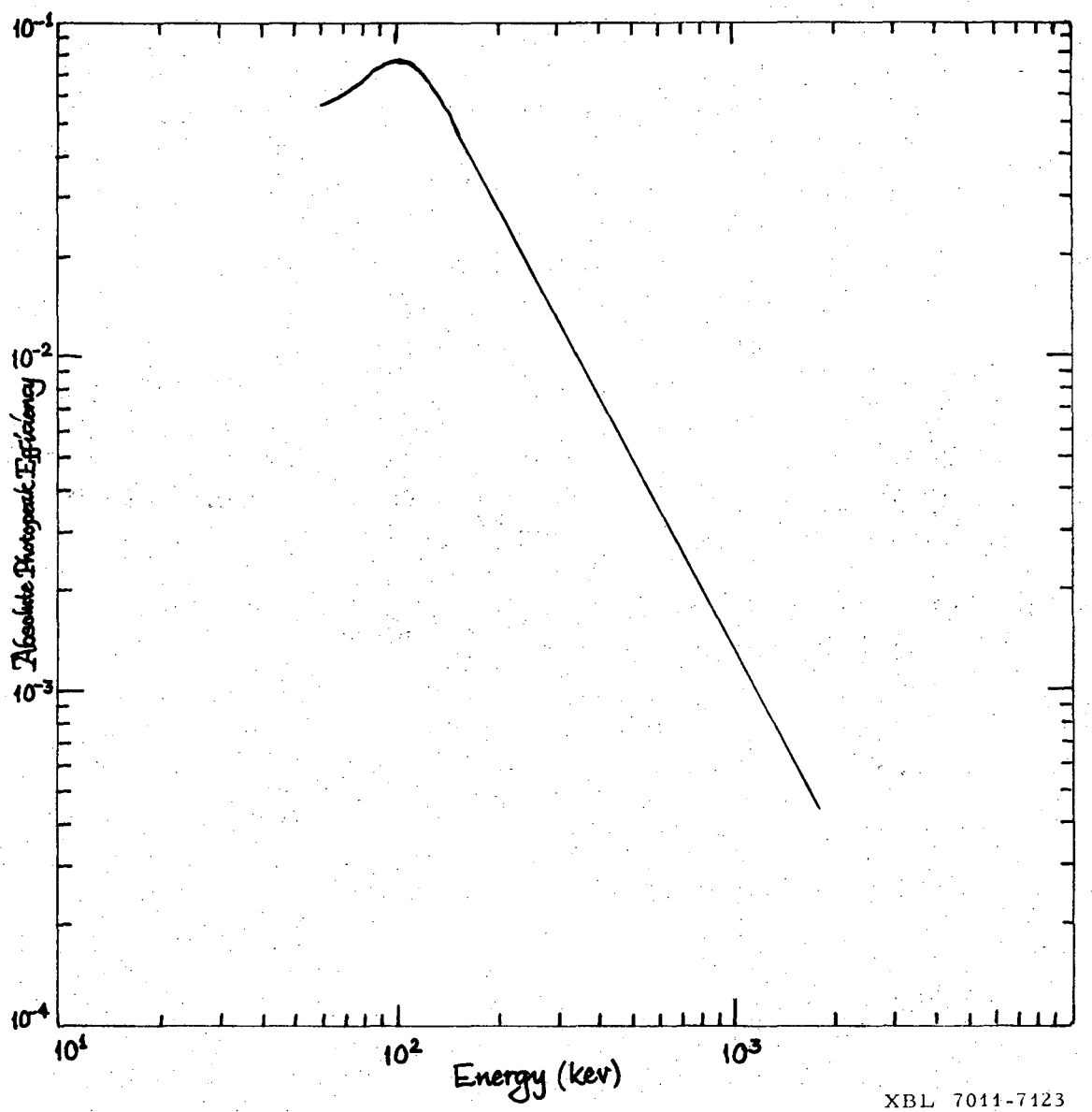

XBL 7011-7123

Fig. III-3. Absolute photopeak efficiency determined at the experimental geometry for the second ~5 cm^3 Ge(Li)-II crystal used in the gamma ray singles measurements.

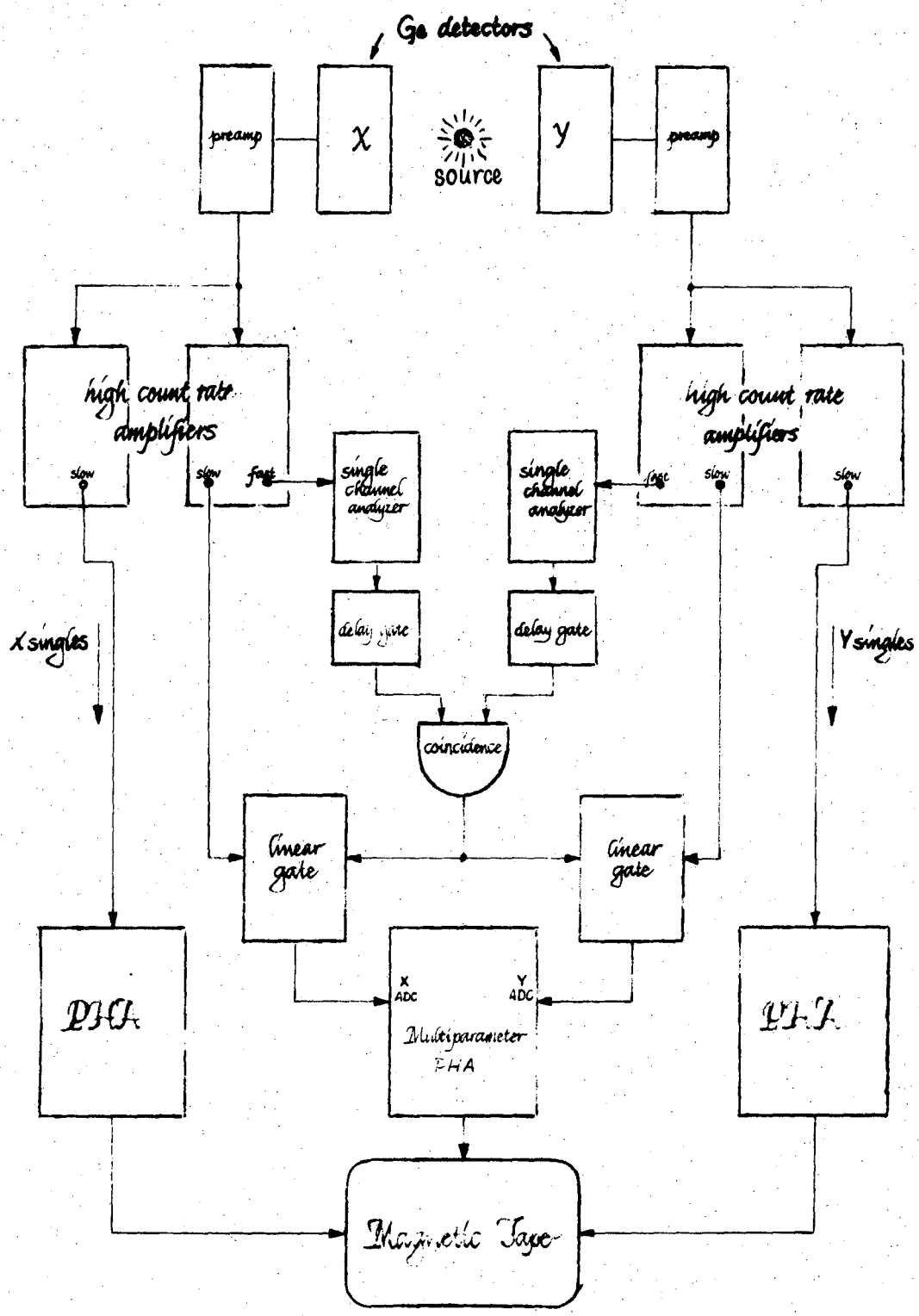

XBL 7011-7124

Fig. III-4. Block schematic diagram of the electronics used in the coincidence studies.

read serially into the buffer memory of a multiparameter pulse-height analyzer. When the buffer became full the contents of the memory were automatically dumped onto magnetic tape.

To analyze the spectra it was necessary to process the raw data with a computer code which sorted the information into desired gamma ray energy intervals. This code (POLLY) is described in the next section.

The geometry of the experimental setup was determined from the following considerations. In general, coincidence spectra exhibit the usual Compton backscattering components found in singles spectra, but in addition the Compton scattering from detector to detector can produce false coincidences. The effect is most pronounced when the detectors can "see" each other as in Fig. III-5(a). A false coincidence will be registered when a gamma is Compton-scattered in crystal 1 and the scattered photon is detected in crystal 2. As the crystals are moved farther apart the false coincidence peaks become weaker owing to the smaller angle through which the gamma ray may be scattered in one detector and still reach the other detector. Increasing the source-to-detector distance is no solution, however, since the coincidence rate decreases as fast as the scattering.

There are some standard anti-Compton shields. False coincidences can be avoided in the geometry shown in Fig. III-5(b) but only at the expense of much lower efficiencies. For gammas of favorable energies the arrangement shown in Fig. III-5(c) can help without unduly reducing the efficiencies.

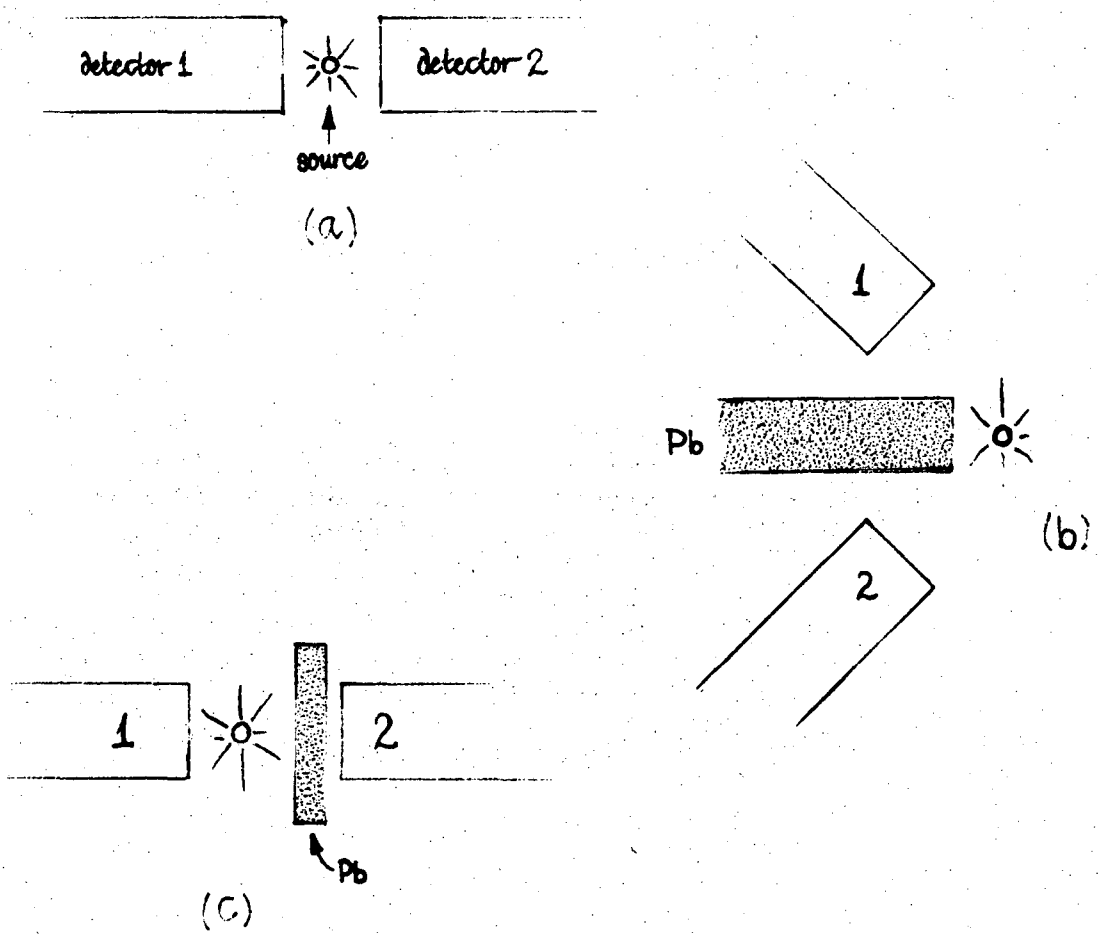

XBL 7011-7125

Fig. III-5. Detector geometry in coincidence measurements. (a) Two detectors at 180°. False coincidences will be seen owing to coincidences with Compton scattered photons. (b) A Compton shield to prevent the detectors from "seeing" each other. However, there is a resultant decrease in efficiency. (c) Low-energy gammas can be detected in crystal (1) and high-energy gammas in coincidence with them will be seen in (2) without accidentals caused by Compton scattering.

We could not afford the loss of efficiency inherent in the arrangement of Fig. III-5(b). The increased source-to-detector distance with our 2.7-cm-diameter Ge(Li) crystals results in an efficiency for each detector 50 times smaller than that in a linear arrangement [Fig. III-5(a)]. This means the coincidence efficiency has decreased by a factor of 2.5×10^3, and we could not make up the difference by increasing the source strength. Since we were interested in coincidences between gammas in a wide energy spectrum, the geometry in Fig. III-5(c) was not satisfactory.

Instead we used the anti-Compton sample holder shown in Fig. III-6. It was modified from one designed earlier by Dr. E. Browne. The source on a 1-in. platinum disk with the activity confined to the center of the disk in a circle of 6 mm diameter was sandwiched between two lead plates. Each of the identical lead plates has a 6-mm-diameter orifice in the center. The thickness leading out from this hole toward the gamma detectors was tapered from 0 at the hole to 0.53 cm (the thickness of the lead plate) at 1.23 cm from the center of the hole. This provided a cone for a gamma emanating from the orifice to reach one of the detectors. The scattered photon had to strike the hole in the shield in order to reach the other detector. The tapering allowed a greater thickness to confront the backscattered photons of higher energy found at larger scattering angles near the crystal edges.

The lead plates were, in turn, sandwiched between two 0.7-mm silver absorber plates in order to stop some of the copious polonium

(a)

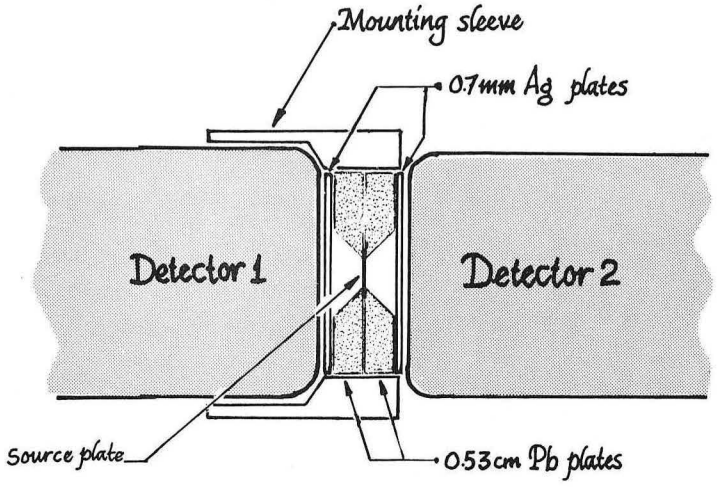

(b)

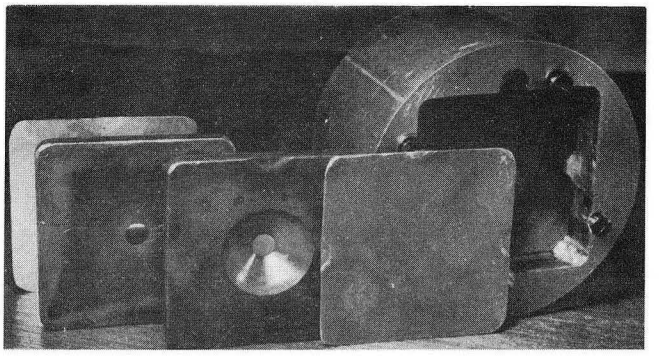

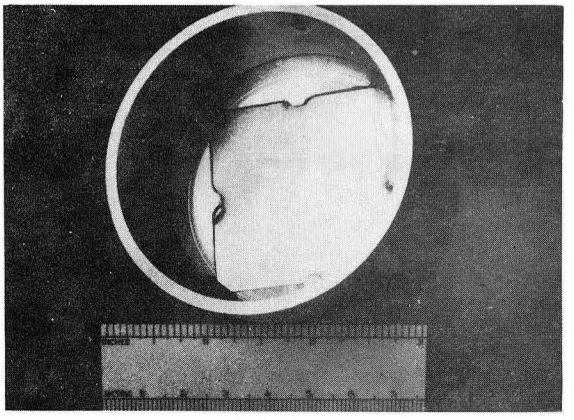

(c)

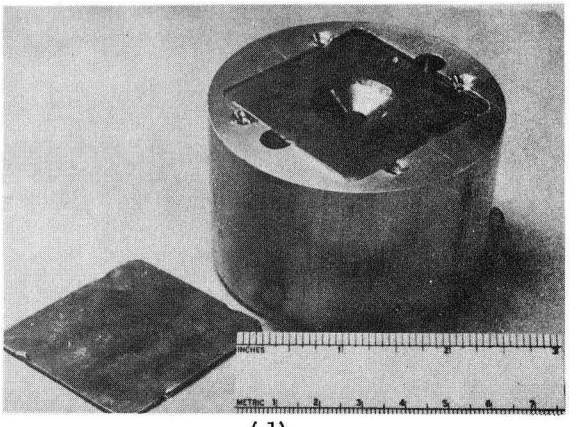

(d)

XBB 7011-5340

Fig. III-6. Sample holder used in the coincidence measurements. (a) Schematic diagram of holder. (b) View of disassembled holder. (c) Bottom view. (d) Top view, with silver plate removed.

and bismuth x rays and thus allow the detection system to handle a hotter source. This thickness of silver transmits only 18% of the 79.29-keV Po K_{α_1} x rays while still transmitting 71% of the 150-keV gamma rays and greater than 90% of all gammas with energies over 300 keV. The whole assembly of the two Ag and two Pb plates fit down into a well on top of a hollow sleeve (Fig. III-6) which was then mounted on one detector. The other detector was positioned adjacent to the front end of the sample holder. The whole arrangement could be assembled in about a minute after the gamma source was in place.

A ^{182}Ta source was placed in the holder to obtain photopeak efficiency curves for both detectors. ^{182}Ta (115 days) has many prominent gamma rays ranging from 67.8 to 1231 keV. The ^{182}Ta was made by reactor bombardment of an 8-mg natural Ta target 0.5 cm in diameter and 1 mil thick. The absolute intensity of each gamma ray was determined by using a detector of known efficiency (the efficiency curve is shown in Fig. III-2). The tantalum was then mounted in the sample holder and its gamma spectra measured with each of the detectors used in the coincidence setup. The efficiency curves obtained in this manner are presented in Figs. III-7 and III-8. The resolution of the gating or "y" Ge(Li) detector was 2.0 keV (FWHM) at 661 keV and the resolution of the "x" crystal was 2.2 keV (FWHM) at 661 keV.

The second curve in Fig. III-8 represents the efficiency curve obtained for the x detector with the same total source-to-detector distance but without the 0.7-mm Ag absorber. The maximum

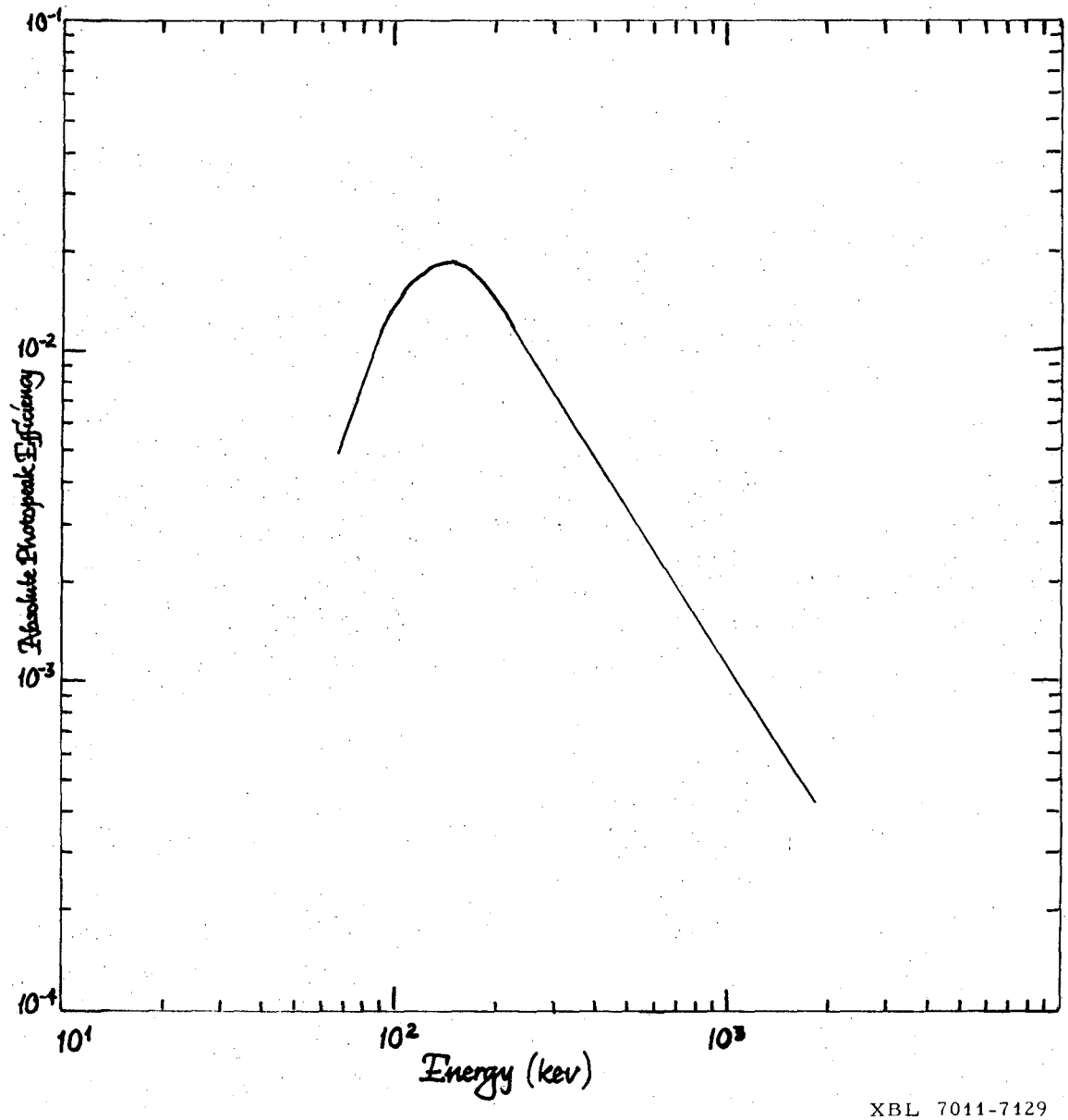

XBL 7011-7129

Fig. III-7. Absolute photopeak efficiency determined at the experimental geometry for "y" or gating Ge(Li) detector of coincidence setup.

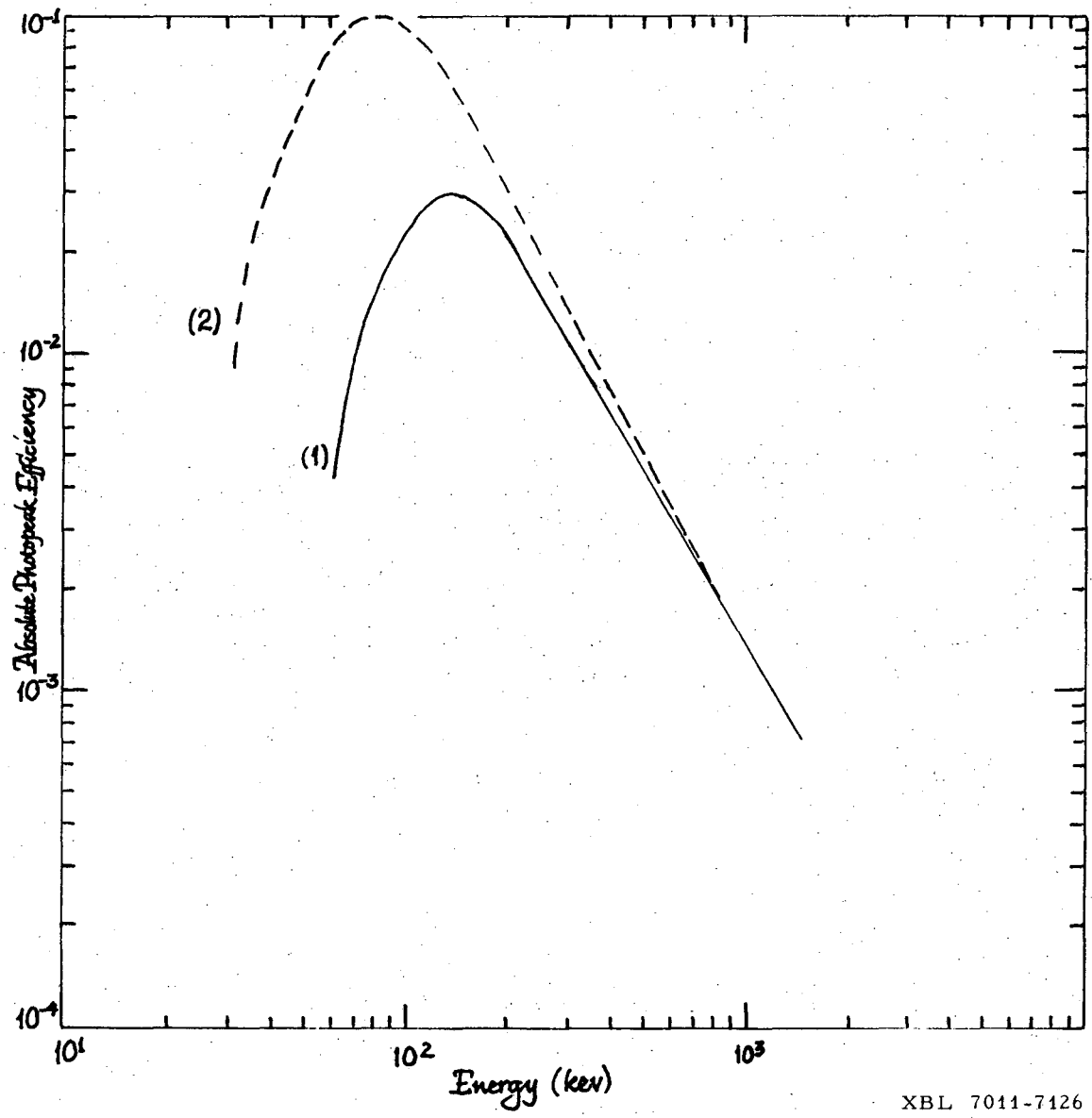

XBL 7011-7126

Fig. III-8. Absolute photopeak efficiency determined at the experimental geometry (1) for "x" Ge(Li) detector of coincidence setup. The second curve (2) represents the efficiency in a sample holder with the same geometry but without the Ag absorber plates.

efficiency has been cut by a factor of ~3.5 with the addition of the silver, but above 200 keV there is very little effect.

B. Data Analysis

1. General Considerations

The advent of high-resolution semiconductor detectors has made possible the rapid acquisition of multitudes of nuclear data. A typical "run," e.g., the singles measurement of the gamma transitions seen in the decay of the daughters of ^{202}At, results in ~30 spectra counted for periods ranging from 4 min to several hours and encompassing a total time span of perhaps 3 days. Each of these spectra contains from 20-120 peaks, each of which must be integrated to yield intensity and for corresponding peaks, half-life information. Quantitative determination of these quantities was possible only by utilizing several computer codes.

The spectrum of a single gamma transition measured in a spectrometer under specified conditions is characterized by a response function. A complex spectra is the sum of many such response functions. Most computer analyses of NaI scintillation spectra (NAS62) are performed by using the measured or calculated response functions corresponding to the individual components of the spectra. Such response functions are not generally available for solid state detectors and it would be extremely difficult to interpolate between the functions to account for responses from crystals of different characteristics and sizes. When the number of peaks and channels in a

spectrum becomes large, the mathematics associated with stripping the response functions quickly become horrendous. With the high-resolution semiconductor detectors, most of the useful information is contained in the photopeaks (full energy and escape peaks), and it is possible to confine the analysis to studying photopeaks only. This method has an advantage in that, although it does not use all the statistical information in the spectrum, it is free from the accumulation of errors that greatly reduces the accuracy attained with spectrum-stripping techniques.

As a first approach, the continuum under a photopeak can be approximated by a smooth curve through points on both sides of the peak. The area of the peak is then defined as the sum of the counts above the continuum, and the center of gravity is taken as the centroid of the peak. This method is only applicable to well-defined single peaks and does not use any statistical information in the peak itself to define the continuum.

A better approach, which can be extended to overlapping peaks (multiplets), is to fit the peaks with a variable-width Gaussian and use an exponential approximation for the background. The continuum under the peaks is due to Compton distributions from gamma rays of higher energy. Without detailed knowledge of the composition of this spectrum we can only observe that the continuum in a short interval under a cluster of peaks is a smoothly varying function of energy except for statistical fluctuations. As such the background can be approximated by a polynomial or, even more accurately, by a polynomial

on a log scale, i. e., an exponential with a polynomial exponent.

Gaussian peak shapes with an exponential background were tried and found to give good fits to the experimental data. The method was developed into the computer code MAGIC. Before describing the code in detail it is important to point out that there are limitations to this method about which the user should be forewarned. First, photopeaks can exhibit low-energy tailing and thus deviate from Gaussian shape. Also the width of the Gaussian should vary smoothly with energy, but in regions of low intensity peaks with poor statistics the width may vary randomly unless extra conditions are imposed. These limitations were considered and did not cause significant error in the present spectra.

To understand when these limitations become significant it is necessary to examine some of the factors that determine the photopeak width. These factors affecting the performance of a Ge(Li) detector system are discussed by Camp.[Cam67] The basic factor determining the width of a photopeak is the statistical fluctuation in the division of the absorbed energy between ionization and heating of the crystal lattice. This gives rise to a Gaussian distribution with a small specified width. The extent to which this distribution is seen in experimental data taken with a particular crystal depends primarily on the inherent quality of the detector, i. e., its resolution. The impurities in the detector as well as its material properties affect the charge collection and the electronic noise associated with leakage current. The combined effects of incomplete charge collection and

incomplete compensation of impurities worsen the resolution and also give rise to low-energy tailing of the photopeaks.

The contribution to the resolution from preamplifier noise is important at low energies and the instabilities of the amplifier and pulse-height analyzer begin to affect the peak width at higher energies, particularly when long counting times are involved. At high counting rates, random summing of pulses also broadens the peaks and gives rise to tailing.

Low-energy tailing is the most significant deviation from a Gaussian shape. In the analysis of the present spectra the increase in the area of any photopeak when the low-energy tailing effect is included (by hand analysis) is less than 5% and more like 1-2% for well-defined peaks. This is probably due in part to the intrinsic quality of the detectors and also to the compressed energy scale, which confines the peaks to only a few channels. As a result the peak widths are small (FWHM ~ 2-3 channels) and fine details of the peak shape (i. e., tailing) are lost.

The Gaussian width was free to vary within certain limitations. As stated previously, the width should increase smoothly with increasing energy. This was generally found to be true except when low-intensity peaks were fit singly. Then the poor statistics could result in a random fluctuation of the width. This problem was avoided by fitting several peaks simultaneously and requiring the width to be the same for all of them in the chosen energy region, which was ~ 40 keV in the actual analysis. This tied down the width parameter and

constrained it to vary smoothly with increasing gamma energy. Since the program was run on-line by means of the cathode ray (CRT) display system, the user was able to make the final decision on acceptance or rejection of the fitted spectra. Any undue variation in peak width was seen immediately and the energy region in question was refit.

It should be noted that a more general and very comprehensive computer code, SAMPO, was developed at this Laboratory by Routti and Prussin[Rou68, Rou69] for the determination of photopeak energies and intensities. This code contains provisions for fitting peaks with significant tails. The central part of a peak is described by a Gaussian and the tails by simple exponentials which join the Gaussian so that the function and its derivative are everywhere continuous. The empirical peak shapes and polynomial backgrounds are fitted in a least-squares sense over a limited energy region. The three shape parameters --the width and the two joining points -- vary smoothly with energy. The values of these parameters for any peak in a spectrum may be found by interpolation between parameters of neighboring peaks. Thus intense single lines in the spectrum are fit as internal standards and the values of their shape parameters stored in an array for interpolation.

SAMPO contains many automated features including peak searching and error analysis. It provides various options for obtaining energy, efficiency, and line-shape calibrations, and allows for on-line use. Output consists of printer plots of the fit along with tabulation

of results and allows the option of CalComp plots or photographs of the CRT displays. It does require good standard shapes and peaks spread over enough channels (at least ~ 10) to allow the calculations to be statistically meaningful. At present it can fit multiplets with up to six components.

Wilhelmy (Wil69) has used SAMPO to analyze the complicated gamma spectra derived from the unseparated fission products formed in the spontaneous fission of ^{252}Cf. He has found that for reasonably good germanium crystals the peak area is increased by between ~ 0.5-10% when the tailing effect is included.

2. Peak Fitting--MAGIC

The present experimental spectra were all analyzed by using the computer code MAGIC, which minimizes the weighted sums of squares

$$\chi^2 = \sum_{x=x_{min}}^{x_{max}} \frac{\left\{ n_x - \left[B(x) + \sum_{j=1}^{np} f(x,j) \right] \right\}^2}{n_x} \qquad (1)$$

where x = channel number,

x_{min}, x_{max} specify the fitting interval ($\leq$ 250 channels),

n_x = counts in channel x,

$B(x) = e^{b_1 - b_2 x - b_3 x^2}$, background function,

np = number of peaks in the fitting interval ($\leq$ 18),

$$f(x,j) = \exp\left[a_{2j-1} - \frac{(x-a_{2j})^2}{2\sigma^2} \right].$$

The parameters b_1, b_2, and b_3 define the continuum, $e^{a_{2j-1}}$ is the height and a_{2j} the centroid of the jth peak, and σ is the width of the Gaussian, constrained to be equal for all peaks in the interval (FWHM = 2.354σ).

The minimization of the sum in Eq. (1) is performed by the subroutine VARMIT, which is an iterative gradient method using a variable metric.[Dav59] This routine uses χ^2, its gradient in the parameter space and the inverse of its second-derivative matrix. The first two quantities are calculated for each iteration step and the third is constructed during the minimization by the method of successive approximation. The size and direction of the next iteration step are determined by all this information. The minimization is terminated when all the components of the next step are less than some preset minimum, here 10^{-8}, or if four successive values of χ^2 are the same.

The results include the best values for χ^2 and the parameters along with the error matrix. The peak locations are expressed directly by the best values of the parameters a_{2j} and their errors by the square root of the appropriate diagonal elements of the error matrix $(d_{a_{2j}a_{2j}})^{1/2}$. The peak areas are obtained by integrating the resulting Gaussians:

$$I = \text{area} = \int_{x=-\infty}^{\infty} e^{a_{2j-1}} \cdot e^{-1/2(x-a_{2j}/\sigma)^2} = A \int_{x=-\infty}^{\infty} e^{-1/2(x-a_{2j}/\sigma)^2},$$

where $A = e^{a_{2j-1}}$ is the maximum amplitude of the Gaussian above the continuum. The integral can be readily evaluated since the

expression for a normal or Gaussian distribution is normalized, i.e,

$$\int_{-\infty}^{\infty} P(x)\,dx = \int_{-\infty}^{\infty} \frac{1}{\sigma\sqrt{2\pi}}\, e^{-1/2(x-x_0/\sigma)^2}\, dx = 1$$

and the area, I, is expressed by

$$I = A \cdot \sigma\sqrt{2}\pi. \tag{2}$$

The uncertainty in the parameters a_{2j-1} and hence in the areas can be obtained from the error matrix. If we write the area in terms of a_{2j-1}, i.e.,

$$I = e^{a_{2j-1}} \cdot \sigma\sqrt{2}\pi,$$

then

$$\begin{aligned} \Delta I &= \frac{\partial I}{\partial a_{2j-1}} \cdot \Delta a_{2j-1} = I \cdot \Delta a_{2j-1} \\ &= I \cdot (d_{a_{2j-1}, a_{2j-1}})^{1/2}, \end{aligned} \tag{3}$$

where $d_{a_{2j-1}, a_{2j-1}}$ is the corresponding diagonal element of the error matrix.

The energy calibration was obtained from the calculated centroids of well-established gamma ray energy standards. The integral linearity of the systems, i.e., the preamplifier and the ADC of the multichannel analyzer was very good. In the range from channels 100-1200 the nonlinearities were less than 0.8 channel. The energy was therefore expressed as a linear function of the channel number in MAGIC. More careful calibrations were subsequently performed on individual spectra, however, using some of the identified strong lines as internal standards and making a polynomial least-squares fit of

their energies. This compensated for any drift in the detector system owing to a change in the dead time between spectra. This final energy calibration resulted in uncertainties of $\leq 0.1\%$ at all energies. In most cases this calibration uncertainty dominates the total uncertainty in the energies of the photopeaks.

The code has been run on the CDC-6600 machines at the Lawrence Radiation Laboratory. It was operated on-line with the remote cathode-ray tube (CRT) display system. The magnetic tapes containing the experimental spectra provided the input data. Each spectrum is displayed in 250-channel segments, one segment at a time, with an overlap of 25 channels at each end [Fig. III-9(a)]. By light-pen interaction it is possible to indicate the fitting interval, three background points, and the photopeaks to be fitted. The resulting fit is then displayed [Fig. III-9(b)] and if it is not acceptable it can be rejected by the user and another attempt can be made to improve the results. Peaks missed in a first trial can be detected and added immediately and the interval refit.

The values of χ^2 and FWHM are also displayed on the CRT screen after each fit to help the user judge the goodness of the fit. If the fit is accepted, the values for the peak centroids and intensities are sent to an output array. The program requires an average of about 0.8 sec per peak. A typical "run" (~30 spectra each with an average of ~100 peaks) requires about 12 hr of actual on-line time for complete analysis which corresponds to about 1 hr of central processing time.

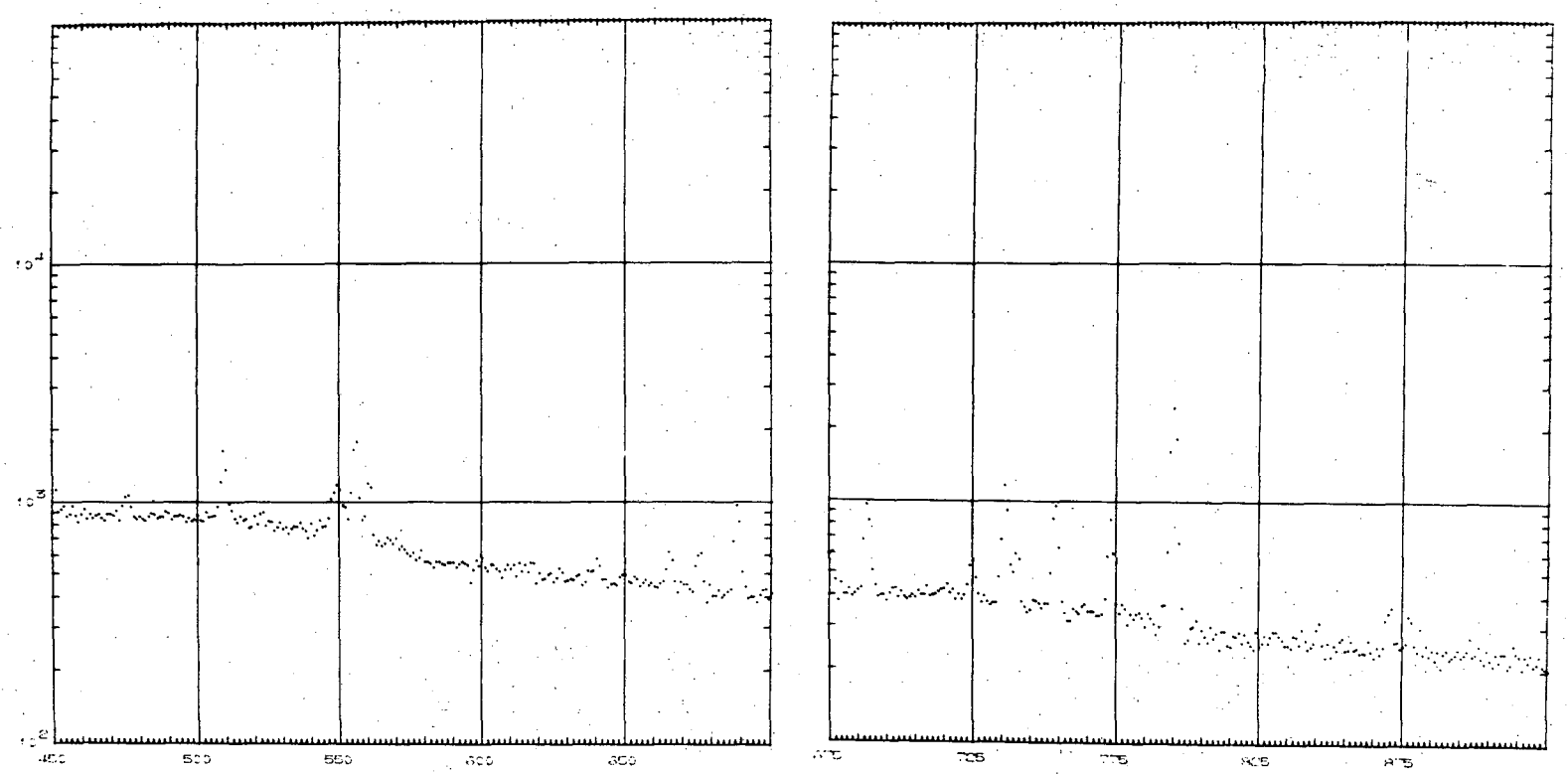

XBL 7011-7094

Fig. III-9(a). A portion of the ^{205}At gamma singles spectrum as displayed on the CRT screen 250 channels at a time.

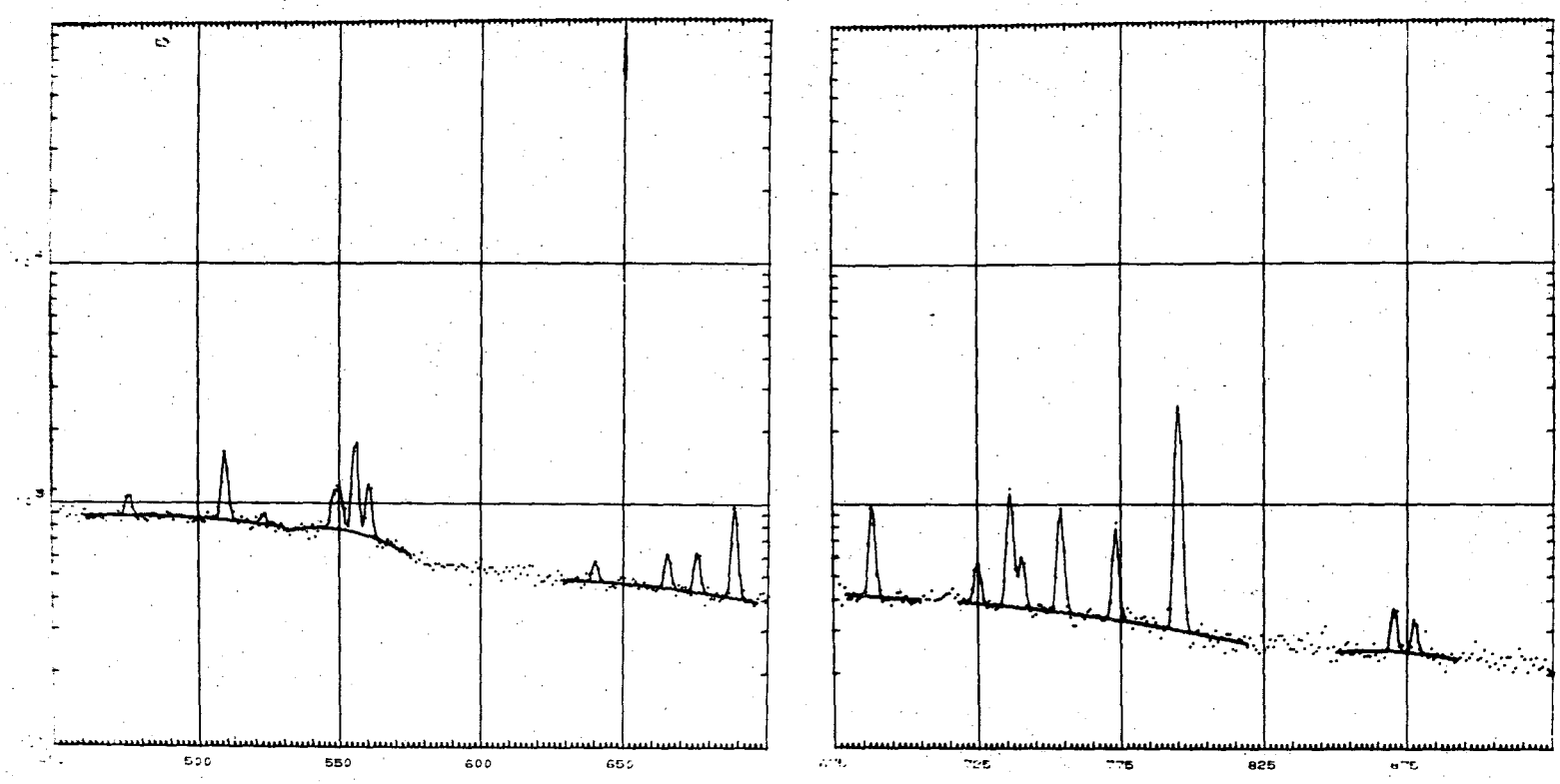

XBL 7011-7095

Fig. III-9(b). Same ^{205}At spectrum with the photopeaks fit by Gaussians, using the computer code MAGIC. The resulting fit is then displayed on the CRT screen.

In addition to the numerical results, the output also includes photographs of the CRT displays of the final fitted spectra. Optional output includes punched cards, one for each peak, containing energy, intensity, and time information. These cards were subsequently used as input data for a program to calculate half-lives for the gamma transitions.

3. Half-Life Determination

The computer code TOYL (Time of Your Life) was developed to calculate gamma ray half-lives. Input data were the punched output of MAGIC containing the intensity of each peak as a function of time (the midpoint of the counting interval). TOYL was also an on-line program; the data were displayed on the CRT screen on a semi-log plot.

The half-life of a given gamma ray that represented only a single component was determined by a least-squares fit to the well-known decay law

$$N = N^0 e^{-\lambda t}, \qquad (4)$$

where N = number of atoms at time t and N^0 = number of atoms at time = 0 (end of bombardment). This can also be expressed in terms of activities,

$$A = A^0 e^{-\lambda t},$$

since $A = \lambda N$.

Again the operator could indicate the fitting interval with the light pen and could also exclude any obvious bad points from the fit.

The resulting calculated decay curve was displayed and the fit accepted or rejected by the user (Fig. III-10).

Composite decay curves of species not related genetically and with well-separated half-lives could be handled by first fitting the linear section of the plot. This occurs at times long compared to the half-life of the first component [Fig. III-11(a)] and is the result of being able to ignore its decreasing exponential terms. The values obtained by extrapolating this linear portion back to the origin are subtracted from the original data and the resulting activities then fit to obtain the half-life of the shorter-lived component. The sum of the resultant decay fits was then displayed and could be rejected if not satisfactory. Although the program can handle five such components, in actual practice no more than three were ever seen.

Photographs of the final decay fits [Figs. III-10 and 11(b)] were included in the output package. The output also consisted of numerical values for the half-life and the extrapolated activity at the end of bombardment (A^0) for each component at a given gamma ray energy. Statistical errors for each of these values were computed from the appropriate diagonal element of the error matrix.

Half-life calculations for daughter radiations observed to grow in and then decay were performed according to the following parent-daughter decay relationships. Radioactive decay follows the principles of first-order kinetics, i.e., the decay rate is proportional to the number of atoms present, namely

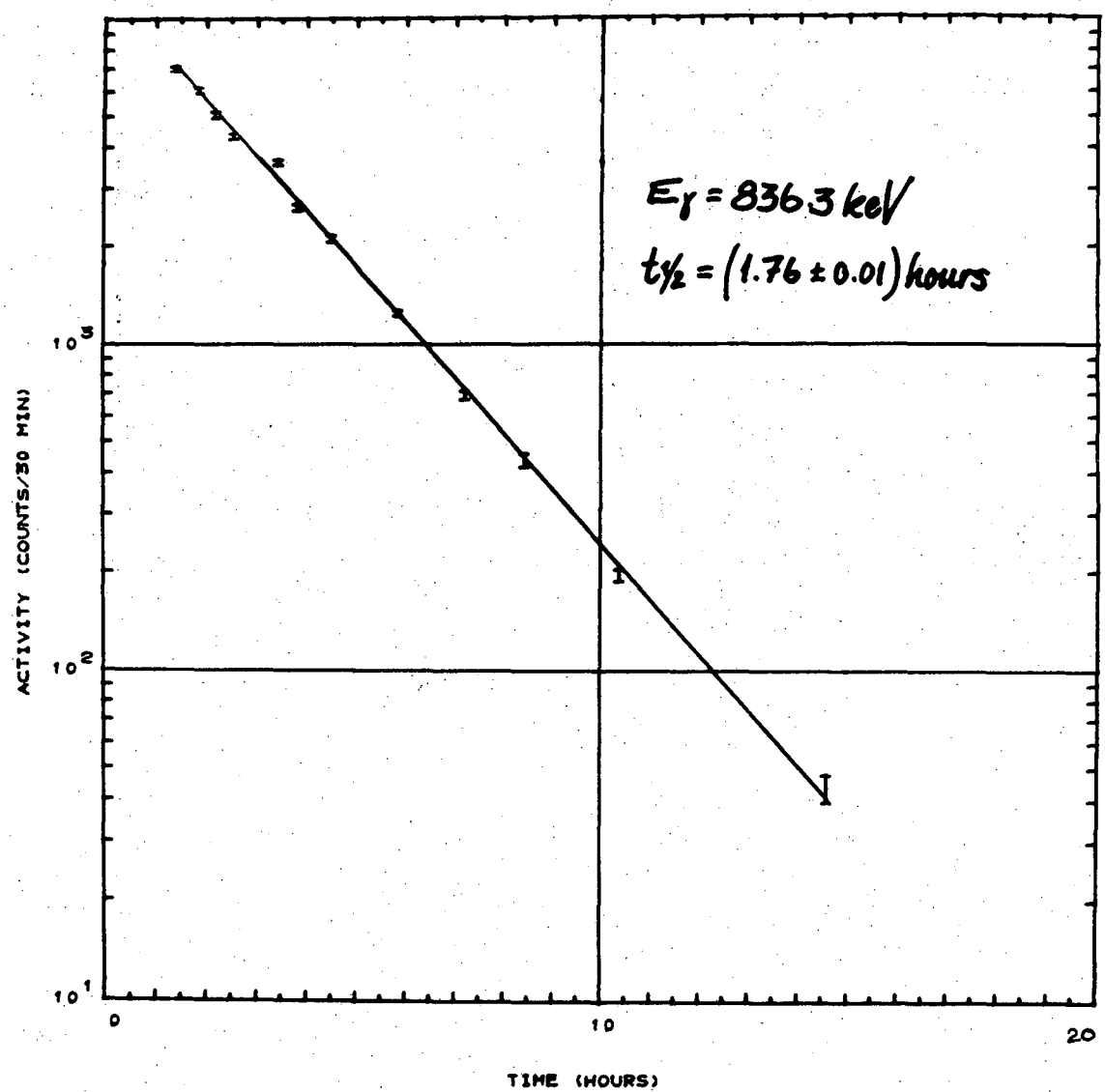

XBL 7011-7127

Fig. III-10. The decay curve of the 836.3-keV gamma transition assigned to the decay $^{205}Po \rightarrow {}^{205}Bi$. The points are experimental data and the solid line represents the least-squares fit performed by computer code TOYL.

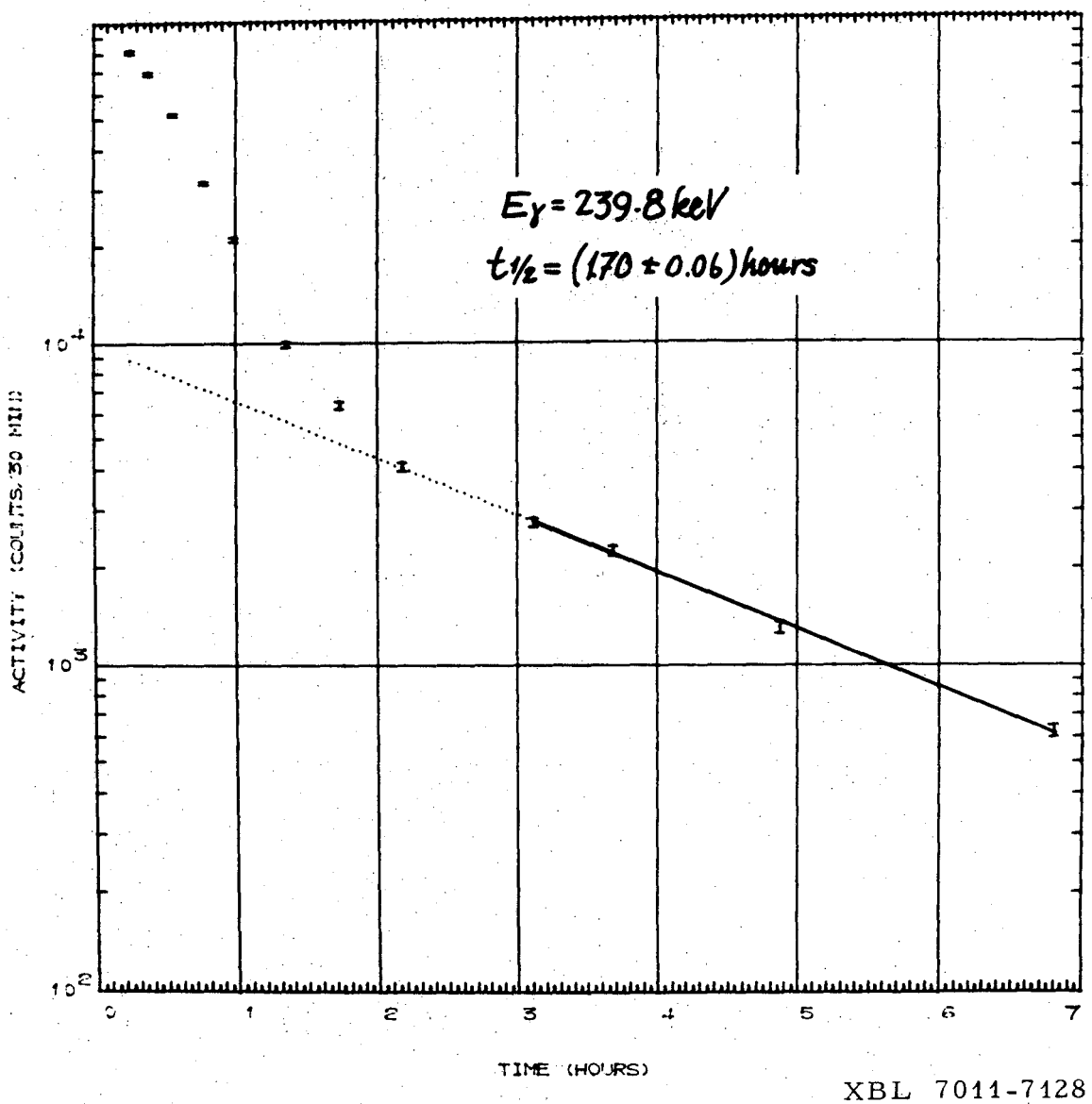

XBL 7011-7128

Fig. III-11(a). Composite decay curve of two independent activities with only the long-lived component (linear portion) least-squares fit by TOYL.

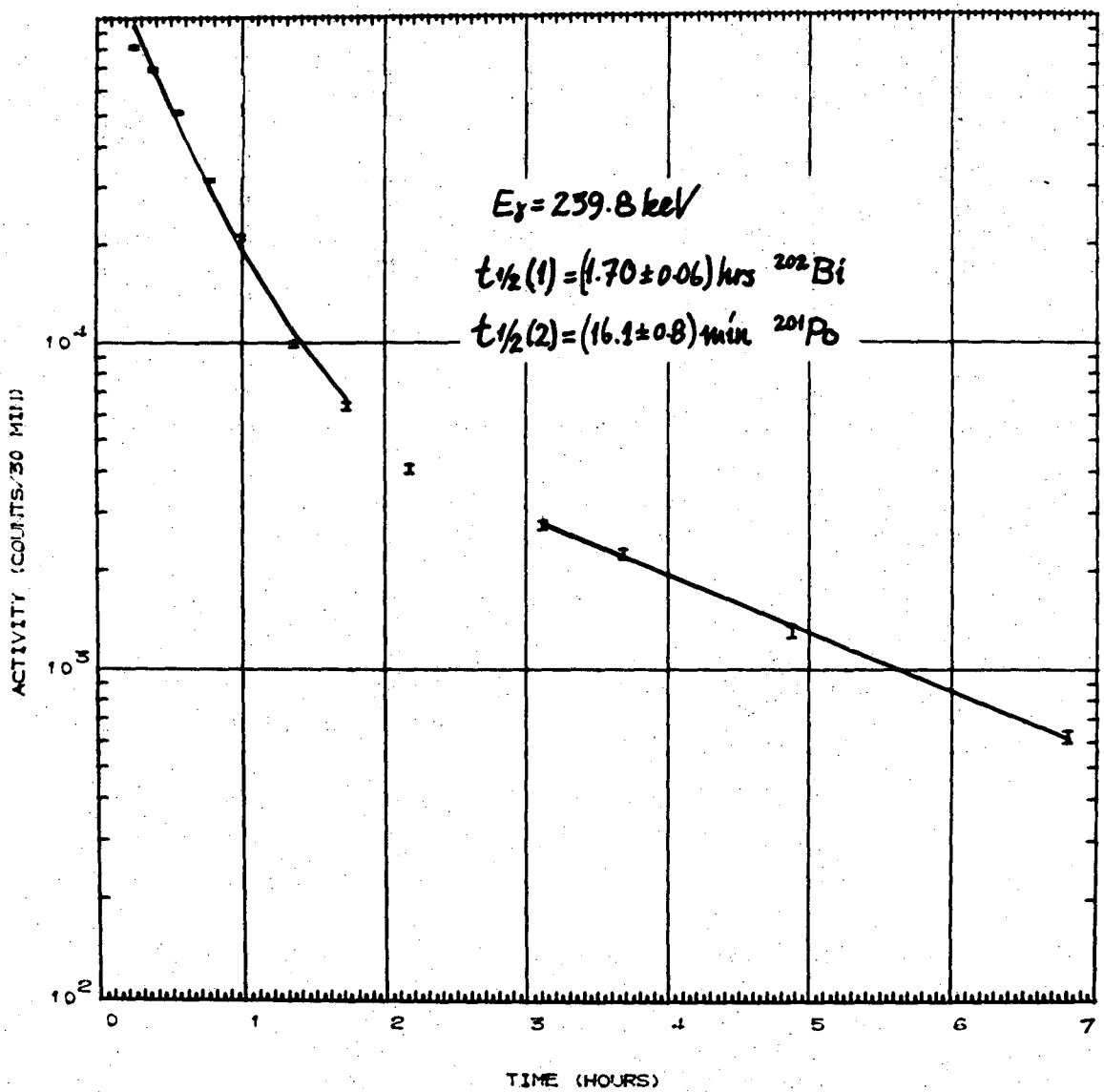

XBL 7011-7130

Fig. III-11(b). The values obtained by extrapolating the linear portion of the decay curve back to the origin are subtracted from the data points. The resulting activities are least-squares fit to obtain the half-life of the shorter-lived component. The sum of the resultant fits is then displayed (solid line).

$$\frac{dN_1}{dt} = -\lambda_1 N_1,$$

where N_1 and λ_1 in this case refer to the number of atoms and decay constant, respectively, of the parent. This, of course, is the relationship which, when integrated, gives rise to Eq. (4). The second species (daughter) is formed at the rate at which the first decays, $\lambda_1 N_1$, and, in turn, decays itself at the rate $\lambda_2 N_2$. Thus

$$\frac{dN_2}{dt} = \lambda_1 N_1 - \lambda_2 N_2$$

or

$$\frac{dN_2}{dt} = \lambda_1 N_1^0 e^{-\lambda t} - \lambda_2 N_2. \tag{5}$$

This can be solved by assuming the solution to be of the form

$$N_2 = U e^{-\lambda_2 t}. \tag{6}$$

Upon differentiation this gives

$$\frac{dN_2}{dt} = -\lambda_2 U e^{-\lambda_2 t} + \frac{dU}{dt} e^{-\lambda_2 t}. \tag{7}$$

Substituting (6) and (7) back into (5) we obtain

$$\frac{dU}{dt} = \lambda_1 N_1^0 e^{(\lambda_2 - \lambda_1)t}$$

or

$$U = \frac{\lambda_1 N_1^0}{\lambda_2 - \lambda_1} e^{(\lambda_2 - \lambda_1)t} + C.$$

After substituting back into (6) and imposing the boundary condition that $N_2 = N_2^0$ at $t = 0$ to evaluate the constant C, we have

$$N_2 = \frac{\lambda_1 N_1^0}{\lambda_2 - \lambda_1}\left(e^{-\lambda_1 t} - e^{-\lambda_2 t}\right) + N_2^0 e^{-\lambda_2 t} . \tag{8}$$

In most cases where growth was observed there was no equilibrium attained; i.e., the parent was shorter lived than the daughter. Since the daughter radiation was observed to grow in and decay, its half-life could be determined by using TOYL and fitting Eq. (4) to only the decay (linear) portion of the curve (Fig. III-12). It was also desired to obtain the parent half-life, primarily as an aid for gamma identification. In the case of no equilibrium the parent half-life can be obtained from an analysis in terms of t_{max}, the time required for the daughter to reach its maximum activity.

Differentiating Eq. (8) we find that

$$\frac{dN_2}{dt} = -\frac{\lambda_1^2}{\lambda_2 - \lambda_1} N_1^0 e^{-\lambda_1 t} + \frac{\lambda_1 \lambda_2}{\lambda_2 - \lambda_1} N_1^0 e^{-\lambda_2 t},$$

since $N_2^0 = 0$ if we start with an initially pure parent. Then, requiring that $dN_2/dt = 0$ when $t = t_{max}$ yields

$$\frac{\lambda_2}{\lambda_1} = e^{(\lambda_2 - \lambda_1) t_{max}} \tag{9}$$

or

$$t_{max} = \frac{2.303}{\lambda_2 - \lambda_1} \log \frac{\lambda_2}{\lambda_1} .$$

Once the daughter half-life and t_{max} were obtained with the use of TOYL, the parent half-life was approximated by finding the root of the function $f(\lambda_1) = \lambda_1 e^{(\lambda_2 - \lambda_1) t_{max}} - \lambda_2$ obtained from

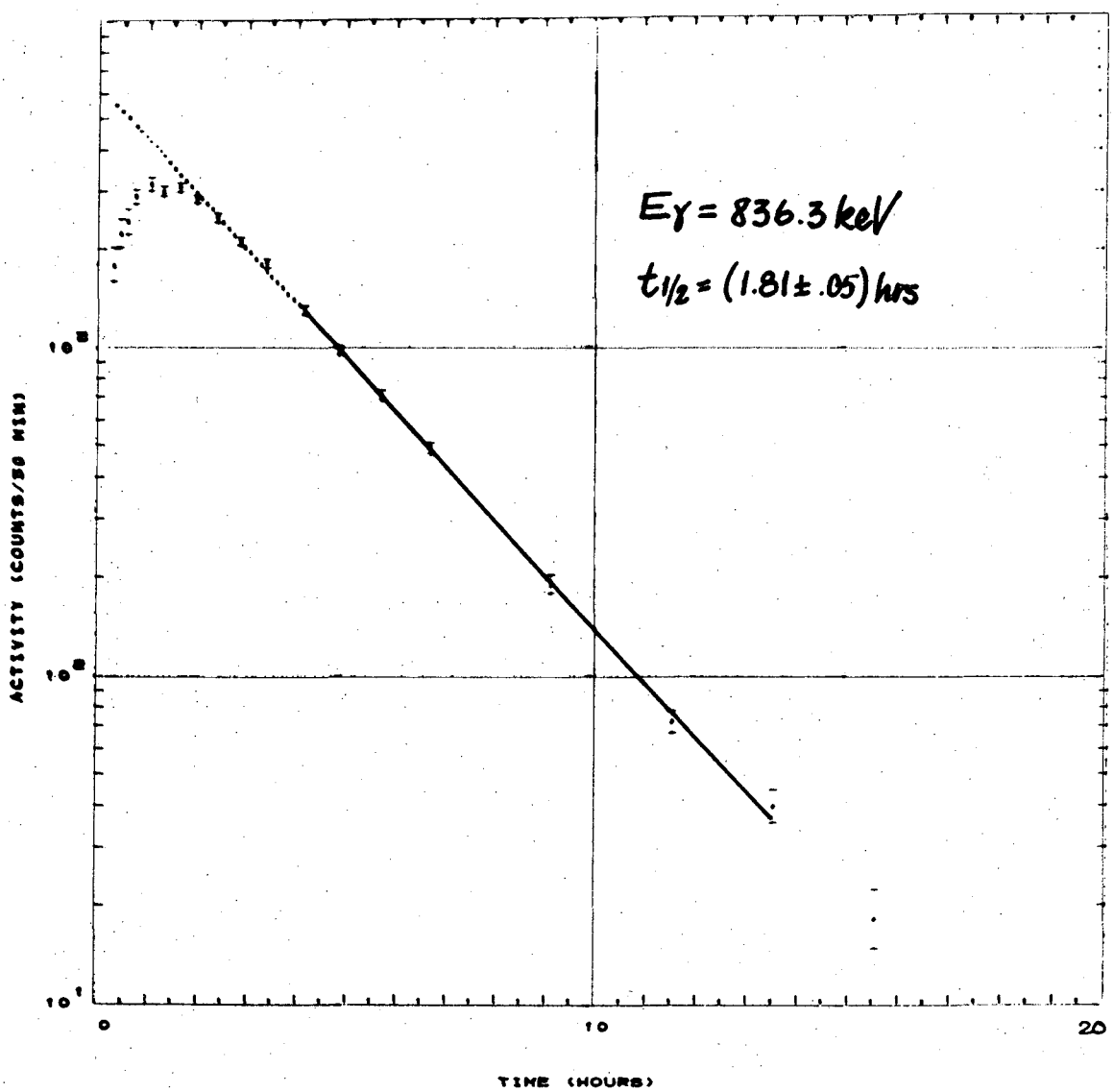

XBL 7011-7131

Fig. III-12. The decay curve of the 836.3-keV gamma seen in the decay of ^{205}Po. The half-life, $t_{1/2}$, was calculated from the least-squares fit of the linear portion of the curve as carried out by the computer program TOYL.

Eq. (9). This was performed by the subroutine ZERO. (Mei65) Given a function f and two points A and B such that f(A) and f(B) have opposite signs, ZERO finds two points X and Y such that $|X - Y|$ is less than a specified tolerance and f(X) and f(Y) have opposite signs. This is done by a combination of the false-position or secant method and the midpoint method. The two points A and B were generated within the code by successive approximations and the requirement that the function have opposite signs at the two points. The difference $|X - Y|$ was required to be less than 1×10^{-7} and the final solution λ_1 was taken as the midpoint of (X, Y).

A separate computer code PDDK was developed to obtain values for the parent and daughter half-lives as well as the initial parent activity A_1^0 directly from Eq. (8). They were obtained by minimizing the weighted sum of squares

$$\chi^2 = \sum_{t=t_{min}}^{t_{max}} \left[\frac{\log A_t - f(t)}{w(t)} \right]^2 ,$$

where t is the time,

t_{min}, t_{max} specify the fitting interval,

A_t = activity at time t with error a_t (from MAGIC),

$$f(t) = \log(\lambda_2 N_2) = \log\left[\frac{A(2)\, e^{A(3)}}{A(2) - A(1)} \left(e^{-A(1)t} - e^{-A(2)t}\right) \right],$$

$$w(t) = \log(A_t + a_t) - \log(A_t - a_t).$$

Again this assumes $N_2^0 = 0$ at $t = 0$. The initial parent activity is obtained from the parameter A(3) defined by $A_1^0 = \lambda_1 N_1^0 = e^{A(3)}$.

The decay constants λ_1 and λ_2 are equal to A(1) and A(2), respectively.

The minimization is again performed by the VARMIT routine. Initial guesses for the three parameters were supplied by cards. The activity and time information were again provided by the punched output of MAGIC.

Output included a photograph of the fitted decay curve as well as numerical printout. Figure III-13 shows the complete fit of the decay curve of the ^{205}Po 836-keV gamma shown in Fig. III-12.

4. Coincidence Sorting--POLLY

To analyze the coincidence data stored on magnetic tape it was necessary to sort the information into desired gamma ray energy intervals. This was done by the computer code POLLY.* All the coincidence data were stored event-by-event in a 1600×1600 matrix. Individual window sorts were performed by summing slices of the matrix over the number of channels in the window. The windows or energy gates were chosen from the y data and the coincidence spectrum D(x) then obtained by stripping the x data according to

$$D(x) = \sum_{y=y_i}^{y_f} D(x, y),$$

---

*This code represents the work of many people. The initial impetus and constant surveillance is due to Duane Mosier. He was aided by D. Harrell and the late Jo Drake in the development of the code. D. Gorman has added many refinements. In the course of the present work it was necessary to do a thorough revision to correct several elusive bugs.

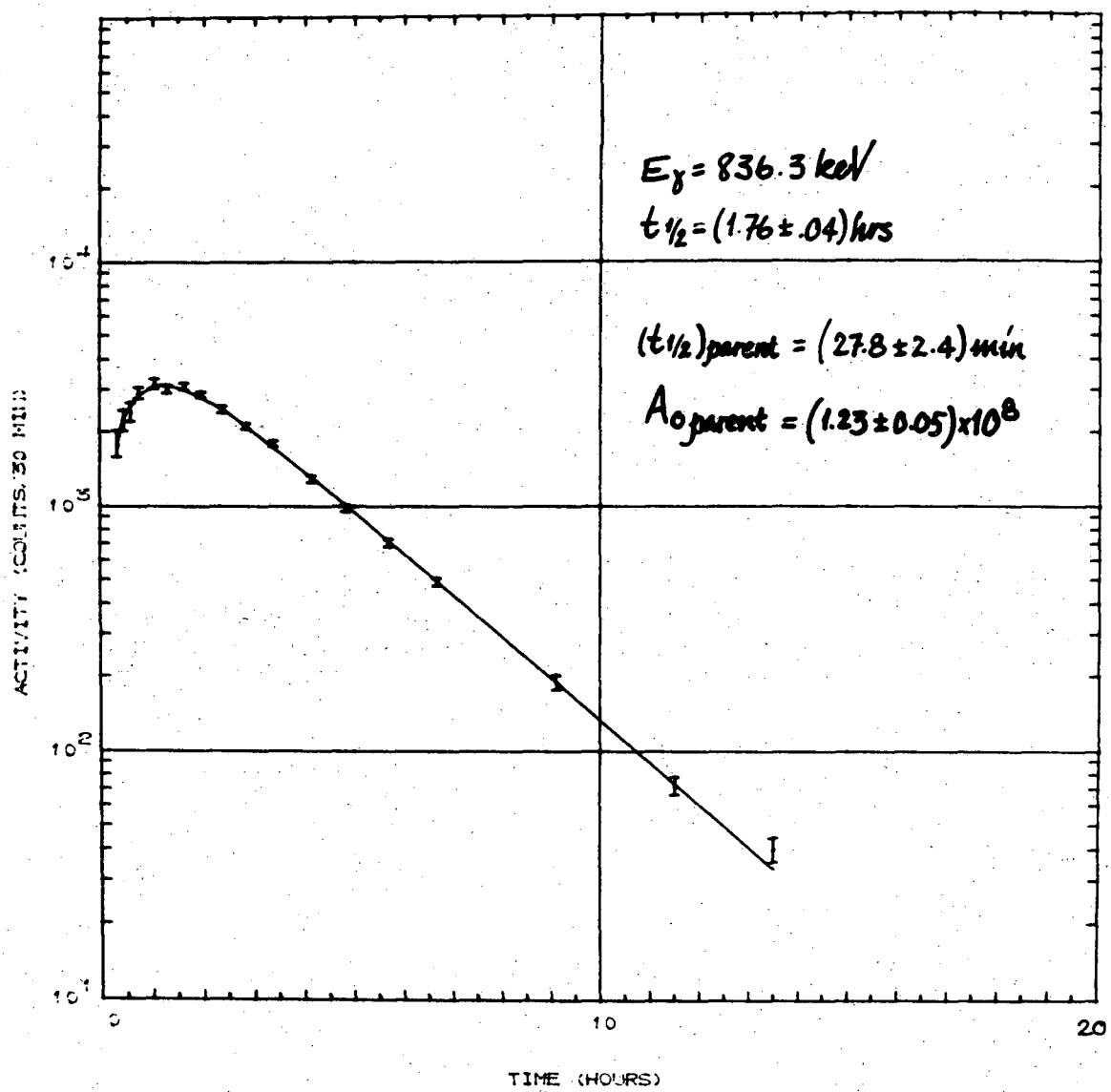

XBL 7011-7132

Fig. III-13. A complete fit of the decay curve of Fig. III-12 performed by the computer code PDDK using Eq. (8). The parent and daughter half-lives as well as the initial parent activity are indicated. The half-life values support the assignment of the 836.3-keV line to ^{205}Po growing from ^{205}At.

where y_i and y_f are the initial and final channels of the window. Each spectrum was listed and CalComp plotted. The photopeaks were hand integrated in order to calculate coincidence intensities.

The code also allowed the option of obtaining a two-dimensional printer map of all coincident gammas within desired energy limits. This proved to be especially valuable as a first survey of the results.

IV. RESULTS: DECAY OF ASTATINE ISOTOPES

A. Even-Mass Isotopes

1. ^{206}At

In the course of measuring the gamma spectrum of ^{205}At, several gamma rays of ^{206}At and ^{204}At were also observed. The spectrum is shown in Fig. IV-1. On the basis of their half-lives, four gamma lines were definitely assigned to ^{206}At decay and two others designated as probably belonging to ^{206}At. Table IV-1 presents the relative intensities of these observed ^{206}At gamma rays.

Using the lifetime values found from the three strongest transitions, the half-life of ^{206}At was determined to be 31.4 ± 0.7 min, in good agreement with previous values.(Led67) The assignment of some of the weaker gamma lines observed in the spectrum was made difficult by the fact that ^{205}At has a very similar half-life: 27.2 ± 0.6 min (results of this work). This leads to earmarking the tentative assignments as "probable" in Table IV-1.

Since electron capture accounts for ~99% of ^{206}At decay, the observed gamma rays must be transitions between levels of its ^{206}Po daughter. Gamma-gamma coincidence measurements (see Table IV-2) showed that the three most intense gamma transitions form a triple cascade and their relative intensities led to the ordering shown in the ^{206}Po level scheme proposed in Fig. IV-2.

The assignment of spins 2^+, 4^+, and 6^+ to the low-lying excited states was made by analogy to the first excited levels found in both

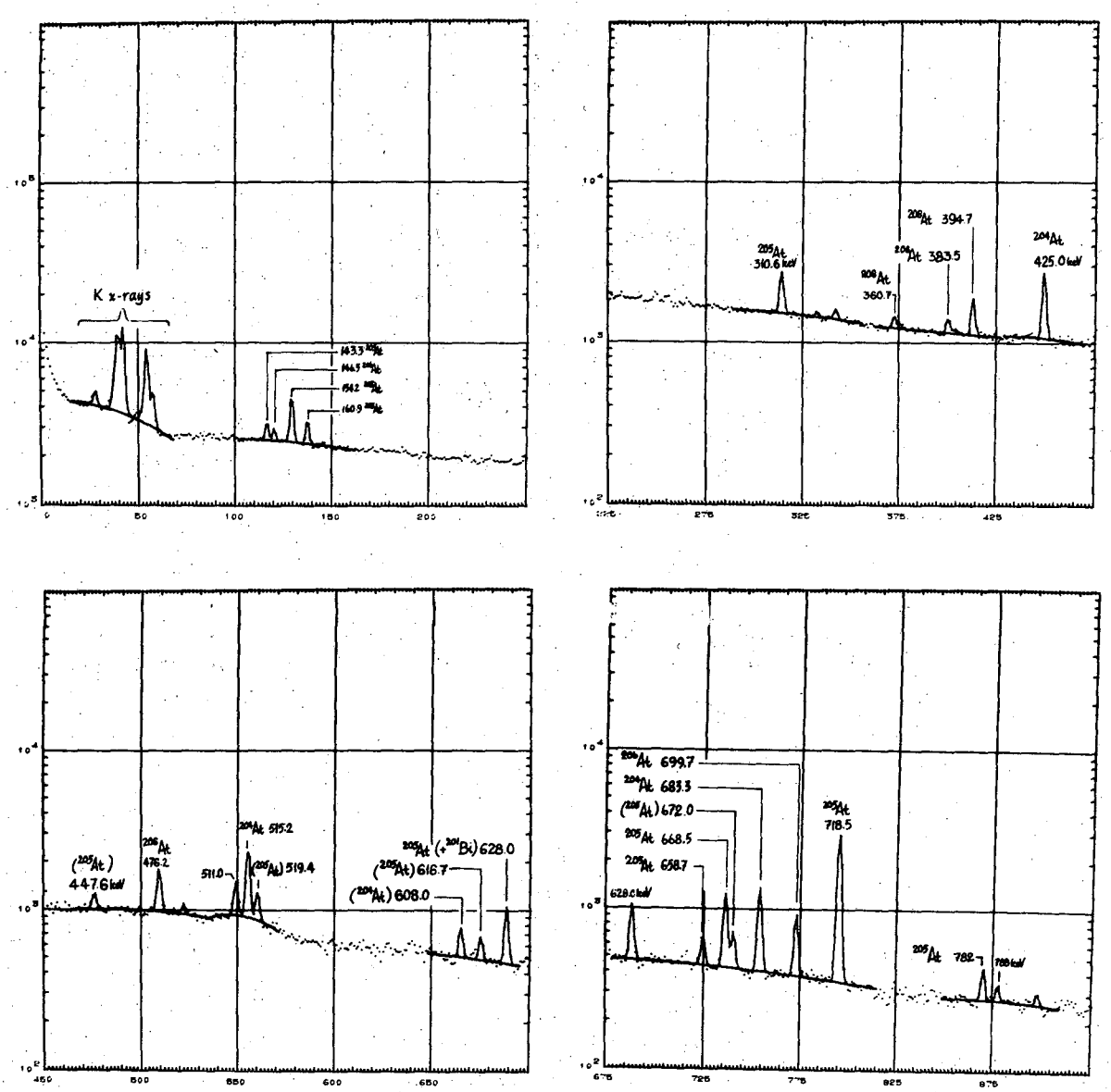

XBL 7011-7106

Fig. IV-1. Gamma spectrum of ^{206}At, ^{205}At, and ^{204}At 8 min after bombardment of a 0.25-mil Au target with 74-MeV ^{12}C ions (5.25-mil Al absorber).

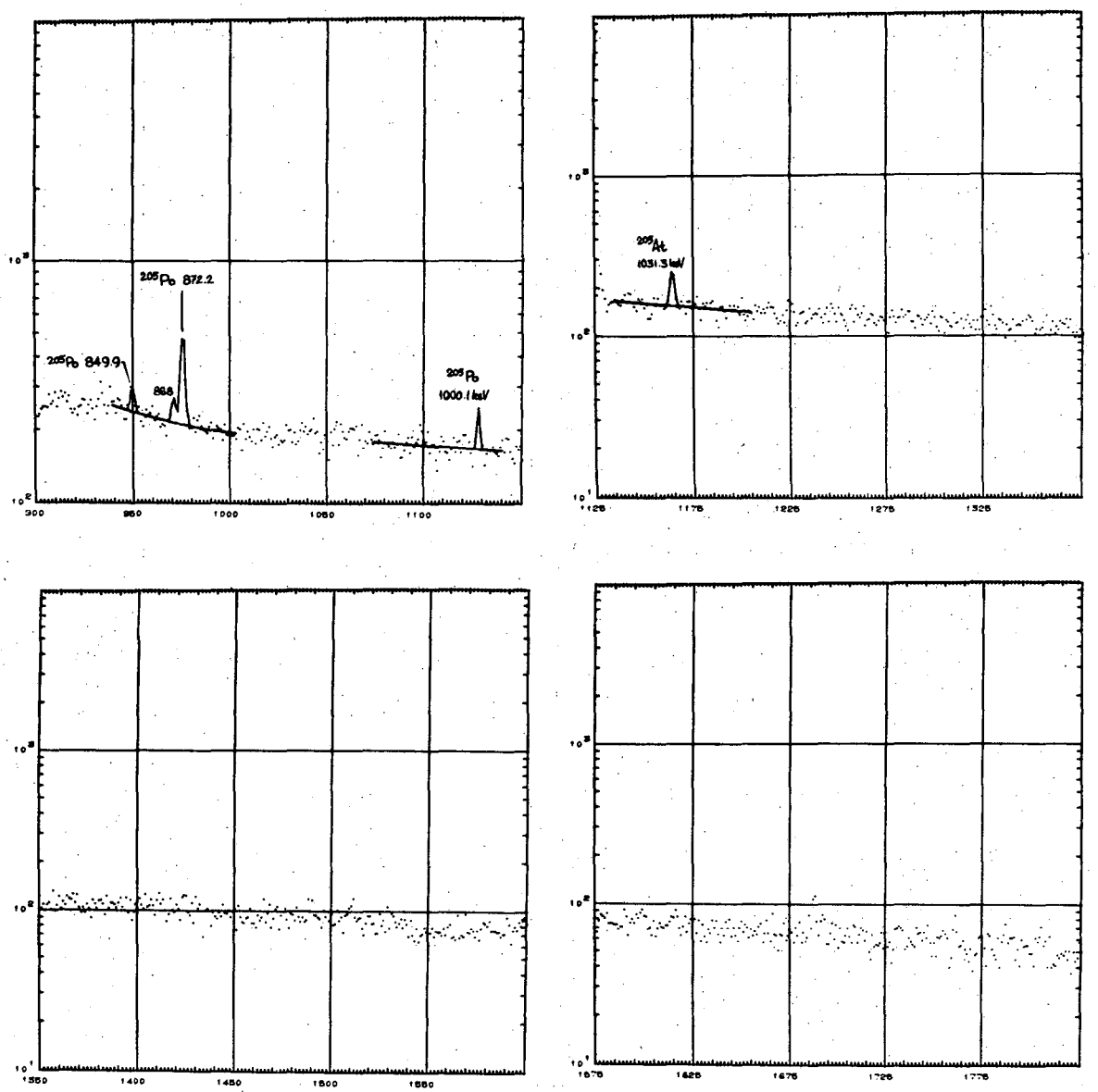

XBL 7011-7108

Fig. IV-1 (cont.)

Table IV-1. Relative intensities of gamma rays assigned to $^{206}At \rightarrow ^{206}Po$ decay.

Energy (keV)	Half-life (min)	Relative intensity
146.5 ± .3	31.4 ± 2.0	6.8 ± 0.6
394.7 ± .4	31.1 ± 0.7	53.0 ± 2.6
476.2 ± .4	30.5 ± 0.7	89.1 ± 6.3
699.7 ± .6	32.6 ± 0.7	100
Probably ^{206}At		
360.7 ± .5	31.0 ± 3.2	14.9 ± 1.3
383.5 ± .5	32.1 ± 3.5	15.3 ± 1.5

Table IV-2. Coincidence results for transitions observed in the decay $^{206}At \rightarrow ^{206}Po$.

Energy (keV)	Energy of gate (keV)				
	360.7	383.5	394.7	476.2	699.4
146.5					
360.7					
383.5					
394.7				x	x
476.2	?		x		x
699.7			x	x	

^{210}Po(Pru67) and ^{208}Po.(Tre68) Using known single-particle energies of the odd proton in ^{209}Bi, Hoff and Hollander(Hof58) calculated the two-proton level structure of ^{210}Po with a delta function force. It was assumed that the two protons beyond the closed 82-

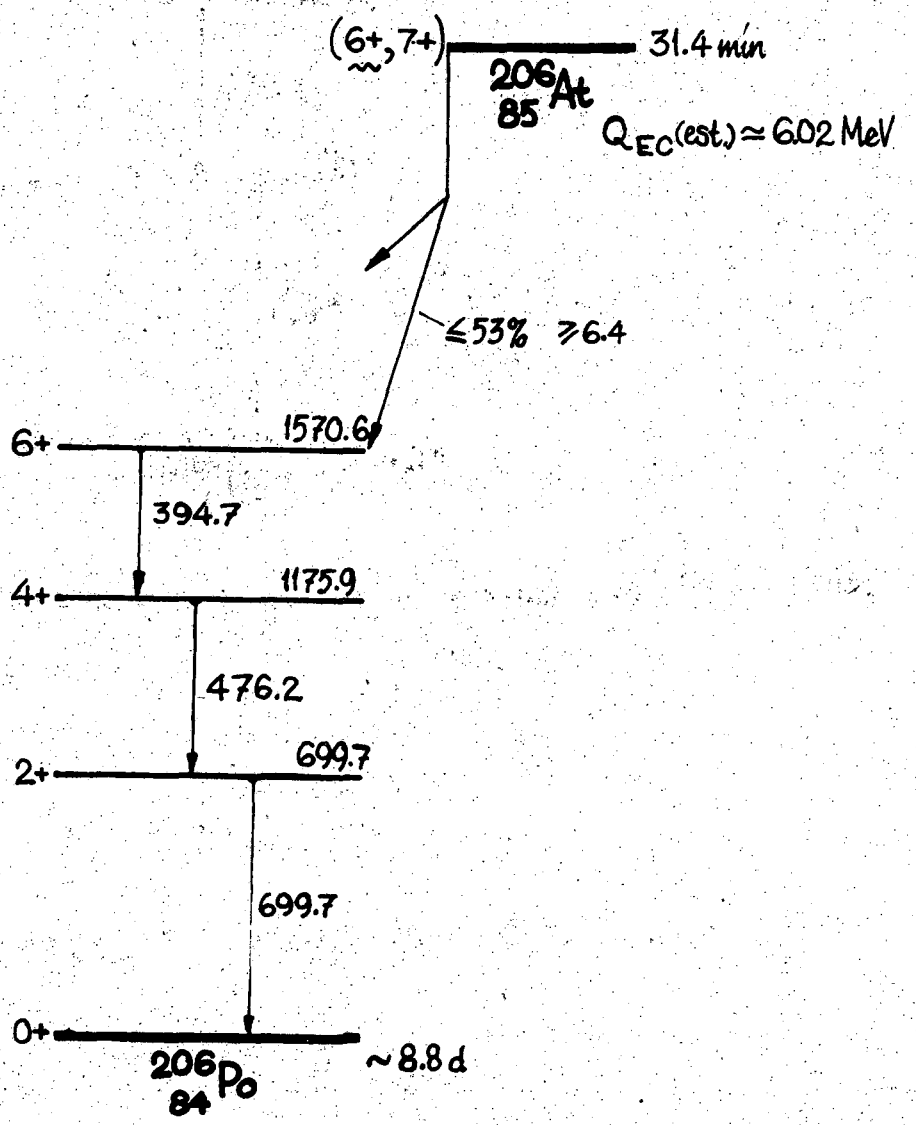

XBL 7011-7133

Fig. IV-2. Proposed decay scheme for $^{206}At \rightarrow {}^{206}Po$.

proton shell occupy the $h_{9/2}$ orbital in the ground state. Their calculations clearly predicted a ground state band of levels due to the coupling of the 83rd and 84th protons in the $(h_{9/2})^2$ configuration. The calculated energy values of these low-lying levels (2^+, 4^+, and 6^+) were in good agreement with the energies observed experimentally. The same low-energy ordering was established in ^{208}Po(Tre68) by measurement of gamma intensities and conversion coefficients. It is reasonable to expect the same $(h_{9/2})^2$ configurations to occur in ^{206}Po.

The ground state spin of the ^{206}At parent has never been reported. It can be predicted from the simple shell model. The ordering of the subshells near the closed shells at $Z = 82$ and $N = 126$ is shown in Fig. IV-3. The ground state of ^{206}At ($Z = 85$, $N = 121$) should then have the configuration $\pi(h_{9/2})^3$, $\nu(p_{1/2})^{-2}(f_{5/2})^{-3}$. The coupling of the unpaired $h_{9/2}$ proton and the $f_{5/2}$ neutron hole results in a probable ground state spin 7^+ according to Nordheim's weak rule. (See Ref. May 55.)

A ground state spin of 7^+ was, indeed, found to be consistent with the log $\underline{ft}$ values obtained for ^{208}At electron capture decay(Tre68) although other spin values could not be definitely excluded. The measured spin (Lin59) of the Bi isotone of ^{206}At (^{204}Bi with $N = 121$) is 6^+, which is not inconsistent with Nordheim's rule. Therefore we can state only that the ^{206}At ground state has a high spin, probably 6 or 7.

The Q value for ^{206}At electron capture decay has been estimated as 6.02 MeV, by using the mass table of Mattauch et al. (Mat65)

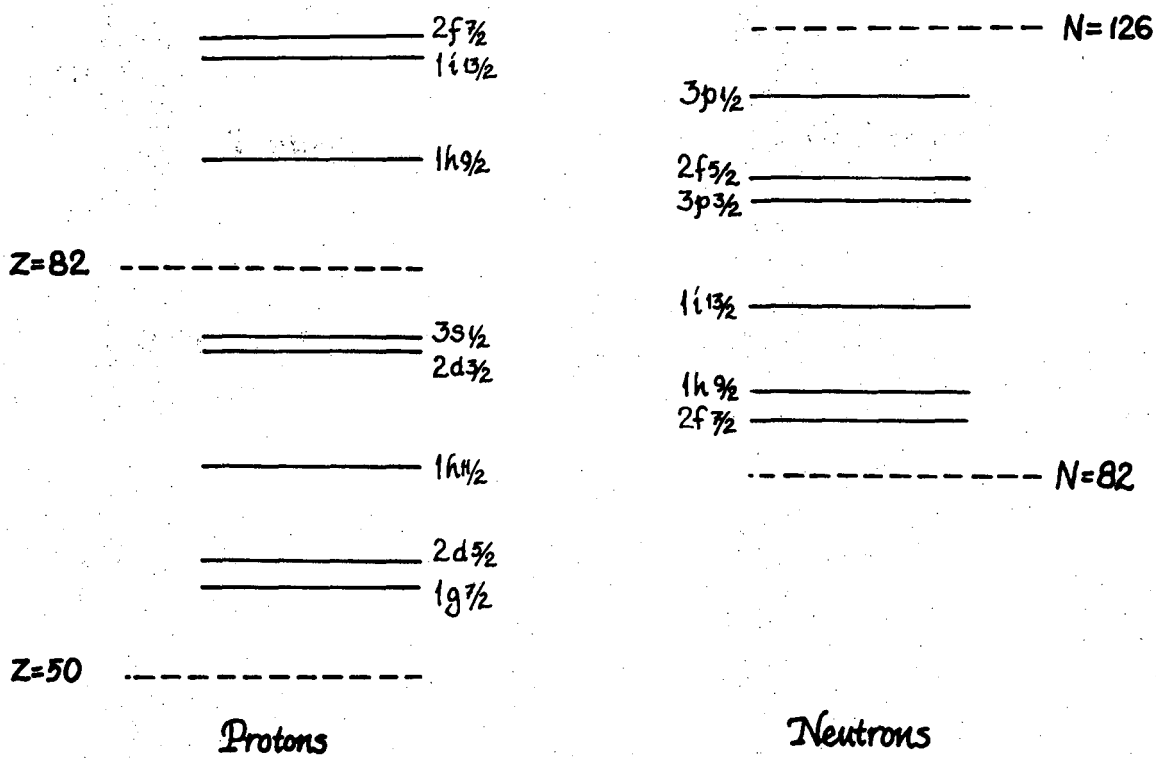

XBL 7011-7135

Fig. IV-3. Single-particle shell model states near the closed shells at Z = 82 and N = 126.

Because of the high intensities of the three prominent ^{206}At gamma lines, it can be concluded that the triple cascade is involved in the majority of decay events ($\geqslant 53\%$). Consequently these lines have been assigned to the $2^+ \rightarrow 0^+$, $4^+ \rightarrow 2^+$, and $6^+ \rightarrow 4^+$ level transitions. Due to the high spin of the ^{206}At ground state, direct decay to the ground or first few excited states of ^{206}Po (spin $< 6^+$) is very improbable. In order to explain the observed relative gamma intensities there must also be considerable electron capture decay to higher-lying states in ^{206}Po that subsequently de-excite by a series of gamma rays that (in part at least) proceed via the cascade to the ground state. A more detailed study of the high-energy gamma rays emitted in ^{206}At decay must be made before these higher-lying states will be seen. Certainly no other gammas of $> 10\%$ abundance were observed in the current experiments, which included the energy region up to 1500 keV.

If we assume that the 1570.6-keV 6^+ ^{206}Po level directly receives a maximum of 53% of the total ^{206}At electron capture decay, we obtain an estimate for the log $\underline{ft}$ value: 6.4. This value seems reasonable since the transition

$$[\pi(h_{9/2})^3 \nu(p_{1/2})^{-2}(f_{5/2})^{-3}]\, 6^+ \text{ or } 7^+ \rightarrow [\pi(h_{9/2})^2]\, 6^+$$

is forbidden because $\Delta\ell = 2$.

The 146.5-keV gamma transition has not been placed in the decay scheme. It was not observed to be in coincidence with any of the three intense lines in the triple cascade and may be a transition between some of the higher levels.

Previous information on the nuclear levels of ^{206}Po was obtained

by Yamazaki (Yam70) in an (α, xn) reaction on ^{204}Pb and by Thoresen (Tho66), who observed the three cascade gamma transitions in a study of the electron capture decay of ^{206}At. Yamazaki observed that the 395-, 476-, and 700-keV transitions (depopulating the 6^+, 4^+, and 2^+ members of the ground band) follow a decay of 160 ± 40 nsec. He postulated that this lifetime is due to the low energy $8^+ \rightarrow 6^+$ transition which was unobserved in his spectra. [In ^{208}Po this $8^+ \rightarrow 6^+$ transition is ~10 keV and highly converted; this 8^+ level is directly populated (Tre68) in ^{208}At decay (7%), supporting the 7^+ astatine ground state spin assignment.]

More intense study of this nucleus--particularly the high energy levels--should certainly prove to be interesting. Conversion studies, in particular a search for the low-energy $8^+ \rightarrow 6^+$ transition, would also be informative.

2. ^{204}At

The gamma transitions assigned to the decay of ^{204}At have been labeled in Fig. IV-1. Their relative intensities are listed in Table IV-3. The best value of the half-life was determined to be 9.2 ± 0.5 min. Half-life values found previously are 8.9 min (Tho63) and 9.3 min. (Hof63)

Gamma-gamma coincidence measurements (see Table IV-4) showed that the three intense gammas form a triple cascade analogous to that observed in ^{206}At. Gamma singles intensities indicate that the 425.0-keV transition is the first of the chain as shown in Fig. IV-4.

Table IV-3. Gamma rays observed in ^{204}At decay.

Energy (keV)	Half-life (min)	Relative intensity
425.0 ± 0.3	8.8 ± 0.3	75.7 ± 6.9
515.2 ± 0.3	9.9 ± 0.4	96.5 ± 6.7
608.0 ± 0.6	8.9 ± 1.0	19.3 ± 2.2
683.3 ± 0.5	8.8 ± 0.4	100

Table IV-4. Gamma-gamma coincidences observed in the decay ^{204}At → ^{204}Po.

Energy (keV)	Energy of gate			
	425.0	515.2	683.3	608.0
425.0		x	x	?
515.2	x		x	
608.0				
683.3	x	x		

The order of the 515- and the 683-keV gamma rays, however, remains rather ambiguous since both have the same intensity. A comparison with the decay scheme of ^{206}At suggests the order shown in Fig. IV-4. Yamazaki in ^{204}Pb(α, xn) reactions (Yam70) observed the same three transitions in ^{204}Po and placed them in the same tentative order. He found that all three followed a half-life of 190 ± 20 nsec, which he attributed to the unobserved 8^+ level, identical to the ^{206}Po situation.

The 608-keV gamma line has very tentatively been assigned to a

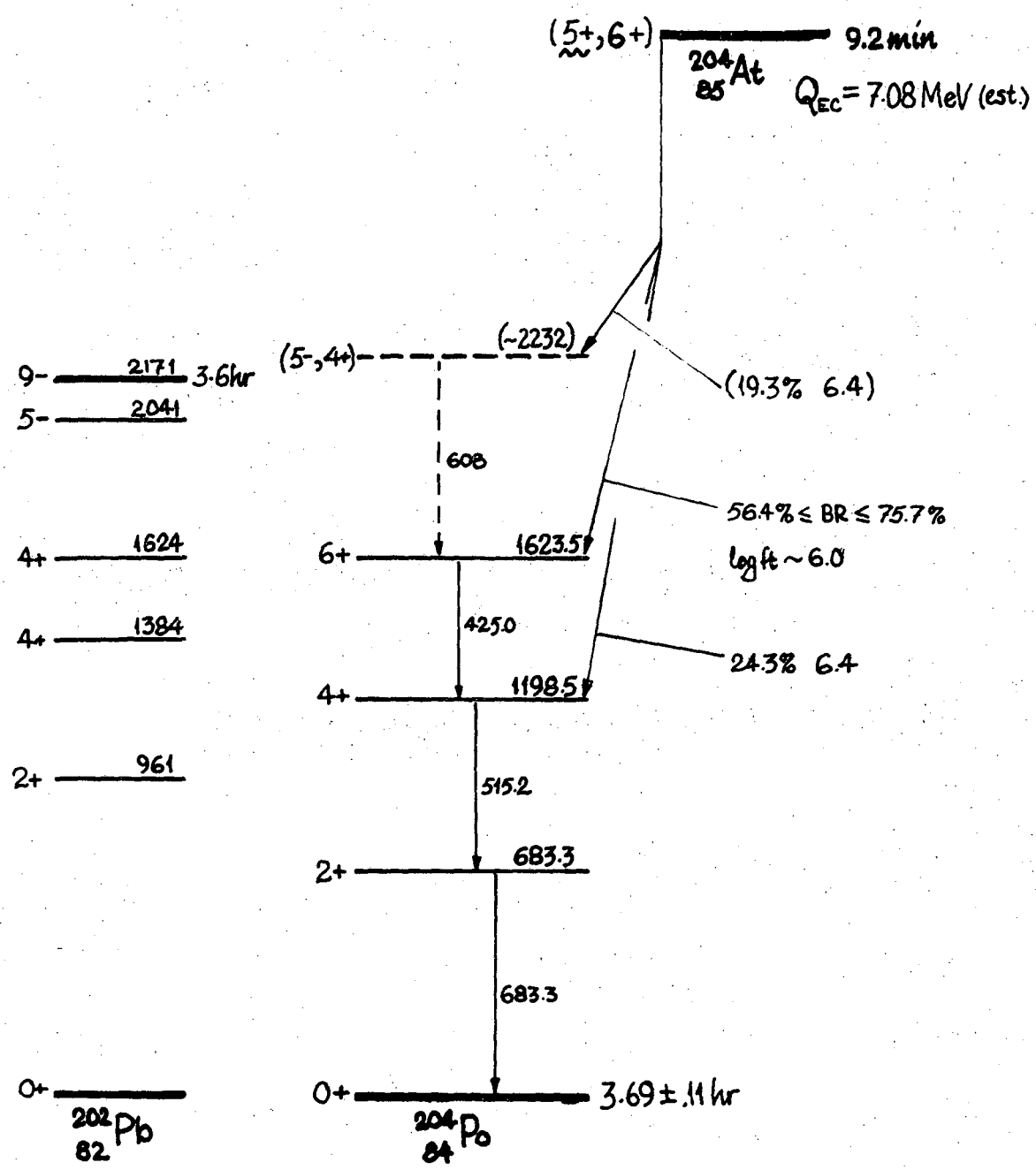

XBL 7011-7134

Fig. IV-4. Proposed decay scheme of ^{204}At. The level scheme of ^{202}Pb (N = 120) is shown for comparison.

level at 2232 keV. There are no coincidence data to support this assignment. Lacking evidence to the contrary, it is reasonable when one takes note of the 5^- (two-neutron) level in ^{202}Pb which is fed directly by ^{202}Bi electron capture decay.

The spin of the ^{204}At nucleus has not been measured. The shell model predicts a ground state configuration $\pi(h_{9/2})^3 \nu(p_{1/2})^{-2}(f_{5/2})^{-5}$ which would lead to a spin $\leq 7^+$. The bismuth isotone, ^{202}Bi (N = 119), has a measured spin of 5 (Lin59) with positive parity inferred. It is reasonable to expect the same sort of coupling to occur in ^{204}At.

Assuming there are no gamma transitions of intensity > 10 % from higher-lying unobserved ^{204}Po levels, the estimated log ft values are certainly good approximations. The estimated Q value for ^{204}At electron capture decay (95.5% of total decay) is 7.08 MeV (Mat65) If we include 19% decay to the 2232-keV level, there is 56.4% direct feeding of the 6^+ 1623.5-keV level (log ft = 6.0), and the remaining 24.3% of the decay leads directly to the 4^+ 1198.5-keV level (log ft = 6.4). If we assume the 608-keV gamma ray does not feed the 6^+ level then this level must receive 75.7% of the ^{204}At decay directly; this leads to a log ft value of 5.9. These log ft values are consistent with an ℓ forbidden transition, i.e.,

$$[\pi(h_{9/2})^3 \nu(p_{1/2})^{-2}(f_{5/2})^{-5}](5^+) \rightarrow [\pi(h_{9/2})^2 \nu(p_{1/2})^{-2}(f_{5/2})^{-4}]\, 6^+, 4^+, 5^-,$$

where an $h_{9/2}$ proton is converted into an $f_{5/2}$ neutron and $\Delta\ell = 2$. If this direct feeding of the 1198.5-keV 4^+ level is real, i.e., there is no substantial feeding of this level from higher-lying ^{204}Po states to

account for the observed intensity of the 515-keV transition, then this is evidence for a 5^+ ground state in ^{204}At. If the ground state spin were 6^+, the transition to the 4^+ level would be second forbidden and the log ft value would be much larger (> 10).

3. ^{202}At

Three gamma rays were assigned to ^{202}At (and/or ^{202m}At) decay on the basis of their half-lives. They are labeled in Fig. IV-5. The best half-life was determined to be 2.9 ± 0.3 min--not accurate enough to make any distinction between ^{202}At and its possible isomer ^{202m}At. The excitation functions or intensity as a function of ^{12}C beam energy varied in the same manner as that of the ^{202}Po gamma rays.

The relative intensities of the three gamma lines are shown in Table IV-5. These three undoubtedly represent the same triple cascade seen in the decay of both ^{204}At and ^{206}At. Intensity arguments indicate that the 441-keV gamma represents the $6^+ \rightarrow 4^+$ transition as seen in Fig. IV-6. The order of the remaining two transitions is ambiguous since their intensities are equal. However, in analogy to the level schemes of ^{204}Po and ^{206}Po, the order shown in Fig. IV-6 is reasonable.

^{200}Bi, the isotone of ^{202}At (N = 117), has a measured ground state spin of 7^+. (Lin59) This is difficult to explain on the basis of the extreme single-particle model. With a two-particle configuration the neutron spin must be $\geq 5/2$, since the proton is most likely to

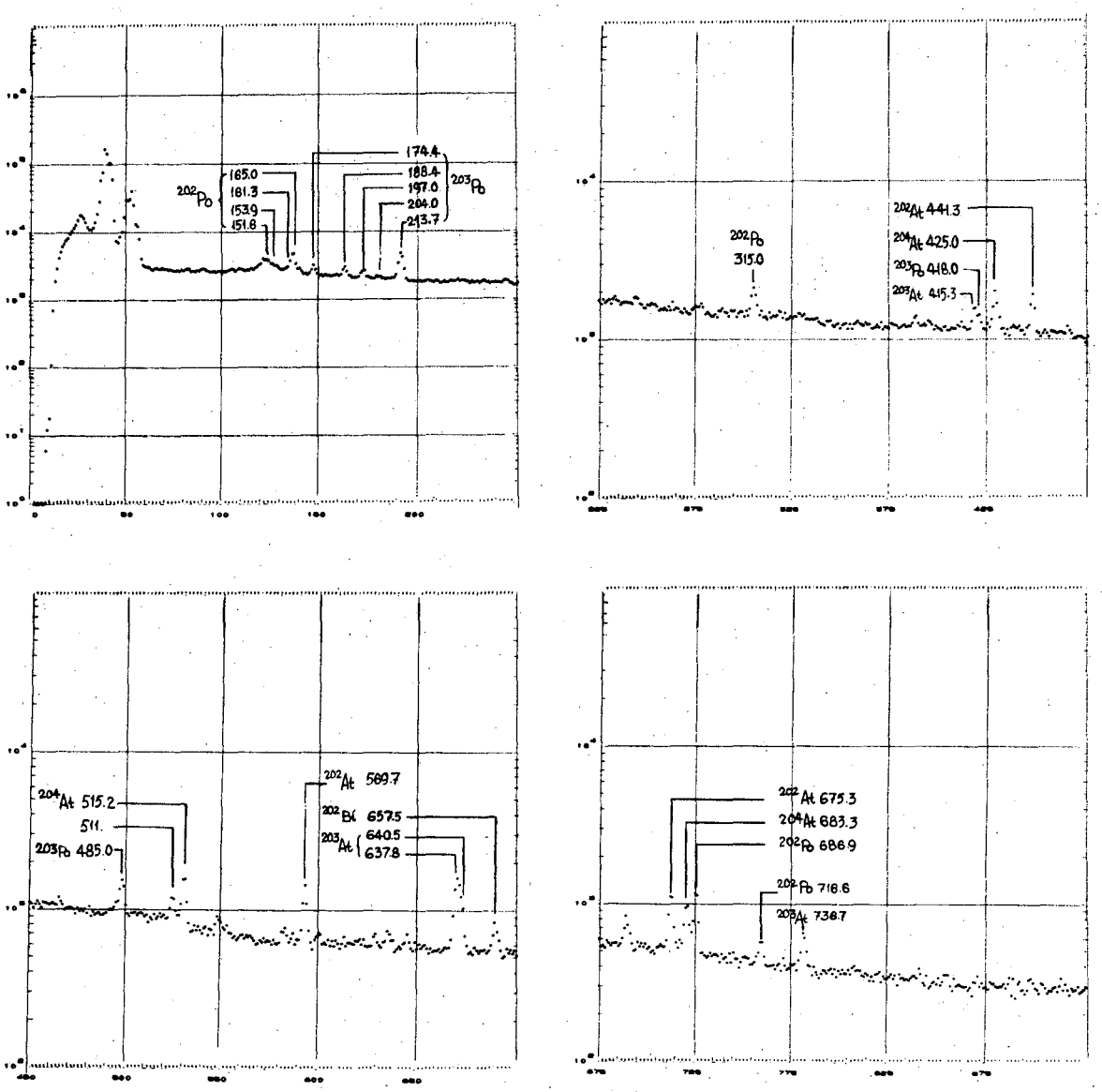

XBL 7011-7100

Fig. IV-5. Gamma spectrum of ^{202}At and ^{203}At (plus their Po daughters) obtained 12 minutes after bombardment of a 0.25 mil Au target with 108 MeV ^{12}C ions. These conditions maximize the ^{202}At concentration while still producing substantial ^{203}At.

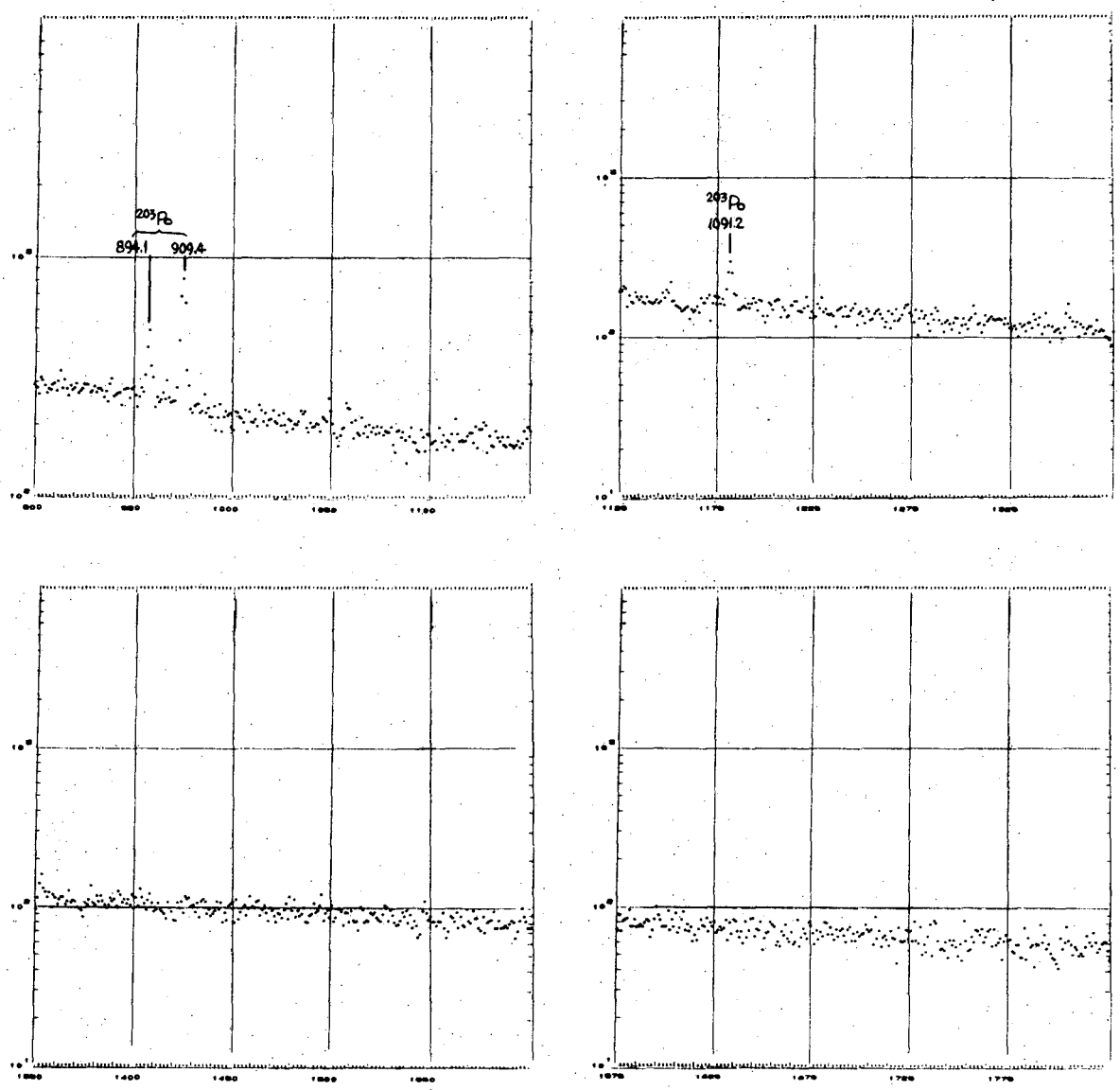

XBL 7011-7101

Fig. IV-5 (cont.)

Table IV-5. Gamma rays observed in ^{202}At decay.

Energy (keV)	Half-life (min)	Relative intensity
441.3 ± 0.3	3.2 ± 0.2	33 ± 2.5
569.7 ± 0.4	2.7 ± 0.3	94 ± 5
675.3 ± 0.5	2.8 ± 0.2	100

occupy an $h_{9/2}$ level. Therefore if the $f_{5/2}$ neutron level is empty, the odd hole must be in one of the levels $i_{13/2}$, $h_{9/2}$, or $f_{7/2}$. A more probable explanation is that there is an irregularity in the filling order of the neutrons so that there is a single neutron in the $f_{5/2}$ level and two holes in another level, e.g., the $p_{3/2}$ level. The spin value 7 would then be in agreement with Nordheim's weak rule. A similar configuration might be expected for ^{202}At, i.e.,

$$[\pi(h_{9/2})^3\, \nu(p_{1/2})^{-2}\, (f_{5/2})^{-5}\, (p_{3/2})^{-2}]\ 7^+.$$

However, one must keep in mind that the extreme single-particle model cannot really be expected to be a very good approximation so far from closed shells; ^{202}At has 9 neutron holes. The total spin might be formed by several particles in the unfilled particle levels.

4. Discussion

A similar decay pattern was found for all the even-mass astatine isotopes investigated. This is shown clearly in Fig. IV-7 where the excited states observed in their even-even polonium daughters are plotted as a function of neutron number.

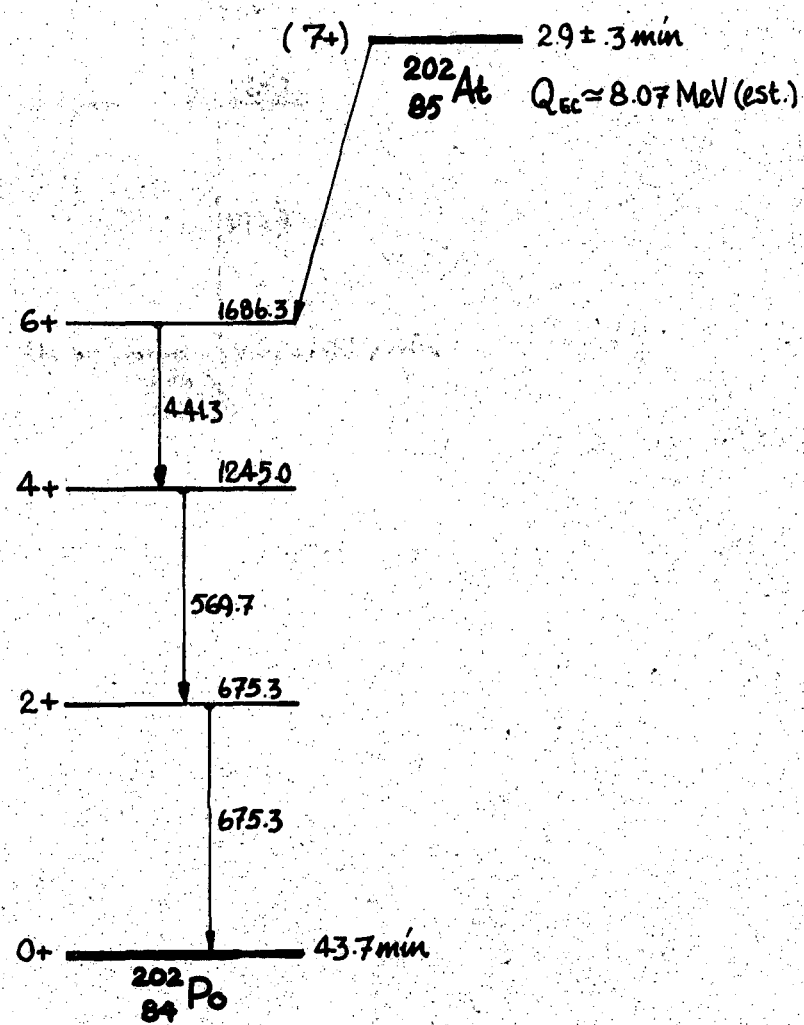

XBL 7011-7136

Fig. IV-6. Tentative decay scheme of ^{202}At.

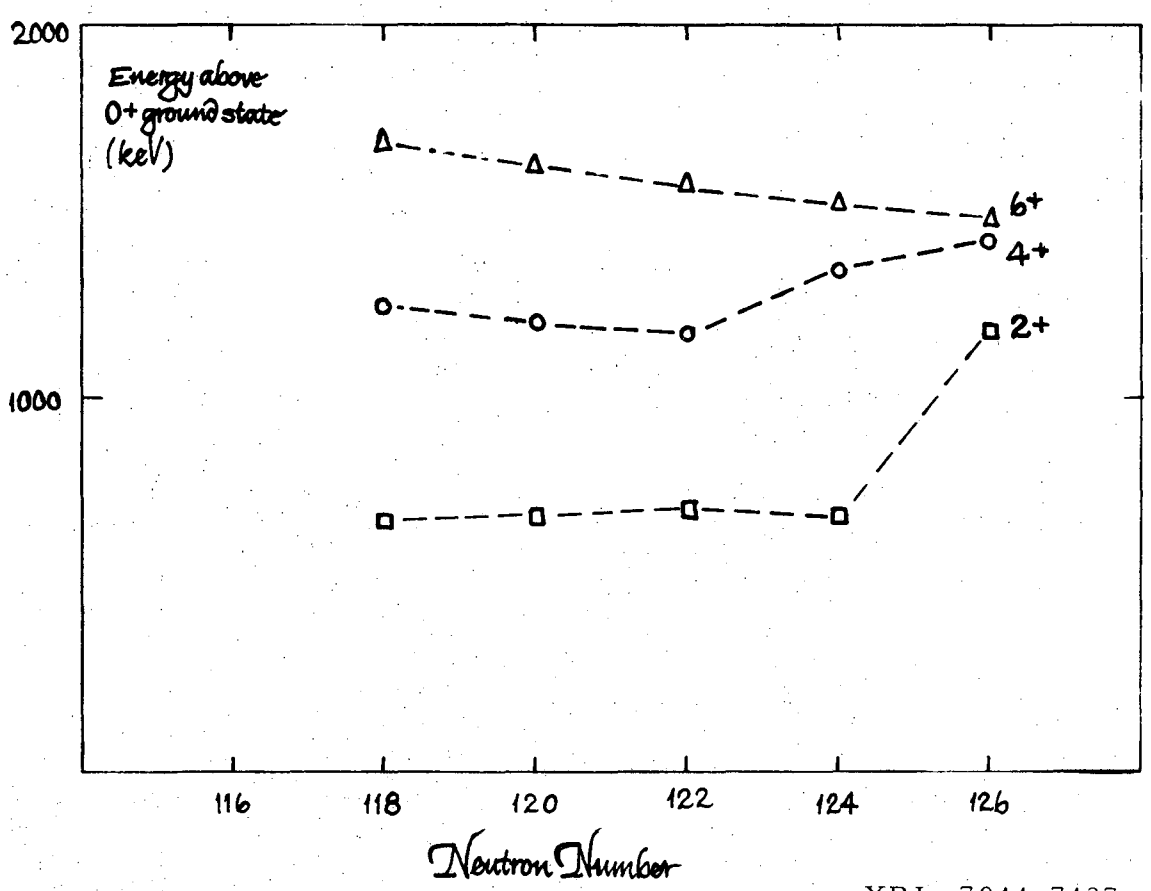

XBL 7011-7137

Fig. IV-7. Excited states of the even-even polonium nuclei, observed in the electron-capture decay of their astatine parents.

All the levels seem to exhibit very regular behavior. As the 126-neutron closed shell is approached, an increase in the energy of the first excited states is observed as one would expect.

The 2^+, 4^+, and 6^+ levels are all attributed to the coupling of the 83rd and 84th protons in the $(h_{9/2})^2$ configuration. Calculated values of the energy of these levels in ^{210}Po (Hof58) using known single-particle energies of the odd proton in ^{209}Bi were in good agreement with the energies observed experimentally. (Pru67) Unfortunately no calculations have been made for the lower-mass isotopes.

B. Odd-Mass Isotopes

1. ^{205}At

Previous studies of the excited states of the ^{205}Po nucleus (Lin57, Har62, Yam70) resulted in the level scheme shown in Fig. IV-8(a). Earlier this year Hopke et al. (Hop70) investigated the electron capture of ^{205}At to ^{205}Po and observed only a single gamma ray--the 718.8-keV transition. They deduced that the decay proceeded entirely to a ^{205}Po $9/2^-$ level at 718.8 keV with an estimated log *ft* value of 6.1.

In this present study several gamma transitions were assigned to ^{205}At decay on the basis of their half-lives. Figure IV-9 shows the decay curves of these gamma rays. The best value obtained for the half-life is 27.2 ± 0.6 min, compared to a value of 26.2 min reported previously. (Hof63) Again, positive identification of the weaker transitions was uncertain due to the similar half-lives of

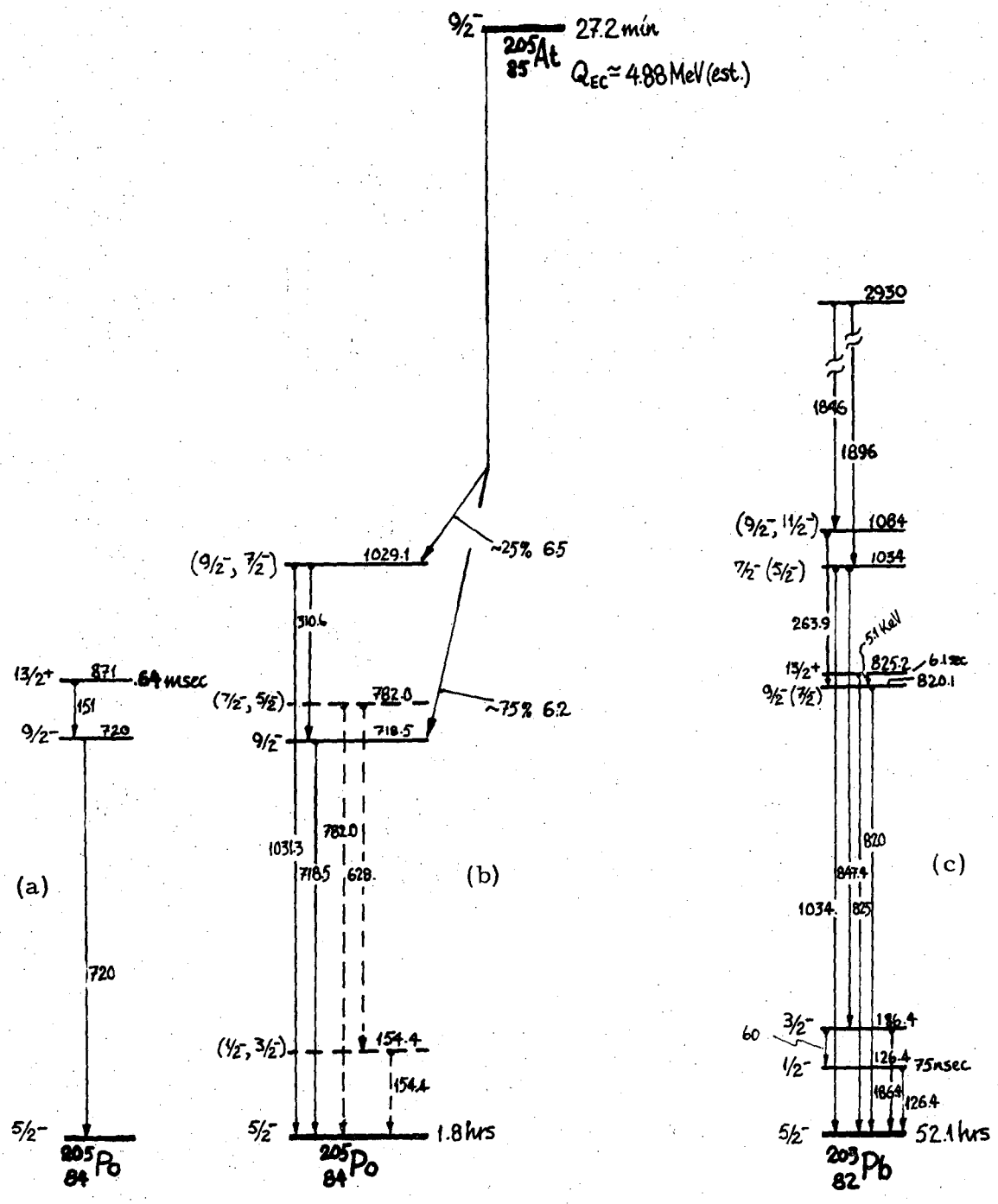

XBL 7011-7138

Fig. IV-8. Decay scheme of ^{205}At. (a) Level scheme of ^{205}Po daughter based on previous information derived from ^{204}Pb (α, xn) (Yam70) and ^{209}Bi(p, 5n)(Har62) reactions. (b) Decay scheme proposed for ^{205}At → ^{205}Po based on the results of this study. (c) Level scheme of ^{203}Pb (N = 121)(Sto60b, Doe68) included for comparison.

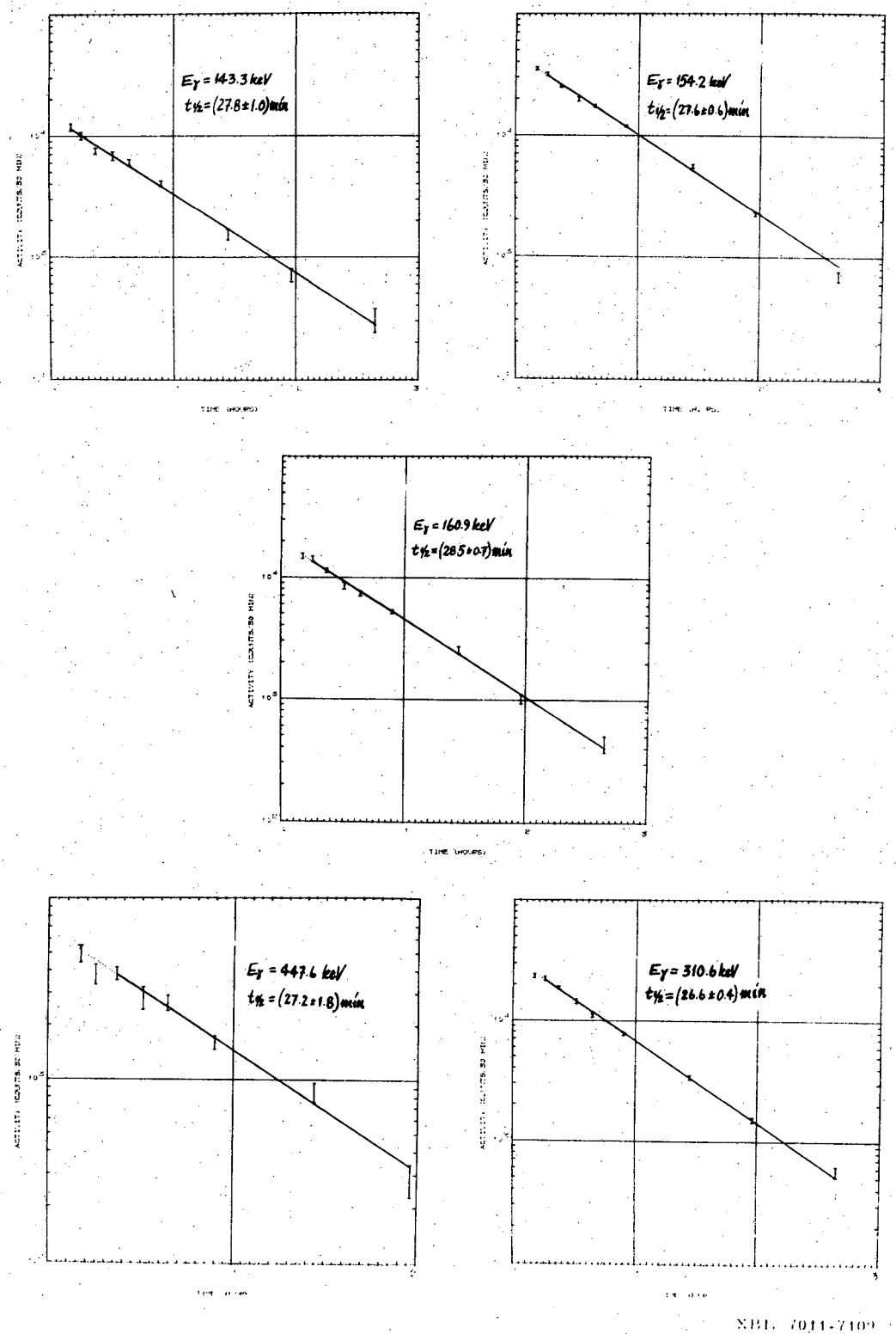

Fig. IV-9. Decay curves of gamma transitions assigned to ^{205}At decay.

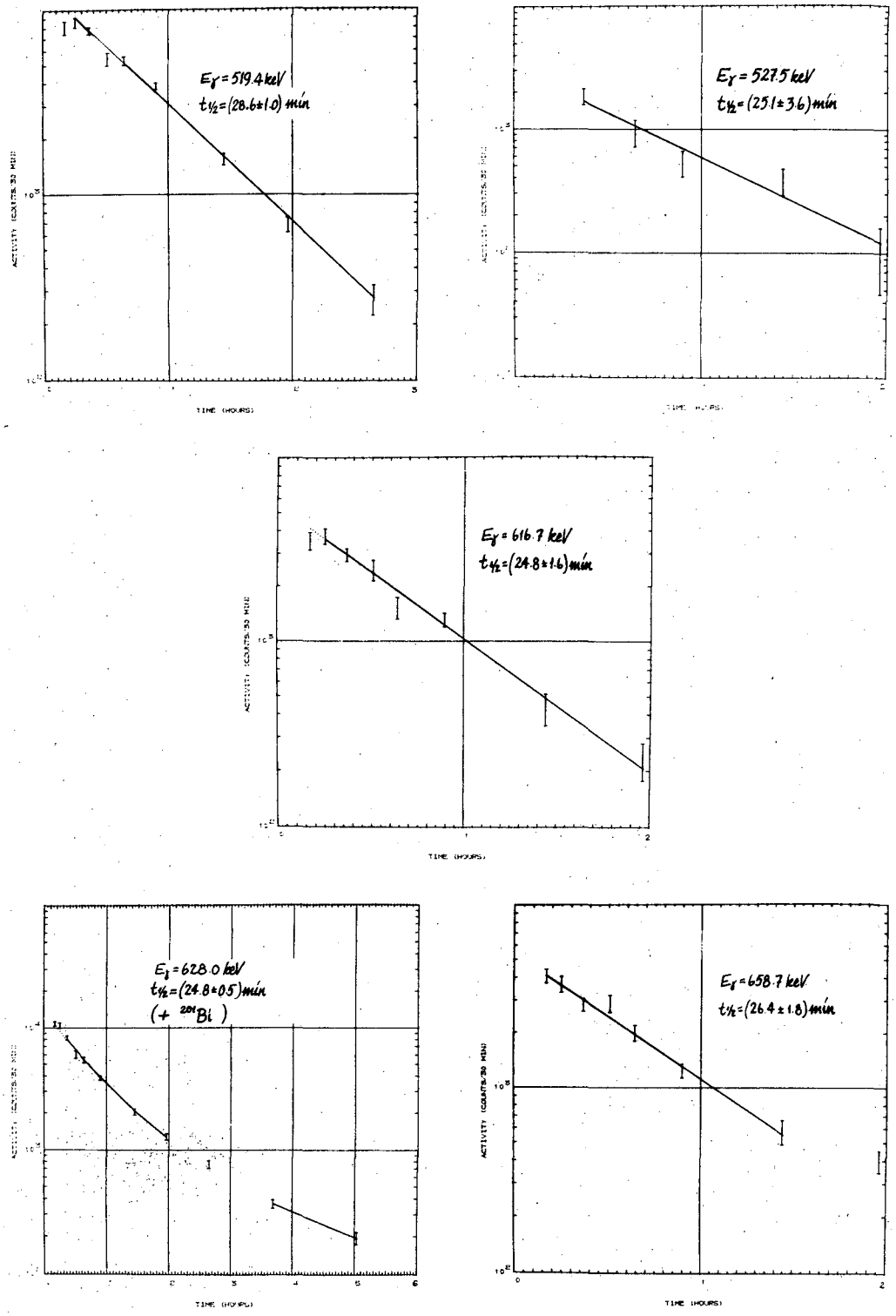

XBL 7011-7110

Fig. IV-9 (cont.)

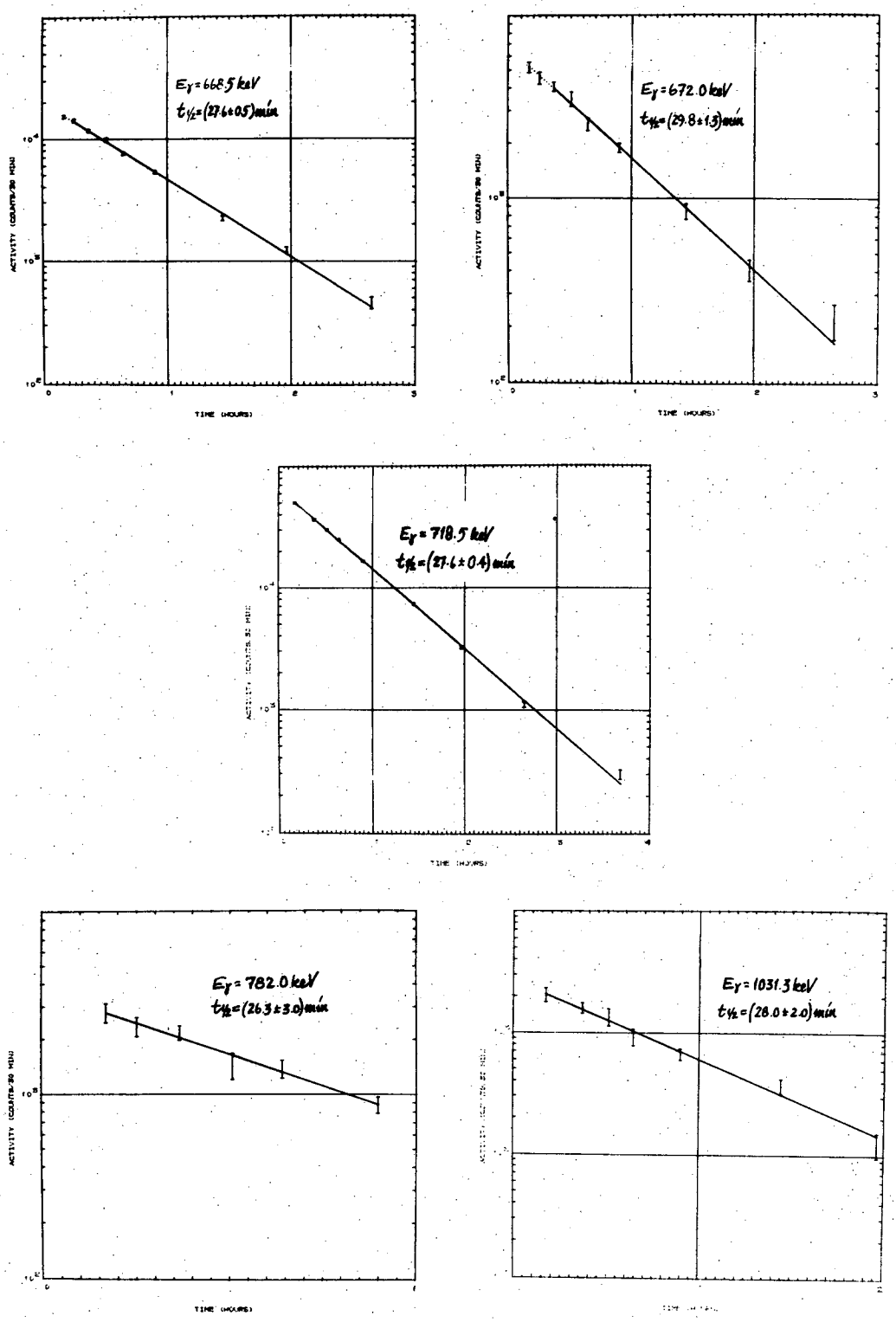

XBL 7011-7111

Fig. IV-9 (cont.)

^{205}At and ^{206}At. The observed spectrum is displayed in Fig. IV-1 and the results summarized in Table IV-6.

Table IV-6. Energies and intensities of gamma rays observed in ^{205}At decay.

Energy (keV)	Half-life (min)	Relative intensity
143.3 ± 0.3	27.8 ± 1.0	2.5 ± 0.2
154.2 ± 0.4	27.6 ± 0.4	7.6 ± 0.4
160.9 ± 0.3	28.5 ± 0.7	3.3 ± 0.2
310.6 ± 0.3	26.6 ± 0.4	13.1 ± 0.7
628.0 ± 0.7	24.8 ± 0.5	14.8 ± 0.7
658.7 ± 0.5	26.4 ± 1.8	7.6 ± 0.5
668.5 ± 0.6	27.6 ± 0.5	28.6 ± 1.7
718.5 ± 0.6	27.6 ± 0.4	100
782.0 ± 0.6	26.3 ± 3.0	6.7 ± 0.5
1031.3 ± 1.0	28.0 ± 2.0	7.6 ± 0.5
Probably ^{205}At		
203.0 ± 0.4	30.0 ± 3.5	1.8 ± 0.2
447.6 ± 0.4	27.2 ± 1.8	5.0 ± 0.4
519.4 ± 0.5	28.6 ± 1.0	12.5 ± 0.8
527.5 ± 0.4	25.1 ± 3.6	3.0 ± 0.3
616.7 ± 0.6	24.8 ± 1.6	6.9 ± 0.8
672.0 ± 0.8	29.8 ± 1.3	9.6 ± 0.7

Gamma-gamma coincidence measurements showed that the 310.6-keV gamma was in coincidence with the intense 718.5-keV gamma. Both of these were also in coincidence with K x rays. It seems likely that the 1031.3-keV line, which was in coincidence with K x rays only, represents the crossover to the ground state. The proposed decay scheme is presented in Fig. IV-8(b); the level scheme of the ^{205}Po isotone ^{203}Pb (N = 121) is also shown for comparison. Results of the coincidence experiment are summarized in Table IV-7.

Table IV-7. Coincidence results for transitions observed in the decay ^{205}At → ^{205}Po.

		Energy of Gate (keV)											
Energy (keV)	K x rays	143	154	161	311	519	628	658	668	672	718	782	1031
143.3													
154.2	x						x						
160.9													
310.6	x					x					x		
628.0	x		x										
658.7													
668.5	x												
718.5	x			?	x								
782.0													
1031.3													
447.6													
519.4	x												
527.5													
616.7			?										
672.0													
203.0									?	x			
K x rays	x	x	x	x	x	x	x	?	?	?	x	?	x

Electron capture to ^{205}Po accounts for 82% of ^{205}At decay; the remaining 18% is due to alpha decay to ^{201}Bi. Only one alpha group has been observed.(Hof63) It is presumably the ground state transition since both ^{205}At and ^{201}Bi have an odd $h_{9/2}$ proton. Consequently all the gammas observed in the decay of ^{205}At must be transitions between levels of ^{205}Po.

The transitions included in the ^{205}At → ^{205}Po decay scheme in Fig. IV-8(b) were all observed in coincidence with polonium K x rays. Some gamma lines, notably the 143.3-, 160.9-, and 519- keV transitions, although in coincidence with the K x rays, have not been placed in the decay scheme. The only intense gamma line not included in Fig. IV-8(b) is the 668.5-keV transition. It seems to belong to ^{205}Po but could not be fit into the level scheme. Conversion studies are definitely needed to determine the multipolarity of these transitions.

The ground state spin of ^{205}Po has been measured(Axe61) as 5/2 and negative parity has been inferred. This is consistent with the ground state configuration $\pi(h_{9/2})^2\,\nu(p_{1/2})^{-2}(f_{5/2})^{-3}$ predicted by the shell model. The ground state spin of ^{205}At should be $9/2^-$ due to the unpaired $h_{9/2}$ proton. Therefore we would expect no electron capture decay directly to the ^{205}Po ground state or to the previously observed $i_{13/2}$ excited state.

The presence of the 310-keV transition and its coincidence with the 718-keV gamma ray are firmly established. In analogy to the situation in ^{203}Pb, this 310-keV line is probably an M1 transition from a $9/2^-$ (or $7/2^-$) level to the $9/2^-$ level at 718.5 keV. Using the

conversion coefficient of 0.46 for a 310-keV M1 gamma[Sli65] and a Q value of 4.88 MeV for ^{205}At electron-capture decay, obtained from the Mattauch[Mat65] mass tables, we can estimate log ft values. The values obtained, 6.2 and 6.5 for decay to the 718- and 1030-keV levels, respectively, are not unreasonable for allowed transitions.

In estimating these log ft values, feeding of the 310- and 718-keV states by the decay of higher energy levels, as well as the direct ^{205}At electron-capture decay to other energy levels have been ignored. The intensity of any of these transitions must be small and their effect on the log ft values will likewise be small. For example, if we include some direct electron capture decay to the 782.0-keV level and balance the intensities accordingly, the log ft values change to 6.3 and 6.6 for decay to the 718.5- and 1030.2- keV levels.

If we assume that the first excited level is one of the low spin states, $1/2^-$ or $3/2^-$, seen in ^{203}Pb, there will not be any direct decay to this level. Intensity balance at the 154.4-keV level demands that the total intensity of the 154.4- and 628.0-keV transitions must be equal (since no feeding from higher levels has yet been observed). Reference to Table IV-6 shows that since the singles intensity of the 628-keV gamma ray is approximately twice the intensity of the 154.4-keV gamma line, half of the 154.4 keV transition must be converted (total conversion coefficient ~1). This corresponds to an E2 transition (calculated total conversion coefficient ≈ 1.2[Sli65] for a 154-keV gamma transition). A spin of $1/2^-$ is thus indicated for the 154.4-keV level. Again referring to the ^{203}Pb level scheme, the ^{205}Po 628-keV

transition is more apt to be an E2 than an M3 transition, supporting the spin assignment $5/2^-$ to the 782-keV level.

Conversion electron measurements are needed to confirm (or refute) these arguments. Both high-energy and low-energy (< 100-keV) gamma measurements should be fruitful in filling in the remainder of the ^{205}At decay scheme.

2. ^{203}At

In the course of gamma measurements of the decay of ^{203}Po and ^{202}Po, some gamma lines were assigned to their astatine parents. No coincidence studies were made, so decay schemes are very tentative.

An intense gamma line at 637.8 keV was found to decay with a half-life of 7.3 ±0.3 min and was, therefore, assigned to ^{203}At. A shoulder on this gamma line, at 640.5 keV, (Fig. IV-5) was found to decay with approximately the same half-life and it was also assigned to ^{203}At. Two other gamma transitions were also identified as belonging to ^{203}At → ^{203}Po decay. The decay of all four assigned gamma rays is shown in Fig. IV-10 and their relative intensities summarized in Table IV-8. The intensity of each gamma varied as a function of bombarding energy in the same manner as did the ^{203}Po gamma intensities, thus supporting the mass assignment.

A tentative decay scheme is shown in Fig. IV-11. The estimated Q value for ^{203}At electron capture is 5.82 MeV.[Mat65] The astatine ground state most likely has spin and parity $9/2^-$ due to the odd $h_{9/2}$ proton; the ground state spin of ^{203}Po has been measured to be

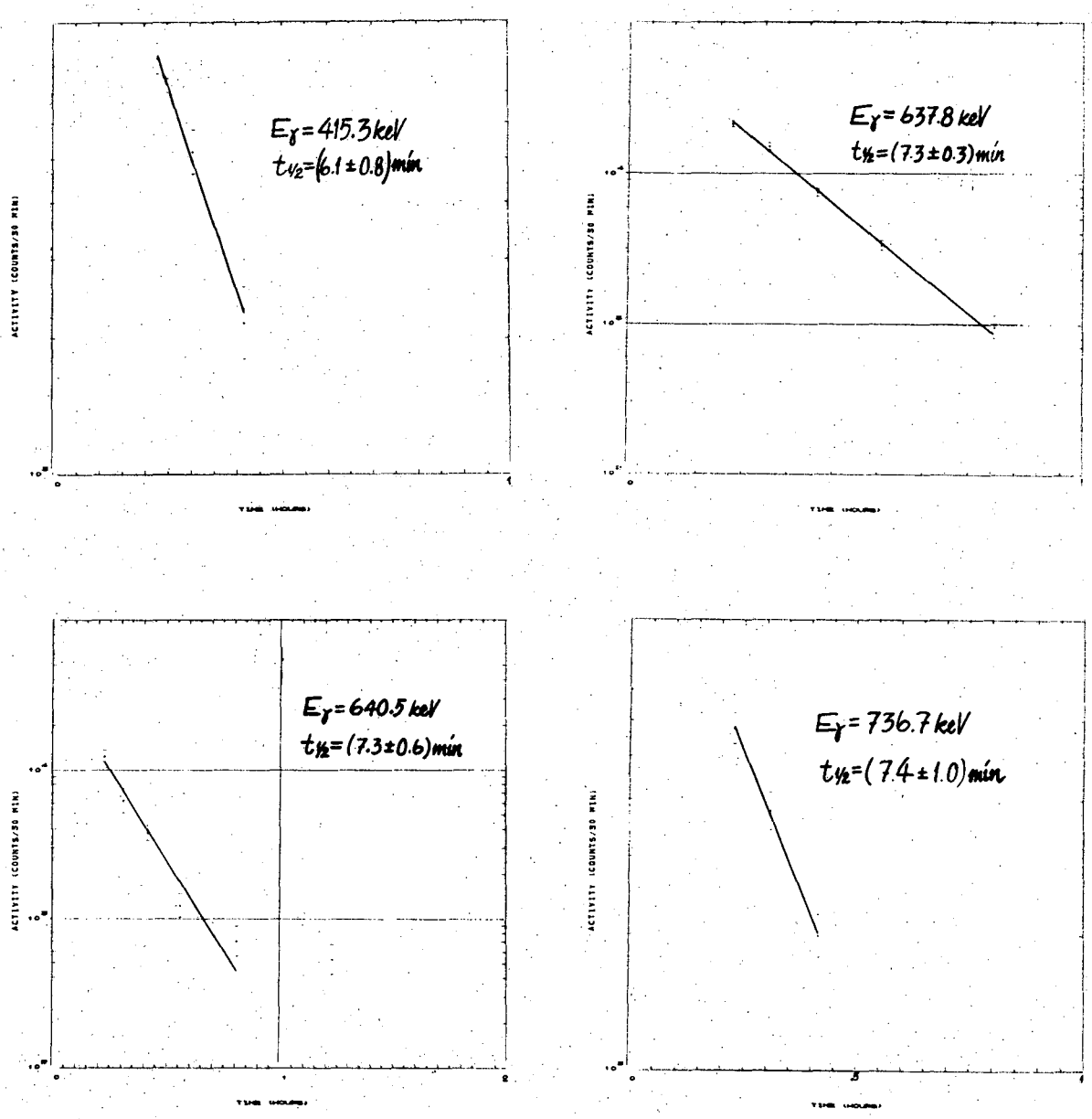

XBL 7011-7112

Fig. IV-10. Decay curves of the four gamma transitions assigned to ^{203}At decay.

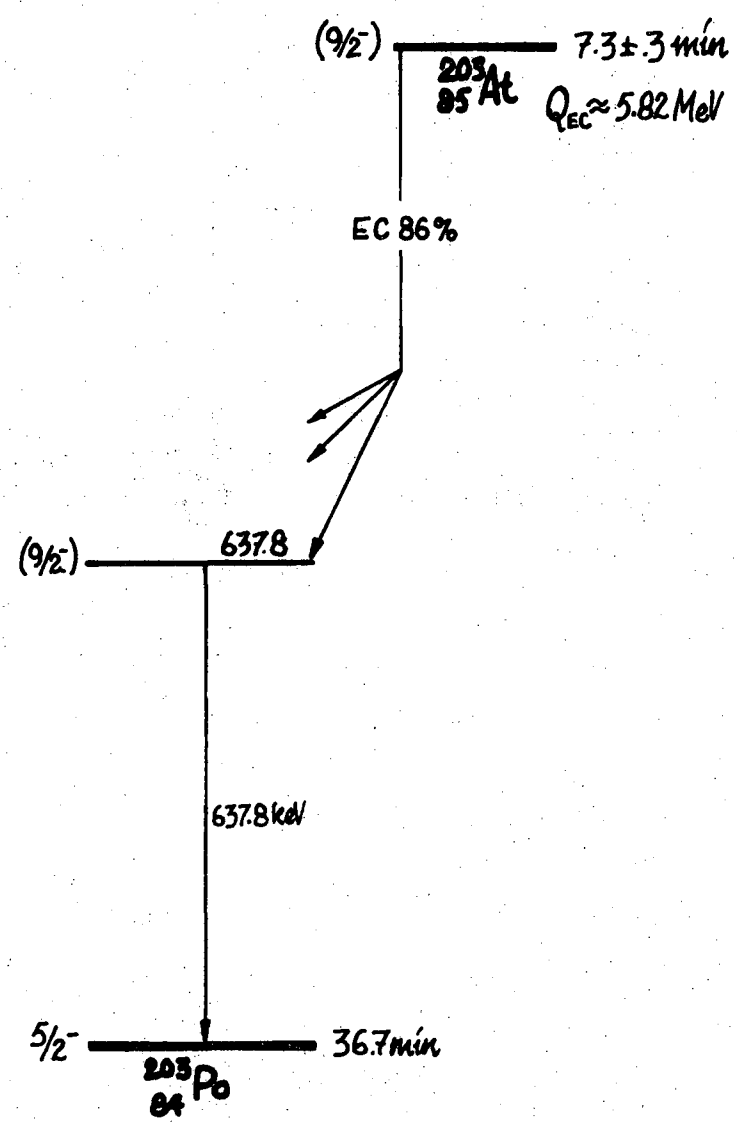

XBL 7011-7139

Fig. IV-11. Tentative decay scheme of ^{203}At.

Table IV-8. Gamma rays observed in ^{203}At decay.

Energy (keV)	Half-life (min)	Relative intensity
415.3 ± 0.4	6.1 ± 0.8	23 ± 3
637.8 ± 0.5	7.3 ± 0.3	100
640.5 ± 0.7	7.3 ± 0.6	52 ± 5
736.7 ± 0.6	7.4 ± 1.0	35 ± 4

$5/2^-$. (Axe61) The 637.8-keV gamma probably represents the E2 transition from the $9/2^-$ excited level to the ^{203}Po ground state--the analog to the 718-keV gamma observed in ^{205}At decay. The other three gammas cannot be placed in the decay scheme without further information--coincidence and conversion measurements.

3. Discussion

The decay of the two odd-mass astatine isotopes studied, ^{205}At and ^{203}At, is characterized by direct feeding of at least one $9/2^-$ level in the polonium daughters. This level is then de-excited by an intense gamma transition to the $5/2^-$ ground state.

The information obtained is summarized in Fig. IV-12 where the observed energy levels are plotted as a function of neutron number. The $9/2^-$ level of the odd-mass Pb isotopes is included for comparison.

The energy levels seem to behave quite regularly. The $13/2^+$ levels of ^{203}Pb (N = 121) and ^{205}Pb (N = 123) are only 5 and 26 keV, respectively, above the $9/2^-$ levels, whereas in polonium these levels

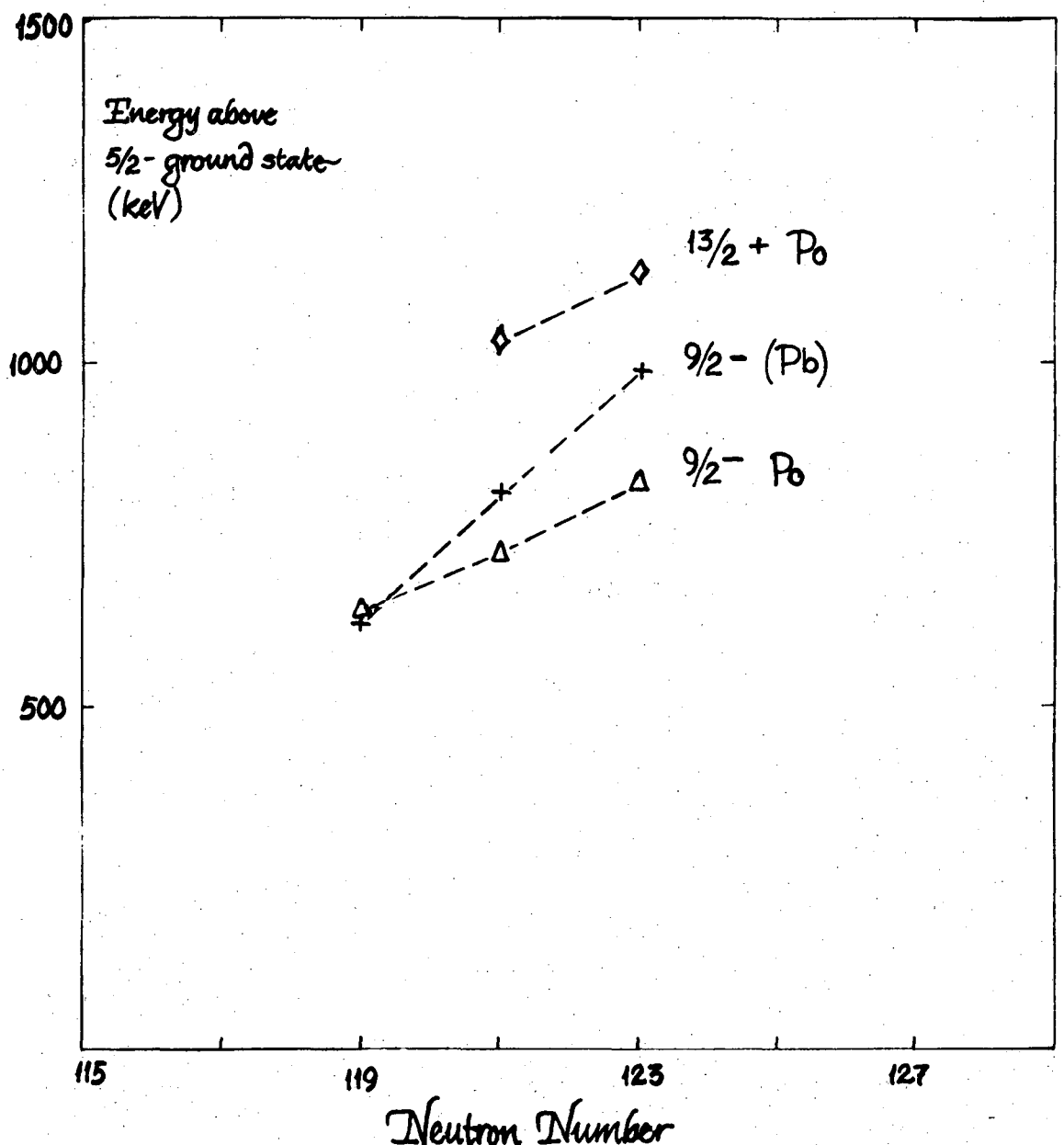

XBL 7011-7141

Fig. IV-12. Experimentally observed excited states of odd-mass Po and Pb isotopes.

are seen to be more widely spaced.

C. Lower Mass Isotopes

Due to their short half-lives, no direct studies of the astatine isotopes with mass A < 202 were made. However, the decay of their daughters was measured. In the course of measuring the gamma spectrum of a target irradiated with a beam energy of 119 MeV, a 571.0-keV gamma was observed to decay with a half-life of ~1 min. It must belong either to ^{201}At or ^{200}At decay.

Reference to Fig. IV-12 indicates that the $9/2^-$ level of ^{201}At might be expected at about 570 keV. The first excited state in ^{200}At--the 2^+ level--will probably appear at about 650 keV (Fig. IV-7) if the regularity of this level continues down to 116 neutrons. On this basis we would propose that the observed 571-keV transition represents the $9/2^-$ to $5/2^-$ ground state transition in ^{201}At. Since these nuclei have so many neutron holes, however, we cannot be completely sure that the level energies determined for the heavier isotopes can be legitimately extrapolated.

V. RESULTS: DECAY OF POLONIUM ISOTOPES

A. Odd-Mass Isotopes

1. ^{205}Po

^{205}Po has a sufficiently long half-life (1.8 hr) that it can be made without many interfering radiations. Two kinds of runs were made. In both, a 0.25-mil gold foil target was bombarded with 74-MeV ^{12}C ions (5.25-mil Al absorber) to maximize the ^{205}At concentration. The astatine was evaporated from the target and collected. In the first runs the gamma singles measurements were begun immediately and the growth of the ^{205}Po radiations could be observed. In later runs the astatine was allowed to decay for an hour to allow the ^{205}Po daughter to reach its maximum growth. The remaining astatine was removed by heating; the polonium was dissolved off the plate with HNO_3 and deposited onto the center of a 1 in. Pt disk (within a circle of diameter 0.5 cm).

The Pt disk was then mounted in the sample holder described in Section III and both singles and gamma-gamma coincidence data taken. The singles spectrum measured 1.4 hr after bombardment is shown in Fig. V-1. ^{204}Po is the primary contaminant, while longer-lived bismuth and lead isotopes are also observed growing in. A low-energy spectrum was also obtained with the Si(Li) detector and showed only the 25.3-keV gamma which decayed with the half-life of ^{205}Po.

The ^{205}Po data obtained from these singles spectra are given in Table V-1 and the coincidence data are summarized in Table V-2.

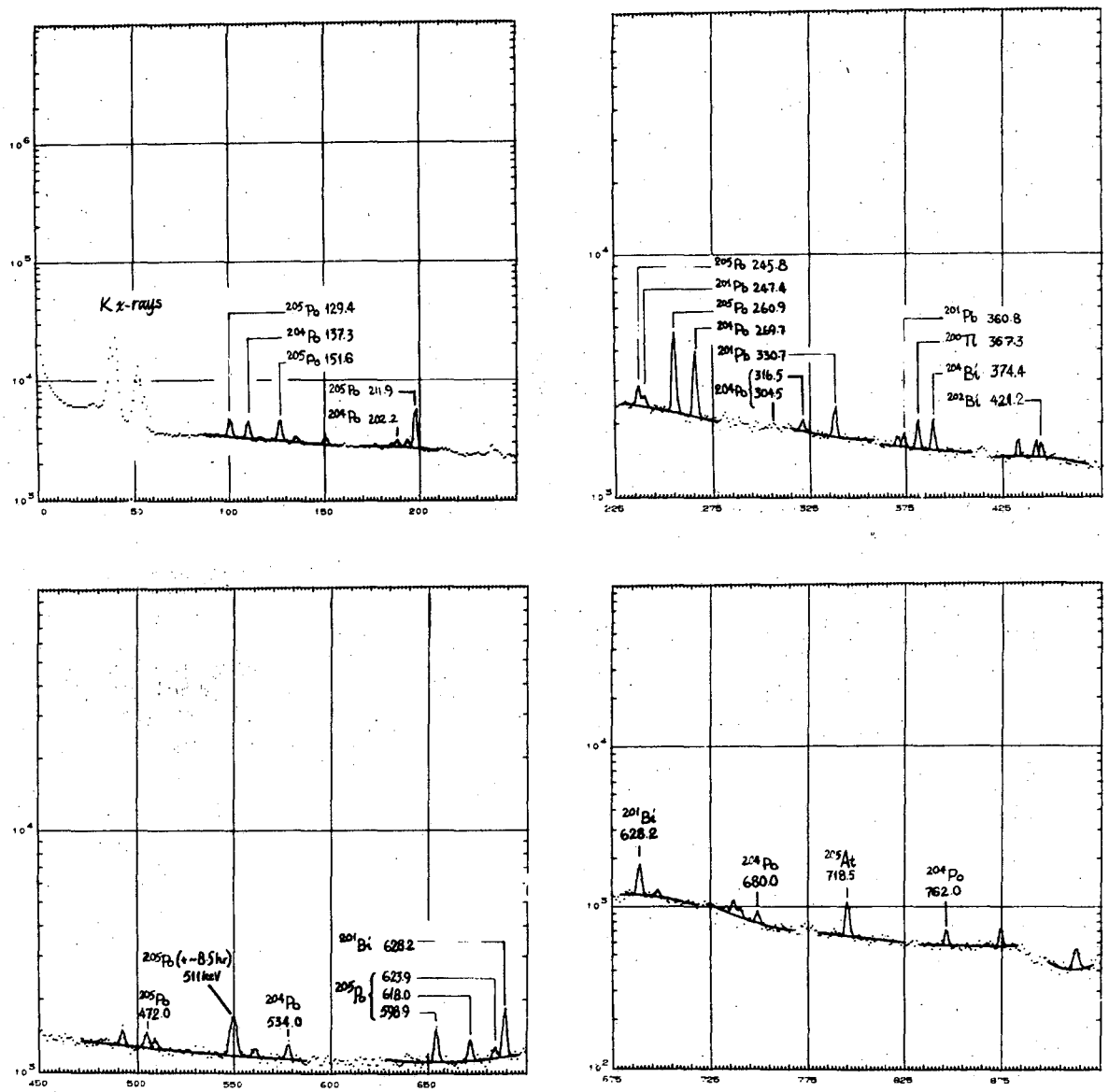

XBL 7011-7104

Fig. V-1. Gamma spectrum of ^{205}Po (+ ^{204}Po). The target was 0.25-mil Au foil bombarded with 74-MeV ^{12}C ions. The sample was allowed to decay 1 hr to allow for maximum growth of the 1.8-hr ^{205}Po from its ~27-min At parent. The remaining At was removed by heating; the Po was dissolved off the plate with HNO_3 and transferred to a Pt disk for gamma measurements.

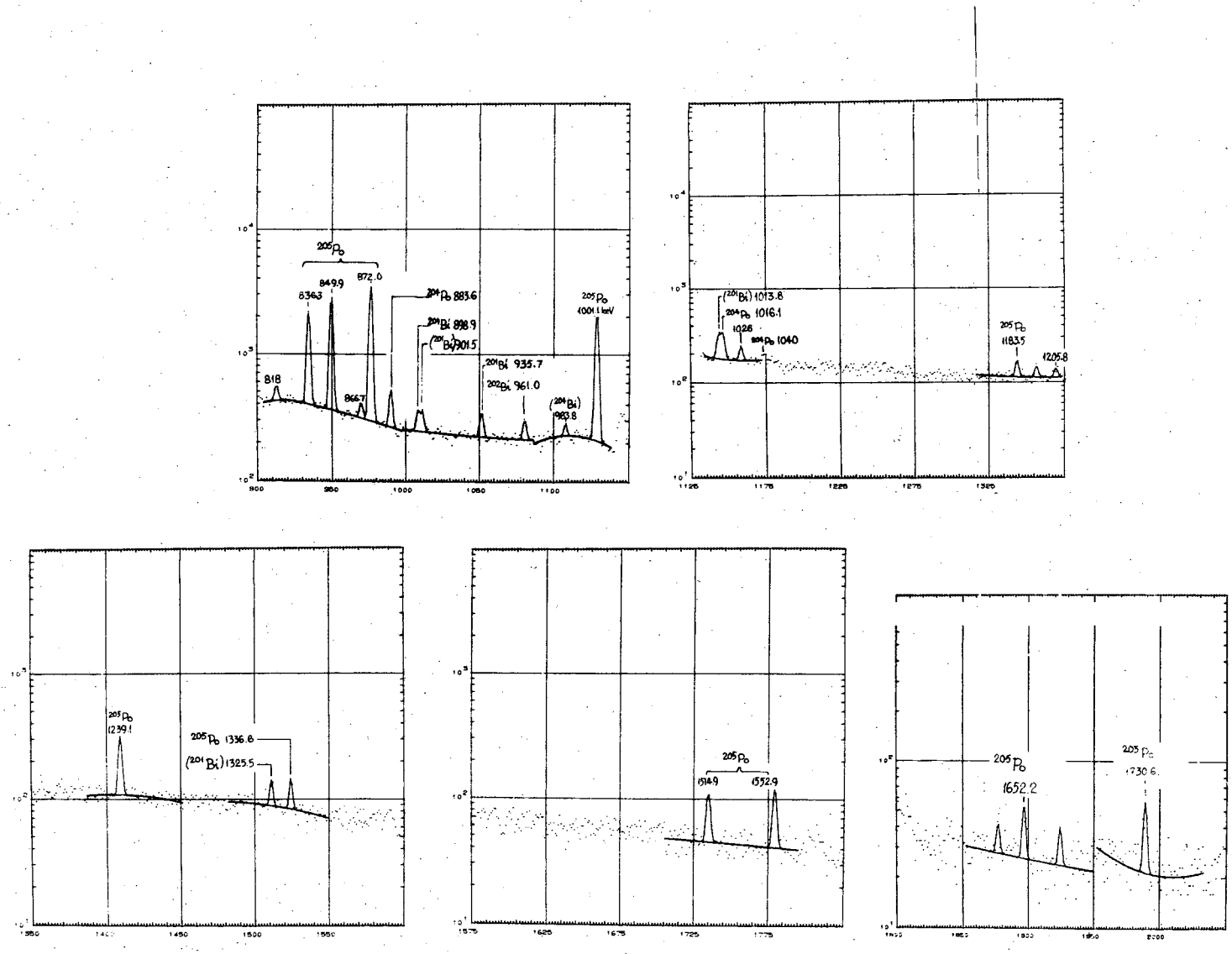

XBL 7011-7105

Fig. V-1 (cont.)

Table V-1. Energy and intensity of gamma transitions observed in $^{205}Po \rightarrow {}^{205}Bi$ decay.

Energy (keV)	I_γ	K-conversion coeff.[a]	K/L ratio[a]	Multipolarity[a]	I_T[c]
25.3±0.15	0.7±.15	~5[b]		(E1)[b]	6.8±1.4
129.4±0.4	2.9±.2	5.6 ±1.2	6	M1	21.8±3.5
151.6±0.4	3.0±.2	3.1 ±0.6	6	M1	13.8±2.5
211.9±0.4	8.0±.5	0.25 ±0.03	2.0	E2+ 15% M1	11.6±1.5
245.8±0.7	2.0±.3	0.25 ±0.15		(E2)	2.7±0.9
260.9±0.3	9.4±.6	0.59 ±0.06	5.5	M1	16.0±1.9
472.0±0.6	2.7±.3	0.031 ±0.006		E2	2.8±0.6
511.0±0.5	5.3±.5				~5.4±0.7
598.9±0.7	6.3±.4	0.014 ±0.003		E2	6.4±1.3
613.0±0.7	4.0±.2	0.065 ±0.009	5	M1	4.3±0.7
623.9±0.7	2.4±.2	0.15 ±0.02	4	M2	2.8±0.5
836.3±0.5	50.7±2.0	0.0034±0.0003		E1	51.0±2.6
849.9±0.5	71.0±2.8	0.020 ±0.002	6	M1+ 8% E2	72±8
872.2±0.5	100	0.007 ±0.0007	6	E2	101
1001.1±0.5	78.6±3.2	0.012 ±0.001	6	M1+ 7% E2	79±7
1183.5±0.7	2.7±.2	0.011 ±0.002		M1	2.7±0.4
1239.1±0.6	12.6±.6	0.0066±0.0010		M1+ E2	12.7±0.7
1336.6±0.8	3.1±.4	0.002 ±0.001		E1	3.1±0.4
1514.9±1.0	5.2±.7				5.2±0.7
1552.9±1.0	6.9±.6				6.9±0.6
1652.0±1.2	2.7±.5				2.7±0.5
1730.6±1.5	4.1±.6				4.1±0.6

[a]All values for K-conversion coefficients, K/L ratios, and derived multipolarities are taken from the experimental results of Ref. Alp69 unless otherwise noted.

[b]The total intensity of the 25.3-keV gamma required by intensity balance was 7. This implied an E1 transition and the K-conversion coefficient is a theoretical value from Sliv and Band.[(Sli65)]

[c]$I_T = (1 + \alpha_K + \alpha_L + \alpha_M + \cdots) I_\gamma$ where α_L were theoretical values obtained from the table of Sliv and Band,[(Sli65)] and $\alpha_M + \alpha_N + \cdots = 0.3\,\alpha_L$.

Table V-2. Summary of observed gamma-gamma coincidences in $^{205}Po \rightarrow {}^{205}Bi$ decay.

	Energy of gate (keV)												
Energy (keV)	129	151	212	261	472	511	599	624	836	849	872	1001	1239
129.4								?			x		
151.6										x			
211.9				x						x			
245.8													
260.9			x		?		x	x	x		x		
472.0													
511.0	x	x	x	x		x		x			x		
598.9													
613.0													
623.9			?							?			
836.3				x							x		
849.9		x											
872.2	x		x	x	?		x	?	x				
1001.1													
1183.5													
1239.1													
1336.6													

The best value obtained for the half-life of ^{205}Po is 1.80 ± 0.04 hr—the same value listed in the Table of Isotopes.(Led67) The relative intensity of the 25.3-keV gamma line is only approximate, since it was calculated from the relative intensities of the Bi K x rays in the low- and higher-energy spectra.

No conversion-electron studies were made during the current work. Two simultaneous investigations, however, have included conversion measurements. The values for the K conversion coefficients,

K/L ratios, and the multipolarity assignments based on them in Table V-1 have been taken from the results of Alpsten and Astner.[Alp69] Identical multipolarities were assigned to these ^{205}Po transitions by Hopke, Naumann, and Spejewski[Hop69] on the basis of their measured electron intensities.

The ^{205}Po decay scheme constructed from the data in Table V-1 is shown in Fig. V-2. It is clear from the coincidences that the 261-, 836-, and 872-keV transitions form a triple cascade. Both singles and coincidence intensity considerations require the sequence to be as shown in Fig. V-2.

The ^{205}Bi ground state spin has been measured as $9/2^-$.[Lin59] Level spins have been assigned from multipolarities and by analogy with the ^{207}Po decay scheme.[Arb58, Hop69, Ast70] Thus the 1708.4-keV level is assigned spin and parity $3/2^+$, whereas the level at 1969.3 keV is assigned spin and parity $5/2^+$. To accommodate the 261-212-624(?)-872 keV coincidence sequence we have placed a level at 1496.3 keV with spin and parity $1/2^+$.

The 1183- and 1239-keV transitions have been tentatively placed to the ground state because of the lack of any coincidences with the transitions depopulating the lower-lying levels. The 1239-keV transition, in particular, is sufficiently intense that it should appear in coincidence if it did populate any of the first three excited levels. A similar lack of any coincidences plus energy sums have led to our placement of the 1001.1-keV line.

The decay scheme constructed is essentially the same as that derived by both Alpsten and Astner and Hopke et al. However, we

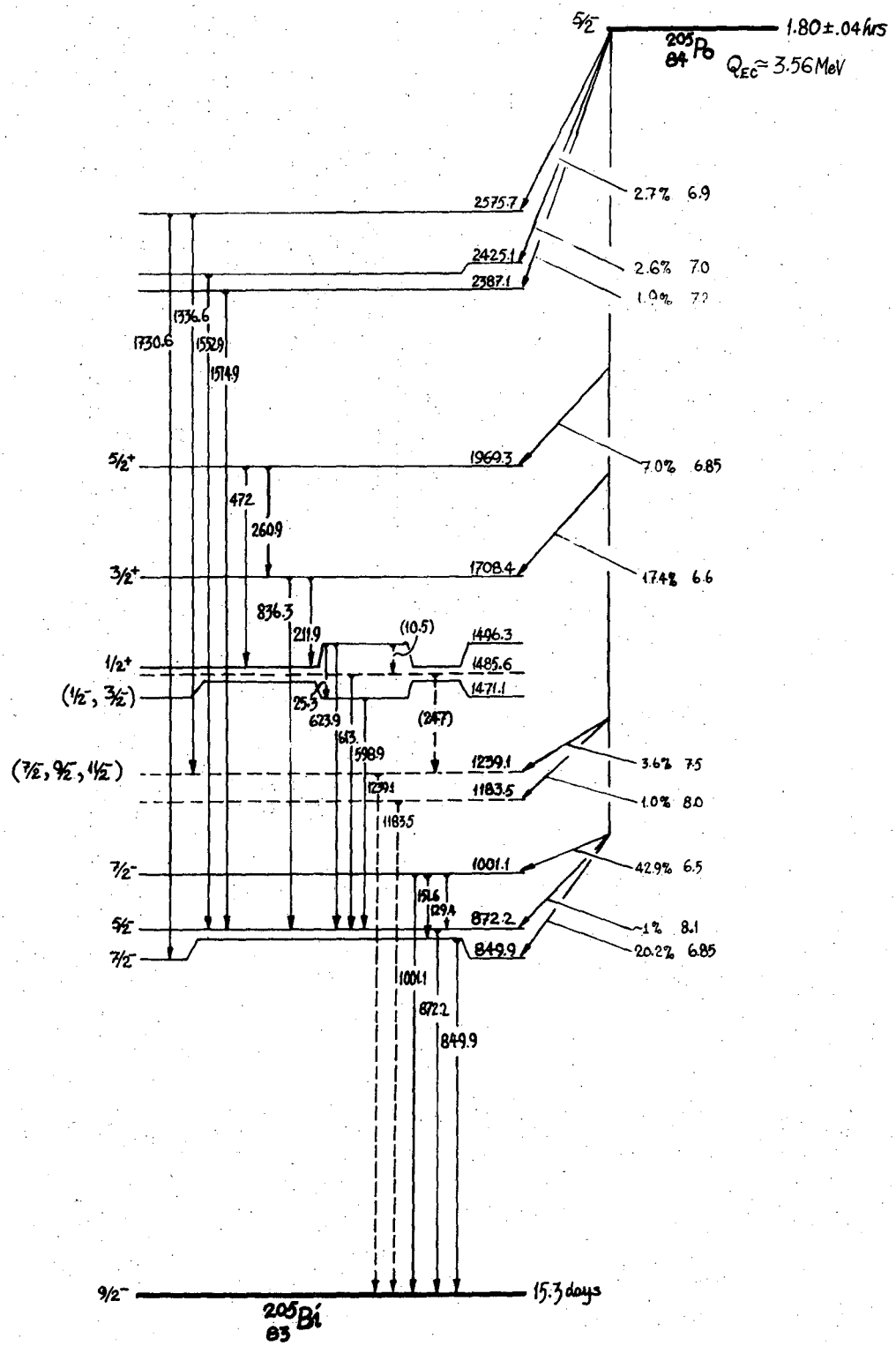

XBL 7011-7097

Fig. V-2. Decay scheme proposed for $^{205}Po \rightarrow {}^{205}Bi$.

have observed the 25.3-keV transition proposed by Alpsten and Astner on the basis of intensity balance arguments. We have placed the 25.3-keV and 598.9-keV gamma transitions in accordance with energy sums. They also placed the 598.9-keV gamma depopulating a 1471.1-keV level. In order to balance intensities at both the 1471.1- and 1496.3-keV levels, the 25.3-keV transition was suggested, although it was unobserved in their spectra. Both of these levels should receive little or no direct feeding from the ^{205}Po decay due to forbiddenness. Within experimental error the intensities of the 25.3- and 598.9-keV gammas are equal; thus there is no observed direct decay to the 1471.1-keV level.

Extending the same reasoning to the 1485.6- and 1496.3-keV levels, Alpsten and Astner found that a gamma of about 10.5 keV was needed to feed the 1485.6-keV level. We could not see a gamma of this low energy with our experimental arrangement; it is undoubtedly highly converted and will be difficult to observe.

The remaining transitions, indicated with dashed lines, were observed in our spectra but were either weak or of high energy so that, although no coincidences with lower-lying transitions were observed, they could not be completely ruled out. Using energy sums and the three high-energy states proposed by both Alpsten and Astner and Hopke et al. as a result of coincidence data, we have also placed these remaining transitions in the level scheme.

The estimated Q value for ^{205}Po electron capture was again obtained from the Mattauch tables[Mat65] and is 3.56 MeV. From this

and the percentage of direct electron-capture decay received by each level, log ft values were calculated. Uncertainties in the intensities (mainly from unplaced weak transitions) and Q value do not appreciably affect the log ft values.

Anomalies in the log ft values do appear. The forbidden decay to the $3/2^+$ and $5/2^+$ states is enhanced while the allowed decay to the three lowest lying levels is retarded. These same anomalies appear in ^{207}Po decay (Hop69, Alp69) and also in ^{203}Po decay, as we shall see.

2. ^{203}Po

The measurement of the gamma lines in the ^{203}Po spectrum (Fig. V-3) confirmed the half-life determined earlier in the alpha measurements. The best value obtained from the gamma data is 36.7 ± 0.5 min (from alpha decay, 36.0 ± 2.5 min).

The energies and intensities of all gammas assigned to ^{203}Po are listed in Table V-3. The K-conversion coefficients and K/L ratios were measured by Alpsten and Astner. (Alp69) There is need for verification of these values and the resulting multipolarity assignments, however. Measurements of these same quantities by Hopke, Naumann, and Spejewski (Hop69) do not agree and have led to a different set of multipolarity assignments. Their resultant decay scheme bears very little resemblance to that of ^{205}Po and ^{207}Po. Believing that nature prefers pattern and order where possible, I have chosen to use the multipolarity assignments of Alpsten and Astner because these lead to a ^{203}Po decay scheme with the same characteristics

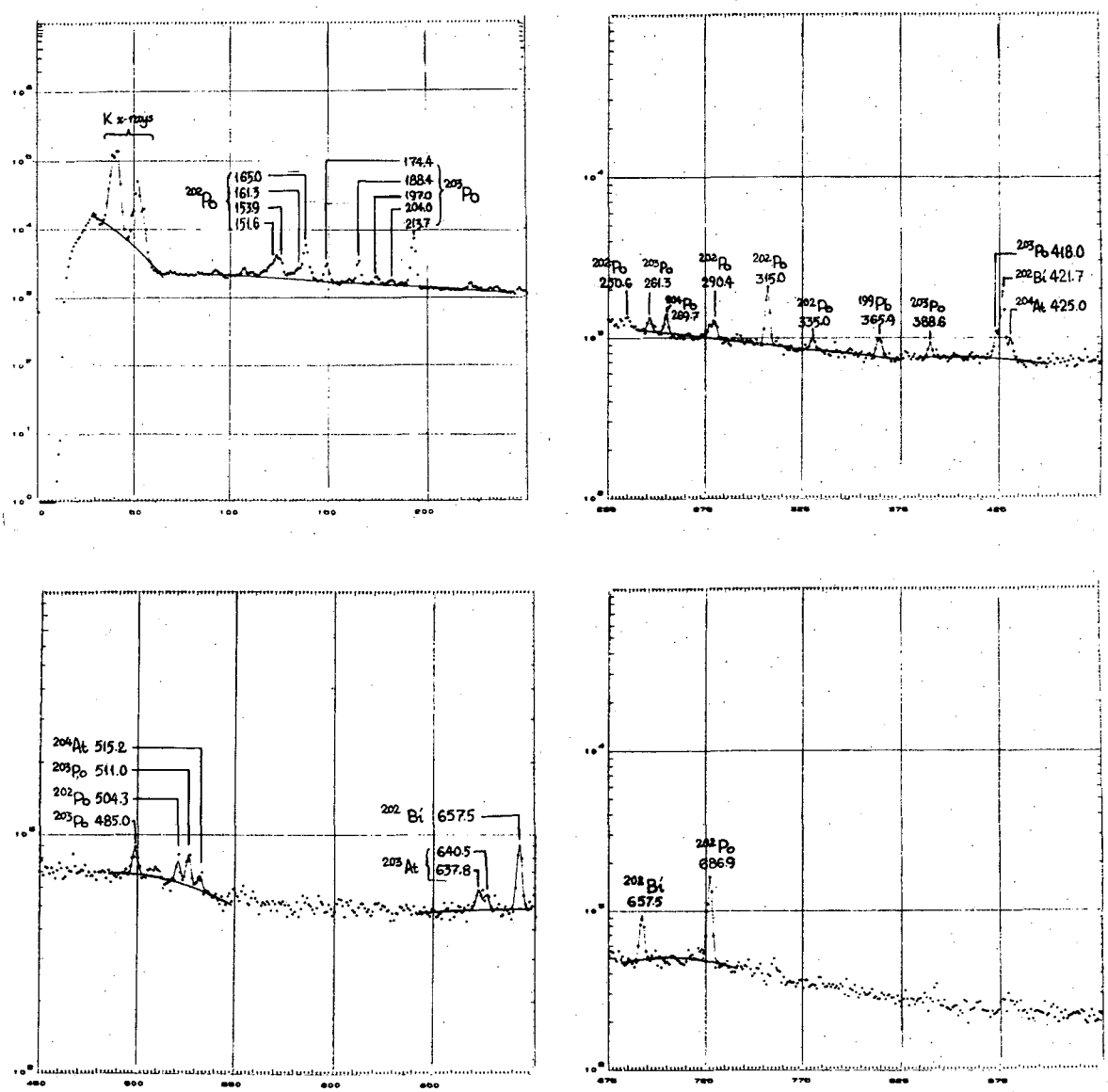

XBL 7011-7102

Fig. V-3. Gamma spectrum of ^{203}Po and ^{202}Po obtained 48 min after end of bombardment (0.25-mil Au target with 108-MeV ^{12}C beam). All short-lived astatine parents have substantially decayed (cf. Fig. IV-5).

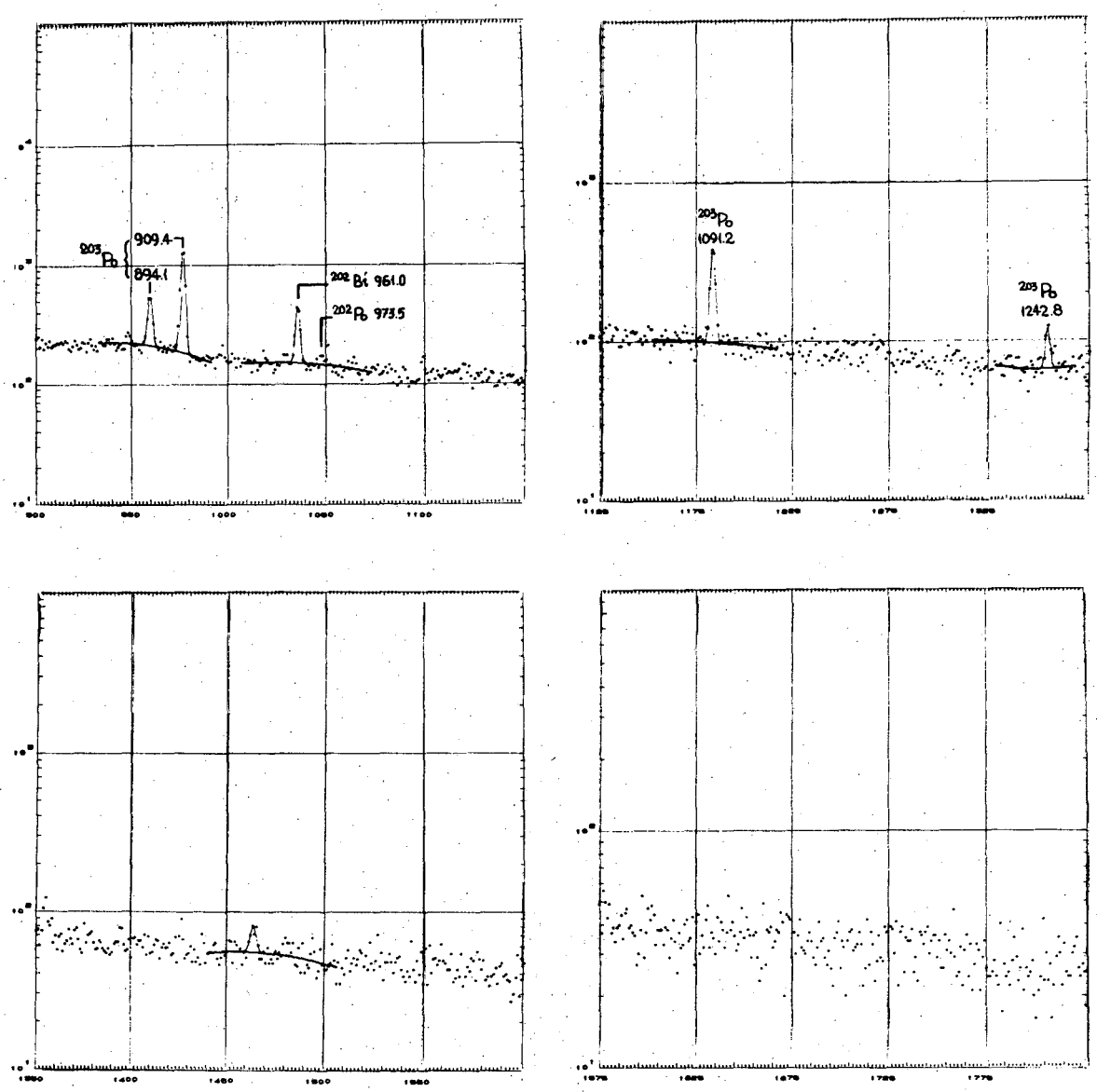

XBL 7011-7103

Fig. V-3 (cont.)

Table V-3. Intensity and energy of all gamma transitions assigned to $^{203}Po \rightarrow {}^{203}Bi$ decay.

Energy (keV)	I_γ	K-conversion coeff.[a]		K/L ratio[a]	Multipolarity[a]	I_T[b]
174.4 ± 0.3	4.6	1.6	±0.1	5	M1	13.5
188.4 ± 0.3	7.1	0.47	±0.04	0.11	E3	35.0
197.0 ± 0.3	1.2	1.4	±0.1		M1	3.2
204.0 ± 0.4	~1	0.75	±0.08	0.3	E3+ 6% M2	5.2
213.7 ± 0.2	27.8	0.18	±0.02	1.2	E2+ 5% M1	40.2
261.3 ± 0.4	2.1					~3
388.6 ± 0.4	2.3	0.034	±0.011		E2	2.8
418.0 ± 0.6	4.1	0.008	±0.005		E1	4.1
485.0 ± 0.4	4.6	0.022	±0.006		E2	4.7
511.0 ± 0.4	17.0					~17
648.2 ± 0.6	2.1	0.04	±0.01		M1	2.2
894.1 ± 0.5	28.0	0.008	±0.001	4.5	E2	28.0
909.4 ± 0.5	100	0.013	±0.001	5	M1+ 50% E2	101
1091.2 ± 0.5	31.4	0.011	±0.001	6	M1+ 25% E2	32.0
1242.8 ± 0.6	7.5	0.0014	±0.0007		E1	7.5

[a]Experimentally determined K-conversion coefficients and K/L ratios, and the multipolarities based on them are taken from Ref. Alp69.

[b]$I_T = (1 + \alpha_K + \alpha_L + \alpha_M + \cdots) I_\gamma$, where α_L were theoretical values obtained from the Sliv and Band tables (Sli65), and $\alpha_M + \alpha_N + \cdots = 0.3\ \alpha_L$.

observed in both ^{205}Po and ^{207}Po decay.

The decay scheme proposed for ^{203}Po in Fig. V-4 is very tentative. No coincidence measurements were made. Therefore the level scheme is supported by energy sums (Table V-4), intensity

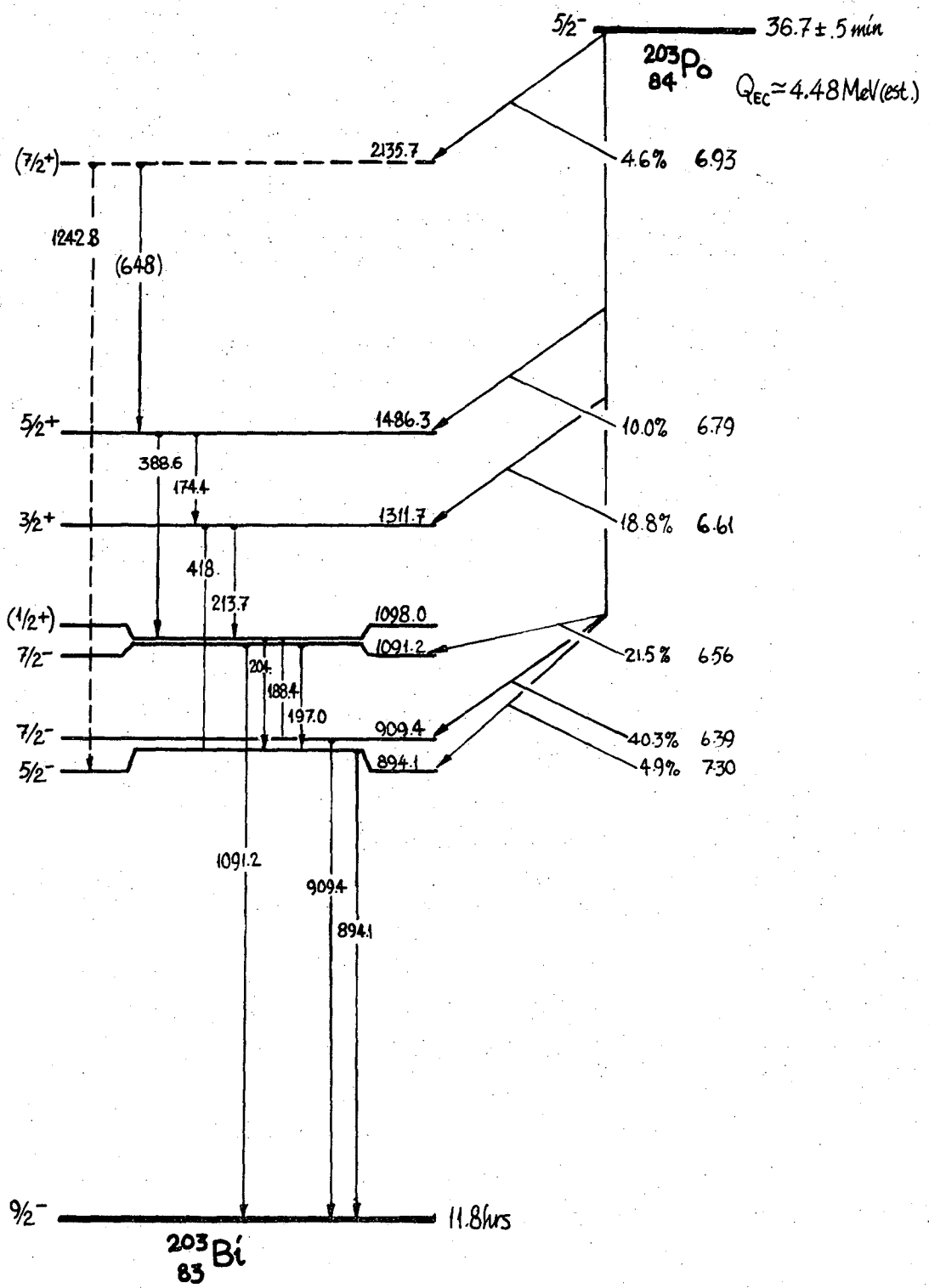

XBL 7011-7140

Fig. V-4. Decay scheme proposed for ^{203}Po.

Table V-4. Energy sums for gamma transitions observed in the $^{203}Po \rightarrow {}^{203}Bi$ decay.

E_1	E_2	Sum	E_3	Used in decay scheme
174.4	213.7	388.1	388.6	yes
188.4	909.4	1097.8	]	yes
204.0	894.1	1098.1	]	yes
197.0	894.0	1091.1	1091.2	yes
213.7	204.0	417.7	418.0	yes
261.3	648.2	909.5	909.4	no

relationships, the multipolarity assignments just discussed, and its similarity with the ^{205}Po decay scheme. It agrees well with the level scheme proposed by Alpsten and Astner. It does not agree with all of the coincidence data presented by Hopke et al., nor with their proposed decay scheme.

The amount of direct electron-capture decay received by the three lowest excited states indicates very clearly that the $5/2^-$ level has dropped down below the two $7/2^-$ states.

We postulated the existence of the 2135.7-keV level from energy sums. The placement of the 1242.8- and 648.2-keV transitions depopulating this level is supported by the coincidence data of Alpsten and Astner.

Alpsten and Astner have also reported a low-intensity (relative $I_\gamma = 0.2$) 182.5-keV M1 gamma which would represent the missing transition between the two $7/2^-$ levels at 1091.2 and 909.4 keV. The presence of a ^{203}Bi gamma ray of about the same energy would have

obscured this weak transition in the present investigation.

Both ground state spins have been measured: ^{203}Po as $5/2^-$ (Axe61) and ^{203}Bi as $9/2^-$.(Lin59) Log ft values were calculated from the estimated Q value (Mat65) and the direct level feedings which were determined by intensity balance.

The features of the decay scheme are very similar to those of ^{205}Po decay. The large percentage of direct decay to the $7/2^-$ levels is again seen: log ft values are 6.6 and 6.4 to the 1091.2- and 909.4-keV $7/2^-$ levels respectively. This is to be compared with values of 6.5 and 6.9 to the analogous $7/2^-$ levels in ^{205}Po → ^{205}Bi decay. The most striking similarity is again the presence of the band of positive parity levels. The $5/2^+$ and $3/2^+$ levels are fed by direct electron-capture decay with log ft values almost identical to those observed for the decay to similar levels in ^{205}Po.

3. Lower-Mass Isotopes

The gamma lines are much more difficult to identify in the low-mass spectra. This is due primarily to the profusion of isotopes produced, many with similar half-lives. The situation is particularly difficult when one is trying to identify short-lived activities.

No gamma transitions could be assigned to 8.9-min ^{201m}Po decay. A 238.8 ± 0.5-keV gamma with a half-life of 17.6 ± 2.1 min was attributed to ^{201}Po decay. The mass assignment is supported by the excitation function. Three other gamma lines were observed to have a similar half-life, but the assignment could not be confirmed by excitation-function measurements. All four gamma rays are listed in

Table V-5. If the 306.2- and 356.3-keV gamma lines do belong to a mass-199 isotope as favored by the excitation functions, this may be evidence for an isomeric state of ^{199}Bi, since currently no nuclide of mass 199 is known to have a half-life of approximately 17 min.

Table V-5. Gamma transitions tentatively assigned to the decay of ^{201}Po.

Energy (keV)	Half-life (min)	Relative intensity	Remarks
238.8 ± 0.5	17.6 ± 2.1	100	
124.4 ± 0.2	17.9 ± 2.0	3	(1)
306.2 ± 0.3	16.2 ± 1.4	100	(2)
356.3 ± 0.3	18.4 ± 1.1	40	(2)

(1) No excitation-function information.
(2) Excitation function tends to prefer mass assignment 199.

The measured ground state spin of ^{201}Po is $3/2^-$.[Axe61] Since the ground state of ^{201}Bi is a $9/2^-$ level,[Lin59] we would expect that ^{201}Po undergoes electron capture to excited levels in ^{201}Bi, possibly to ^{201m}Bi, which is known from alpha decay studies.[Sii64] Alpsten and Astner[Alp69] have observed a strongly converted 846-keV gamma transition with a half-life close to 60 min which they have assigned to the decay of the ^{201m}Bi isomeric state. By assuming that this isomeric transition feeds the ground state directly and interpreting their conversion coefficient measurements as being M4+ (54 ± 20) % E5, Alpsten and Astner have favored the assignment of spin and parity $1/2^+$ to the ^{201m}Bi level. [A multipolarity assignment

of E4 + (26 ± 11)% M5 also agrees with the conversion-electron measurements and has not been ruled out. It is less likely in the light of the data for the heavier isotopes previously discussed. A $1/2^+$ level could well represent the lowest member of the positive parity band previously observed in the level schemes of ^{203}Bi, ^{205}Bi, and ^{207}Bi.]

The 846-keV transition was not seen in the current work. No attempt has been made to incorporate the fragmentary experimental information obtained into a decay scheme for ^{201}Po.

One gamma line was seen with a half-life corresponding to that of ^{199m}Po--4.2 ± 0.3 min. The assignment of this 473.4 ± 0.4 keV gamma transition was supported by the excitation-function measurements.

4. Discussion

The discussion which follows applies equally well to both ^{205}Po and ^{203}Po as well as to ^{207}Po decay which, however, was not observed in the present investigation. Much of the discussion may also be applicable to ^{201}Po, with provision made for its $3/2^-$ ground state, when more information on its decay is available.

The ground state configuration of the odd-mass polonium isotopes is expected to be principally due to the configuration $\pi(h_{9/2})^2 \nu(p_{1/2})^{-2}(f_{5/2})^{-(1+2n)}$, where n = 0 for ^{207}Po, n = 1 for ^{205}Po, and n = 2 for ^{203}Po. The ground state of their respective bismuth daughters can then be assigned a configuration $\pi(h_{9/2})^1 \nu(p_{1/2})^{-2}(f_{5/2})^{-2n}$.

Therefore the ground-state-to-ground-state electron-capture decay of polonium would involve the conversion of an $h_{9/2}$ proton to an $f_{5/2}$ neutron. This transition requires $\Delta I = \Delta \ell = 2$, no, and is therefore expected to proceed very slowly.

The two $7/2^-$ states are readily interpreted as the $2f_{7/2}$ single-proton state, its strength being split on two levels. These states could be strongly fed from the polonium parent if there is a small admixture of $\pi(f_{7/2})^2$ in the ground state wave function of the polonium nucleus. The transition to bismuth would then involve favored conversion of an $f_{7/2}$ proton to an $f_{5/2}$ neutron. Although the log $\underline{ft}$ values are high because of the small admixture, the transition proceeds with sufficient speed to preferentially populate the $7/2^-$ levels.

The most probable explanation for the population of the bismuth positive parity states is that they are due to one hole in the $Z = 82$ proton core with two protons pairing off in the $h_{9/2}$ level. Thus the conversion of a $d_{3/2}$ or $d_{5/2}$ proton in a filled subshell of ^{205}Po (or ^{203}Po) to an $f_{5/2}$ neutron would lead to first forbidden decay to the $3/2^+$ and $5/2^+$ Bi levels ($\Delta I = \Delta \ell = 1$, yes).

If this is the case, the decay should be analogous to that of the odd-mass lead isotopes which also have $5/2^-$ ground states. ^{203}Pb, ^{201}Pb, and ^{199}Pb decay to $5/2^+$ and $3/2^+$ states in their thallium daughters.(Led67) In ^{203}Pb, log $\underline{ft}$ = 7.0 for decay to the $5/2^+$ level and log $\underline{ft}$ = 6.5 for decay to the $3/2^+$ level with < 2% of the electron capture (log $\underline{ft}$ = 8.3) going directly to the $1/2^+$ ground state. In the case of ^{199}Pb, log $\underline{ft}$ = 6.9 and 6.6 for decay to the $5/2^+$ and $3/2^+$

levels, respectively, and no direct decay has been observed to the $1/2^+$ ground state. These log ft values are almost identical to those observed in the polonium decay: 6.85 and 6.6 (cf. Figs. V-2, V-4). Hence this analogy with the lead isotopes supports the notion of "core excitation" in the positive-parity excited levels of these odd-mass bismuth nuclei.

In similar fashion the $1/2^+$ state is attributable to a $\pi(s_{1/2})^{-1}(h_{9/2})^2\,\nu(p_{1/2})^{-2}(f_{5/2})^{-2n}$ configuration. The energy spacings of the three positive-parity states show a pattern similar to that seen in the odd-mass thallium isotopes where the $1/2^+$ level is the ground state. Moreover, the pattern of de-excitation of the $5/2^+$ Tl states, (Led67) i.e., preferential population of the $3/2^+$ state with a small crossover to the $1/2^+$ state, is identical to that observed for the $5/2^+$ level of the bismuth isotopes. The intense $3/2^+ \rightarrow 1/2^+$ transition seen in the thallium isotopes has become much weaker in ^{205}Bi (and ^{203}Bi); rather, the energy available drives the E1 transition down to the low-lying negative parity states.

The multipolarity assignments of the 1242.8- and 648.2-keV ^{203}Bi transitions support the assignment of positive parity to the 2136.9-keV level and indicate a spin of 3/2, 5/2, or 7/2. Due to the high excitation energy of this state, it could be the 7/2 member of the positive-parity band, representing the conversion of a $g_{7/2}$ proton to an $f_{5/2}$ neutron ($\Delta I = \Delta \ell = 1$, yes). The observed log ft value of 6.9 certainly suggests such a first forbidden transiton. The resulting configuration of the ^{203}Bi nucleus would then be $\pi(h_{9/2})^2\,(g_{7/2})^{-1}$

$\nu(p_{1/2})^{-2}(f_{5/2})^{-4}$. This would be in keeping with the configurations of the other positive-parity states where there is also core excitation, i.e., a hole in the 82-proton shell.

B. Even-Mass Isotopes

1. ^{204}Po

The most intense ^{204}Po gamma lines are denoted in the ^{205}Po spectrum presented in Fig. V-1. Four less-intense lines (< 10%) were seen in a separate run which maximized the ^{204}At concentration. The results derived from these spectra are included in Table V-6. The half-life of ^{204}Po was determined to be 3.69 ± 0.11 hr from the gamma measurements, in good accord with the 3.55 ± 0.15 hr obtained from the decay of the alpha group.

The only previous information available on the electron-capture decay of ^{204}Po was acquired by An.[An65]. His results are included in Table V-6 for comparison. The two sets of data agree in half-life determination and in spirit, but there are several discrepancies between the values obtained for both the energy and the intensity of several of the transitions. Additional support for the values obtained in this work comes from the fact that the energies and intensities of ^{205}Po gamma lines seen in the same spectra are in excellent agreement with recently published values [cf. Chapter V-(A)]. This implies that the errors quoted in Table V-6 correctly indicate the uncertainties due to energy and efficiency calibration.

Table V-6. Gamma transitions observed in the decay of ^{204}Po.

This work		Values from Ref. An65	
Energy (keV)	Relative intensity	Energy (keV)	Relative intensity
63.23±0.10	12 ± 2		
115.0 ±0.3	2.3 ±0.3		
120.6 ±0.4	6.2 ±0.7		
126.7 ±0.4	8.7 ± 1.0		
137.3 ±0.3	40.3 ± 3.0	140	66
163.4 ±0.5	6.6 ±0.7		
202.2 ±0.5	9.7 ±0.9	202	13
269.7 ±0.4	100	268	100
304.5 ±0.5	10.0 ±0.9	305	17
316.5 ±0.5	14.9 ± 1.4	316	19
534.2 ±0.6	44.9 ± 3.5	537	52
680.0 ±0.7	30.4 ± 3.6	680	40
762.0 ±0.7	37.6 ± 3.4	764	43
883.6 ±0.6	110.0 ± 8.8	883	101
1016.1 ±0.7	93.0 ± 8.4	1022	77
1040.0 ± 1.1	38.0 ± 3.4	1037	28

The coincidence results are summarized in Table V-7. The 137.3-, 269.7-, and 883.6-keV transitions are all in coincidence, implying a triple cascade. The coincidence data, as well as intensities and energy sums, have been used to construct a decay scheme. The level scheme proposed in Fig. V-5 is one possibility that agrees with all the experimental data.

The 63.23-keV transition was observed only in the low-energy spectrum and thus no coincidence information was obtained. It was

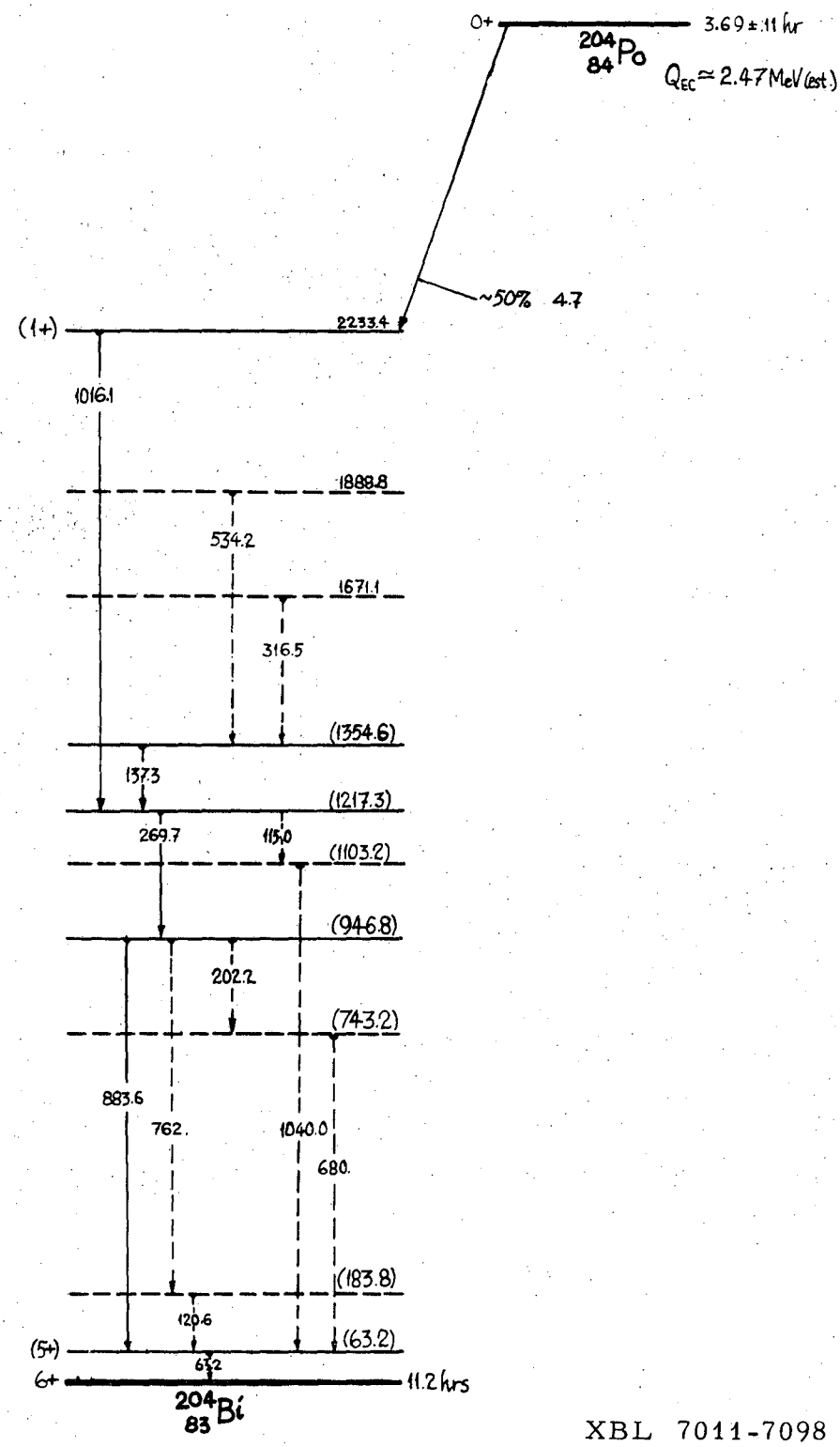

XBL 7011-7098

Fig. V-5. Tentative decay scheme for ^{204}Po.

Table V-7. Coincidence results for gammas observed in the decay $^{204}Po \rightarrow {}^{204}Bi$.

Energy (keV)	Energy of gate (keV) 137	202	269.7	316	534	762	883	1016	1040
63.2									
115.0									
120.6									
126.7									
137.3		x	x	?	x		x		
163.4									
202.2			x						
269.7	x	x		?		x	x	x	
304.5									
316.5			x						
534.2	?						x		
680.0									
762.0									
883.6	x		x		?				
1016.1			x						
1040.0									

assumed to depopulate the first excited level; this is in agreement with the level schemes of both ^{206}Bi(Arb57) and ^{208}Bi(Led67) and with the relative intensities.

Wahlborn(Wah57) has calculated the energies of the nuclear levels expected in ^{206}Bi with three neutron holes. The four lowest-energy configurations-- $\pi(h_{9/2})^1\ \nu(p_{1/2})^{-2}(f_{5/2})^{-1}$, $\pi(h_{9/2})^1\ \nu(p_{1/2})^{-2}(p_{3/2})^{-1}$, $\pi(h_{9/2})^1\nu(p_{1/2})^{-1}(f_{5/2})^{-2}$, $\pi(h_{9/2})^1\ \nu(p_{1/2})^{-1}(f_{5/2})^{-1}(p_{3/2})^{-1}$-- lead to a large density of levels, all with positive parity. The first negative-parity levels have an excitation energy of ~ 1 MeV and arise

from the coupling of an $i_{13/2}$ neutron with the odd $h_{9/2}$ proton. Therefore the gamma transitions between excited levels below ~1 MeV can be expected to have multipolarity M1 or E2. This is born out for ^{206}Bi where only M1 and E2 transitions were observed below the 1379-keV level. (Arb57, Sto56)

One expects the same general level order in ^{204}Bi with five neutron holes. The 63.2-keV ground state transition will then be an E2 or M1 gamma. Intensity balance and reference to Table V-8 would lead to a preference for the M1 assignment.

^{204}Po is an even-even nucleus; hence its ground state is a 0^+ level. ^{204}Bi has a ground state spin and parity of 6^+. (Lin59) There-

Table V-8. Total intensity of ^{204}Po low-energy gamma lines as a function of multipolarity.

Energy (keV)	Relative intensity	Total intensity Assume M1	Total intensity Assume E2
63.2	12	323	1330
115.0	2.3	16	11.5
120.6	6.2	42	31
126.7	8.7	59	43
137.3	40.3	240	85
163.4	6.6	26	14.5
202.2	9.7	26	14.5
269.7	100	158	117
304.5	10.0	15	12
316.5	14.9	21	16

fore we would not expect to see any ^{204}Po electron capture directly to the low-lying Bi levels due to their high spin. Thus the intensities of the 762.0- and 120.6-keV transitions are equal within experimental error; the 120.6-keV gamma probably corresponds to the 121-keV line seen earlier in the study of the alpha decay of ^{208}At. Similarly, requiring the intensities of the 680.0- and 202.2-keV gammas to be equal suggests that the 202.2-keV transition is probably an M1 transition, although their order could be reversed.

Intensities tend to indicate that the 137.3- and 269.7-keV transitions are of multipolarity E2 and M1 respectively. Conversion measurements are necessary before any definite spin assignments can be made.

It appears that the 2233.4-keV level receives ~50% of the direct ^{204}Po decay. Using the Mattauch estimate of 2.47 MeV(Mat65) for Q_{EC}, this corresponds to log $\underline{ft} \approx 4.7$. This would certainly indicate an allowed transition, hence a spin and parity of 1^+ for the 2233.4-keV level. Wahlborn's calculations (Wah57) for ^{206}Bi predict the 1^+ level of the $\pi(f_{7/2})^1\ \nu(p_{1/2})^{-2}(f_{5/2})^{-1}$ configuration at an energy of ~2.16 MeV. The decay to such a state would proceed rapidly if the ^{204}Po ground state configuration has some admixture of $\pi(f_{7/2})^2$. The conversion of an $f_{7/2}$ proton to an $f_{5/2}$ neutron would be allowed; $\Delta I = 1$, $\Delta \ell = 0$, no.

Much more work is necessary before the decay scheme of ^{204}Po is completely elucidated. ^{204}Bi is an extremely complicated nucleus with a huge density of excited levels due to the several configurations possible in the coupling of the odd particles.

2. ^{202}Po

No work has been published concerning the gamma rays or conversion electrons in the electron-capture decay of ^{202}Po.

The ^{202}Po gamma lines observed in the current investigation are labeled in Fig. V-3; the experimental data are summarized in Table V-9. No search was made for low-energy gamma transitions ($E < 100$ keV).

The best value of the half-life obtained from these data is 43.7 ± 1.3 min, to be compared with a value of 43.8 ± 1.5 min obtained previously in the alpha measurements.

As an even-even nucleus ^{202}Po has a 0^+ ground state. The measured spin(Lin59) of the ^{202}Bi nucleus is 5^+. We would thus expect the electron-capture decay to proceed to the higher-lying low-spin states in ^{202}Bi, as was observed for the heavier even-even Po nuclei.

The intense 686.9-keV gamma is probably a transition to the ground state (an analog of the 883.6-keV transition to ground in ^{204}Bi). Any further attempt at constructing a decay scheme would be pure speculation without additional information. Again, in analogy to the heavier odd-odd Bi isotopes, we would expect a large density of available energy levels and hence a complicated ^{202}Po decay pattern.

3. ^{200}Po

No gamma rays can definitely be assigned to ^{200}Po decay. Several gamma lines with the correct lifetime (~ 11 min) were observed.

The majority of these were assigned to ^{198}Bi on the basis of their excitation functions [cf. Chapter VI-A(4)]. The identity of the two remaining 11-min gamma lines at 191.0 and 880.5 keV could not be ascertained; they may belong to $^{200}Po \rightarrow {}^{200}Bi$ decay.

Table V-9. Energy and intensity of gamma rays observed in ^{202}Po decay.

Energy (keV)	Relative intensity	Total intensity	
		Assume M1	Assume E2
151.6 ± 0.4	8.4 ± 0.7	32.5	16.7
153.9 ± 0.5	6.4 ± 0.7	24.4	12.7
161.3 ± 0.4	4.0 ± 0.6	14	7.7
165.0 ± 0.3	25.3 ± 1.7	88	49
250.5 ± 0.4	3.5 ± 0.4	5	3.6
315.0 ± 0.5	22.5 ± 2.2	34	25.4
335.0 ± 0.5	3.0 ± 0.3	4.5	3.7
504.8 ± 0.6	9.8 ± 1.0	10	10
686.9 ± 0.7	100	101	101
716.6 ± 0.8	9.3 ± 1.0	9.4	9.4
789.8 ± 0.7	12.5 ± 1.0	12.6	12.6
973.5 ± 0.8	8 ± 2	8	8

VI. RESULTS: DECAY OF BISMUTH ISOTOPES

A. Even-Mass Isotopes

1. ^{204}Bi

An energy-level scheme has been previously constructed for the ^{204}Pb nucleus by combining results obtained in studies of the isomeric decay of ^{204m}Pb (Her56) with results from studies of the electron capture of ^{204}Bi. (Sto58, Wer56, Fri56) Spins were assigned to the observed low-energy levels, since multipolarity values could be determined for the strong gamma transitions depopulating these levels. By combining the published conversion electron intensities of Stockendal et al. (Sto58) with our relative gamma intensities measured in ^{204}Bi decay, we have determined the multipolarities of some of the weaker gamma transitions and thus deduced spin and parity values for the higher-energy levels of ^{204}Pb.

Conversion coefficients can be calculated from the electron and gamma intensities if the multipolarity (and therefore the K-conversion coefficient) of one transition is known. We were able to use the well-established 374-keV E2 transition as a standard. Then, for a transition with energy E, the conversion coefficient, α_i, is expressed by

$$\alpha_i(E) = \frac{N_i(E)}{N_\gamma(E)} \cdot \frac{N_\gamma(\mathrm{std})}{N_K(\mathrm{std})} \cdot \alpha_K(\mathrm{std}),$$

where i refers to conversion in the ith shell. A value of $\alpha_K(374.4) = 0.0392$ was obtained from the Sliv and Band tables. (Sli65) By using the conversion coefficients determined by this expression and

the K/L ratios of Stockendal, the multipolarities of many transitions could be determined. The results are shown in Table VI-1. Our derived multipolarities for the strong transitions agree with those of Stockendal et al.; in addition, several new assignments were possible.

The results of gamma-gamma coincidence measurements are summarized in Table VI-2. They support the decay scheme that was previously derived. This decay scheme is reproduced from the Table of Isotopes[Led67] in Fig. VI-1; our additional spin assignments and estimates of branching ratios have been inserted.

The transitions shown in dashed lines in Fig. VI-1 were placed by Stockendal after being observed in the electron spectra. These transitions were not seen in the current gamma measurements. This may be explained by the source strength. All the data acquired on the electron capture of ^{204}Bi in the present investigation were obtained by following the decay of a ^{204}Po sample for a long period of time. A much more active source could be prepared and the polonium allowed to decay away before any gamma measurements were made. In this way these very weak transitions might be observed.

The triple cascade of the 911.5-, 374.4-, and 898.9-keV transitions was first demonstrated by Herrlander et al.[Her56] who also ascertained the spins and parities of the 898.9-, 1273.6-, and 2185.1-keV levels in their study of the isomeric decay of ^{204m}Pb.

The spin of the 1562.8-keV level is definitely 4^+; this is shown by the 289.2-keV M1 and the 663.4-keV E2 transitions de-exciting this level and leading to 4^+ and 2^+ states respectively. In similar fashion

Table VI-1. Energies and intensities of gamma transitions observed in ^{204}Bi decay.

Energy (keV)	I_γ	K-electron intensity[a]	K/L ratio[a]	K-conversion coefficient	Multipolarity	I_T[c]
176.0 ± 0.4	1.6	50	≈ 5	1.22 ±0.20	M1	4 ± 1
215.9 ± 0.4	3.1	41	6 ± 2	0.52 ±0.10	M1	5 ± 1
219.2 ± 0.4	4.0	13	4 ± 2	0.127 ±0.025	(E2 or M1)	5 ± 1
222.0 ± 0.4	1.5	24	6 ± 2	0.627 ±0.09	M1	2.5 ± 0.4
289.2 ± 0.3	4.4	38	5.8 ± 1	0.338 ±0.04	M1	6.0 ± 0.6
374.4 ± 0.3	100	100	2.4 ± 0.4	0.0392[b]	E2	100
404.8 ± 0.5	2.6	2.3	≈ 3	0.035 ±0.006	E2	2.5 ± 0.5
663.4 ± 0.5	6.0	1.8		0.012 ±0.002	E2	5.7 ± 1.2
670.3 ± 0.7	12.5	19	5.8 ± 0.6	0.060 ±0.006	M1	12.7 ± 1.5
691.4 ± 0.7	6.2	≈ 1		0.006 ±0.002	(E1 or E2)	(~6 ± 1)
709.5 ± 0.8	5.0	1.5		0.0118±0.0016	E2	4.8 ± 0.7
898.9 ± 0.4	125	23	4.4 ± 0.4	0.0075±0.0008	E2	119 ± 12
911.5 ± 0.6	26.0	36	1.6 ± 0.2	0.054 ±0.006	E5	25.4 ± 3.0
918.0 ± 0.6	13.3	2.9	≈ 5	0.0086±0.0009	E2	12.6 ± 1.3
983.8 ± 0.6	69.0	0.7(L_I)		0.00038(α_{L_I})	(E1)	65 ± 10

[a]Values obtained from Ref. Sto58.

[b]The well-established 374.4-keV E2 transition was used as a standard to calculate the K-conversion coefficients. The value of its conversion coefficient (0.0392) was obtained from Ref. Sli65.

[c]Total transition intensity normalized to I_T (374.4) = 100.

Table VI-2. Results of ^{204}Bi gamma-gamma coincidence measurements.

	Energy of gate (keV)									
Energy (keV)	289	374	670	899	911	918	984	216	219	222
176.0										
215.9			?							
219.2							?	?		
222.0								?		
289.2		x		?						
374.4	x		x	x	x		x	x	?	x
404.8										
663.4										
670.3										
691.4										
709.5										
898.9	x	x	x		x	x	x	x	x	x
911.5		x								
918.0				?						
983.8		x						?	?	x

the E2 multipolarity of the 918.0-keV transition from the 1816.9-keV level to the 2^+ first excited state fixes the spin and parity of the 1816.9-keV level as 4^+.

By contrast the 983.8-keV gamma is most likely to be an E1 transition judging by the L_I conversion coefficient. This means that the 2257.4-keV level must be a negative-parity state with spin equal to 4 or 5. (The spin value 3 has been eliminated since these lowest-energy negative-parity states are undoubtedly due to the coupling of

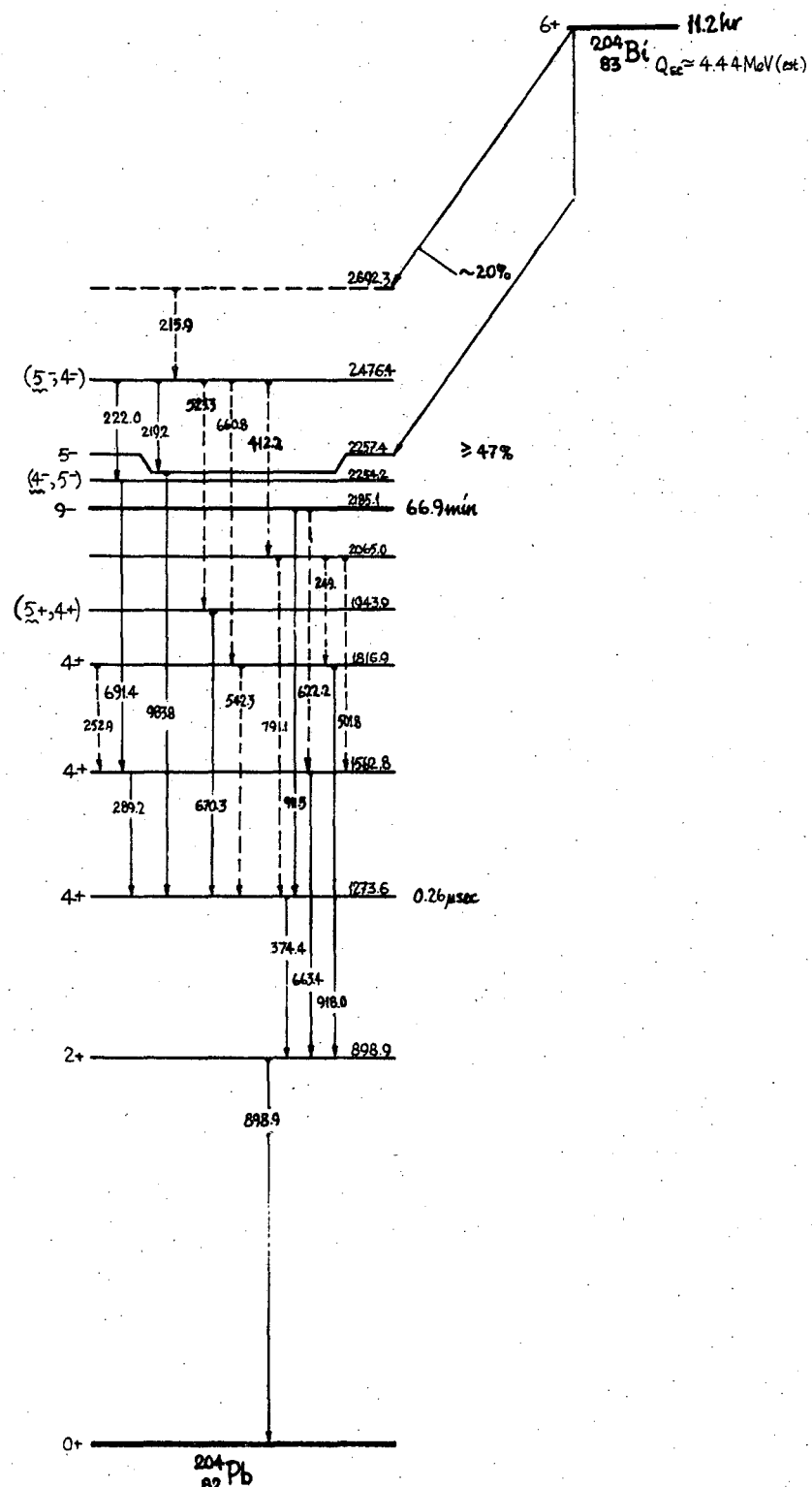

XBL 7011-7099

Fig. VI-1. Decay scheme of ^{204}Bi taken from Table of Isotopes. (Led67) The spin assignments and decay branching based on this work are also included.

odd neutrons in the $f_{5/2}$ and $i_{13/2}$ levels. This results in states with spin values between 4^- and 9^- being possible.) Moreover, since the 2257.4-keV level receives a substantial portion of direct feeding from the ^{204}Bi ground state with a measured spin of 6^+ (Lin59) a spin of 5^- is preferred for this excited Pb level. A 5^- level is seen in ^{202}Pb at ~2 MeV, and 95% of the electron-capture decay of ^{206}Bi (ground state = 6^+ also) proceeds to two high-lying 5^- states in its lead daughter.

In order to assign consistent spins to the 2476.4- and 2254.2-keV levels, the 219.2-keV gamma ray must be an M1 transition. Such a multipolarity assignment is not strongly supported by the calculated K-conversion coefficient, but certainly is not excluded.

The relatively high intensity of the 911.5-keV gamma line indicates that ~20% of the ^{204}Bi electron-capture decay is proceeding through the ^{204m}Pb state. Because of the spins the decay cannot be direct; the 2185.1-keV ^{204m}Pb level must presumably be fed by gamma transitions from higher-lying levels, although no such transitions have yet been observed.

Intensity balance at each level in the existing decay scheme requires ~50% direct population of the 2257.4-keV level. This corresponds to a log ft value of ~7. For comparison, a log ft value of 6.9 was obtained in this work for the decay of ^{202}Bi to the 5^- level in ^{202}Pb at 2036 keV (cf. next section), while ^{206}Bi decay to the two high-energy 5^- states in ^{206}Pb entails log ft values of 6.3 and 6.7. Intensity balance requirements also indicate 5 to 10% direct decay to

the 2476.4-, 2254.2-, and 1943.9-keV Pb levels. However, these levels may all be fed by transitions (thus far unobserved) from higher lying states.

The resulting level scheme still needs further clarification. The additional spin and parity assignments we have been able to include in the decay scheme shown in Fig. VI-1 are the most probable values according to all available data. But they, in turn, must be regarded as tentative. Because of the complexity of the decay more experiments are needed. Additional measurements of both gamma-ray and electron spectra, including coincidence studies, with a strong ^{204}Bi source would be helpful.

2. ^{202}Bi

From observation of the gamma rays emitted in the isomeric decay of 3.62-hr ^{202m}Pb, a level scheme had been previously established for ^{202}Pb. (McD56) Karracker and Templeton(Kar51) first reported the electron-capture decay of ^{202}Bi in 1951; they observed two gamma lines at 421 and 961 keV which decayed with a half-life of ~1.6 hr. No further information has been published concerning ^{202}Bi decay.

In the current ^{202}Po measurements, several gamma lines, including the 421- and 961-keV activities mentioned above, were observed to grow in (with the ^{202}Po 45-min half-life) and then decay with a half-life of 1.79 ± 0.03 hr. These lines have been assigned to ^{202}Bi electron-capture decay and are so listed in Table VI-3.

Table VI-3. Energies and intensities of gamma transitions observed in ^{202}Bi decay.

Energy (keV)	Relative intensity	Multipolarity[a]	I_T
167.6 ± 0.3	4.5 ± 0.5		
239.8 ± 0.3	3.8 ± 0.4	(M1)	6.4 ± 0.7
319.2 ± 0.4	2.0 ± 0.5		
345.9 ± 0.4	3.2 ± 0.4		
421.7 ± 0.4	75.2 ± 4.3	E2	79 ± 5
514.1 ± 0.5	1.6 ± 0.3		
568.7 ± 0.5	3.3 ± 0.4		
577.9 ± 0.6	8.0 ± 0.9		
657.5 ± 0.4	56.3 ± 4.0	E1	57 ± 4
928.0 ± 0.7	4.5 ± 0.7		
954.8 ± 0.7	8.2 ± 0.8		
961.0 ± 0.5	100	E2	100
(124.9 ± 0.3)[b]	1.5 ± 0.4		
(224.5 ± 0.4)	2.5 ± 0.5		

[a]Assignments obtained from Table of Isotopes.(Led67)
[b]Transitions in parentheses are probable.

The ^{202}Bi gamma lines are shown in the spectrum of Fig. VI-2. It is apparent that substantial ^{198m}Tl and ^{198}Pb activity is also present. Both have half-lives similar to ^{202}Bi, making positive identification of some of the weaker transitions--where the growth was not always detected-- difficult. Hence these assignments are indicated in parentheses in Table VI-3.

Without further experiments the weak transitions cannot be definitely placed in the decay scheme (Fig. VI-3). The absence in the

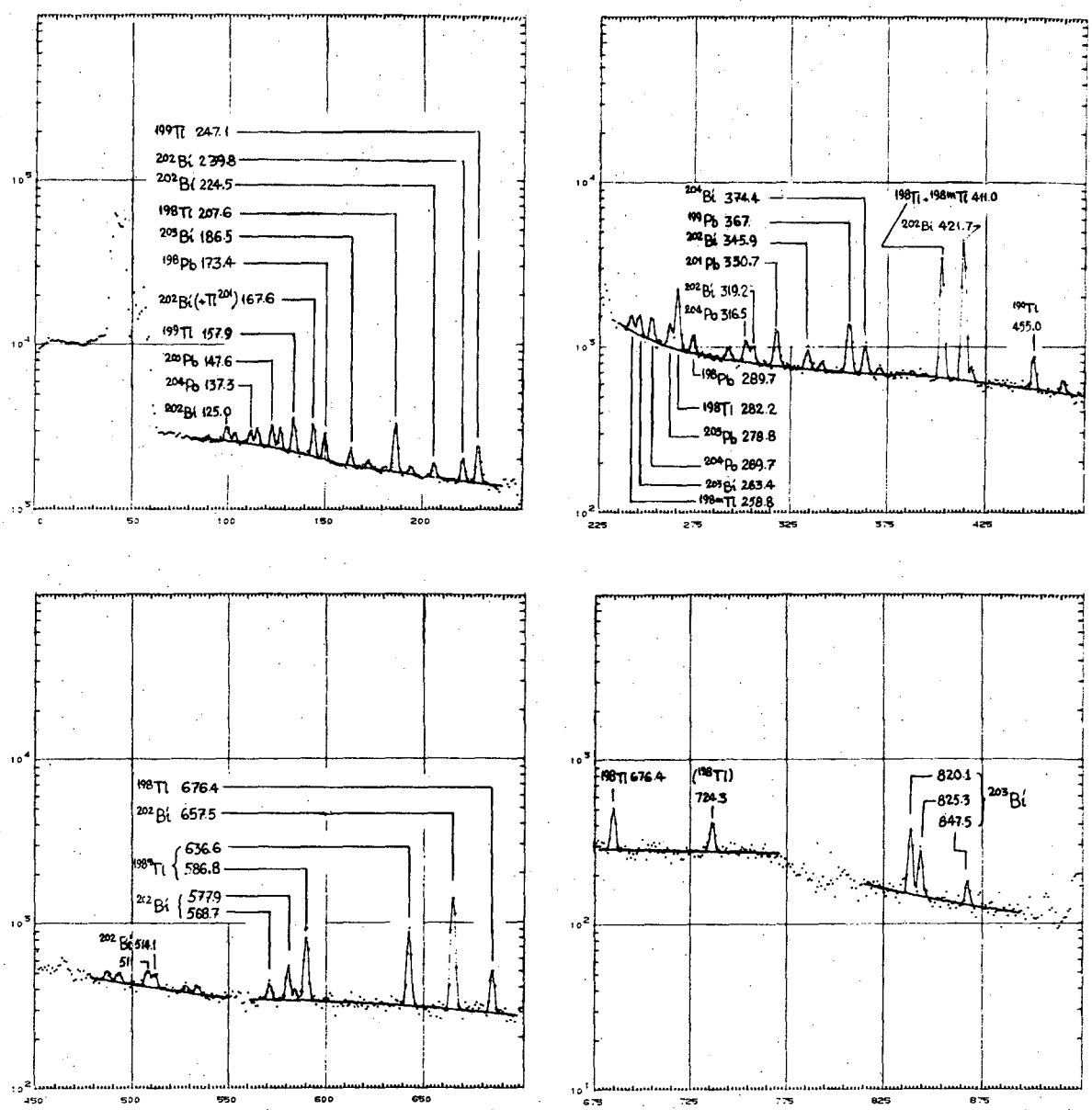

XBL 7011-7113

Fig. VI-2. Gamma spectrum of ^{202}Bi obtained 6 hr after bombardment of a 0.25-mil gold target with a 110-MeV ^{12}C beam. The shorter-lived Po isotopes have decayed away, but there is substantial ^{198m}Tl (1.87 hr) and ^{198}Pb (2.4hr) activity. Longer-lived lead and thallium isotopes can also be observed growing in.

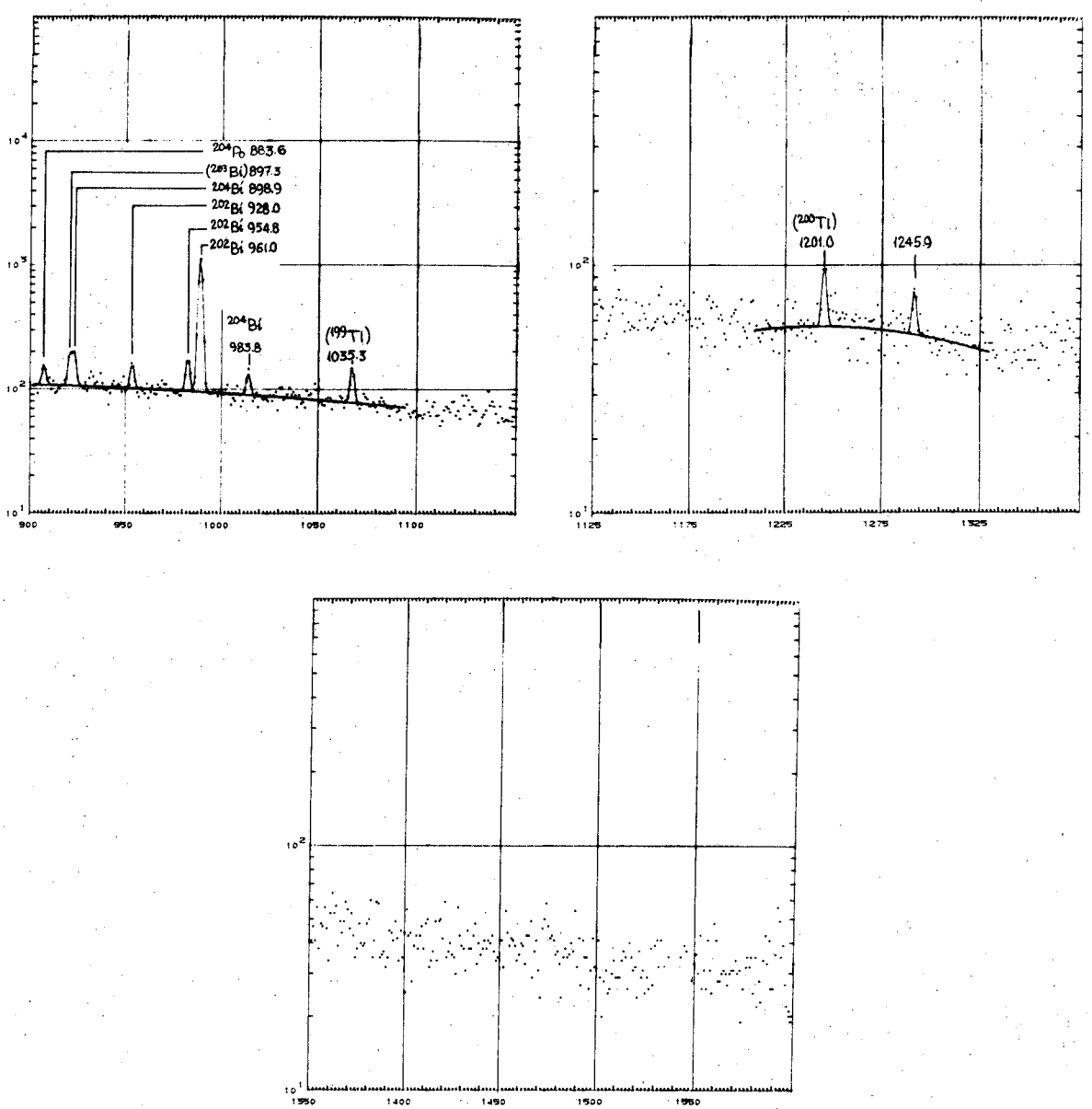

XBL 7011-7114

Fig. VI-2 (cont.)

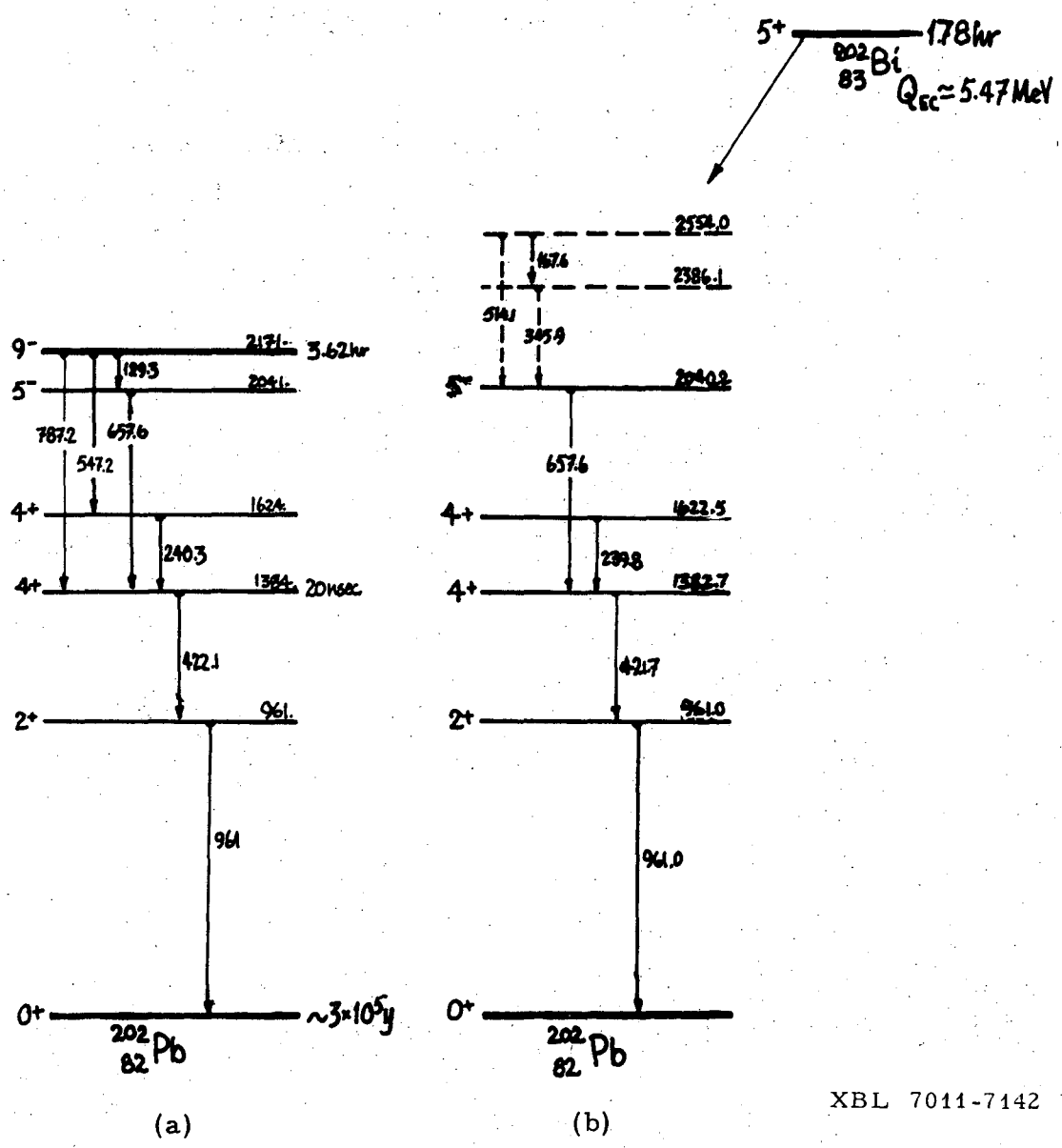

Fig. VI-3. Energy-level scheme for ^{202}Pb.

(a) Level scheme from Table of Isotopes,[Led67] based on the study of ^{202m}Pb decay.
(b) Tentative level scheme proposed in this work from the observation of ^{202}Bi electron capture decay.

spectrum of the three gammas that depopulate the ^{202m}Pb isomeric level indicates there is very little or no feeding of this level from any higher excited states of ^{202}Pb. However, the observed weak transitions may feed the 4^+ levels. Therefore, the levels and transitions indicated with dashed lines are reasonable but by no means conclusive.

Intensity balance at the 961-keV level requires extra feeding from higher levels, since we would expect no direct bismuth decay to this 2^+ level. Again, by intensity arguments, there may be a small percentage of direct decay to the two 4^+ levels (5 to 10%). As indicated in the decay scheme the 5^- level at 2040.2-keV would need to receive ~50% of the direct electron-capture decay to account for the intensity of the 657.6-keV gamma. Undoubtedly this level is populated directly but, in all likelihood, is also fed by some of the observed weak transitions (other than the tentative ones indicated). Taking into account the extra feeding required at the 961-keV level, the 5^- state probably receives ~30% of the direct bismuth ground state decay. Using an estimated Q value (Mat65) of 5.47 MeV, this would mean a log ft value of 6.9, similar to the value obtained in ^{204}Bi decay.

3. ^{200}Bi

Electron capture of ^{200}Bi has been observed(Neu50) to occur with a decay time of ~35 min. Nothing more has been published about the energy levels of ^{200}Pb.

Four gamma lines observed in the current investigation could be definitely assigned to ^{200}Bi (Table VI-4). Our best value obtained

Table VI-4. Energies and intensities of gamma transitions assigned to the electron-capture decay of ^{200}Bi.

Energy (keV)	Relative intensity
245.0 ± 0.3	50
419.4 ± 0.5	90
461.4 ± 0.4	95
1027.1 ± 0.5	100

for the half-life is 36.4 ± 0.5 min.

Since the intensities of the three strongest transitions are roughly equal within experimental error, their order in the decay scheme is difficult to determine. By referring to the ^{202}Bi and ^{204}Bi decay schemes previously discussed, the 1027.1-keV gamma is probably the $2^+ \rightarrow 0^+$ ground state transition as shown in Fig. VI-4. The order of the 461.4- and 419.4-keV transitions could quite possibly be reversed, but their intensities certainly indicate that they are consecutive transitions. Further evidence in support of the ordering is taken up in the discussion section that follows.

4. ^{198}Bi

In three of the runs, the ^{198}Pb 173-keV transition was observed to grow in with a half-life of ~10 min. In these same runs five gamma rays with a half-life of 11.1 ± 0.4 min could be assigned a mass number 198 on the basis of their excitation functions. Thus we have assigned these five transitions to the decay of ^{198}Bi.

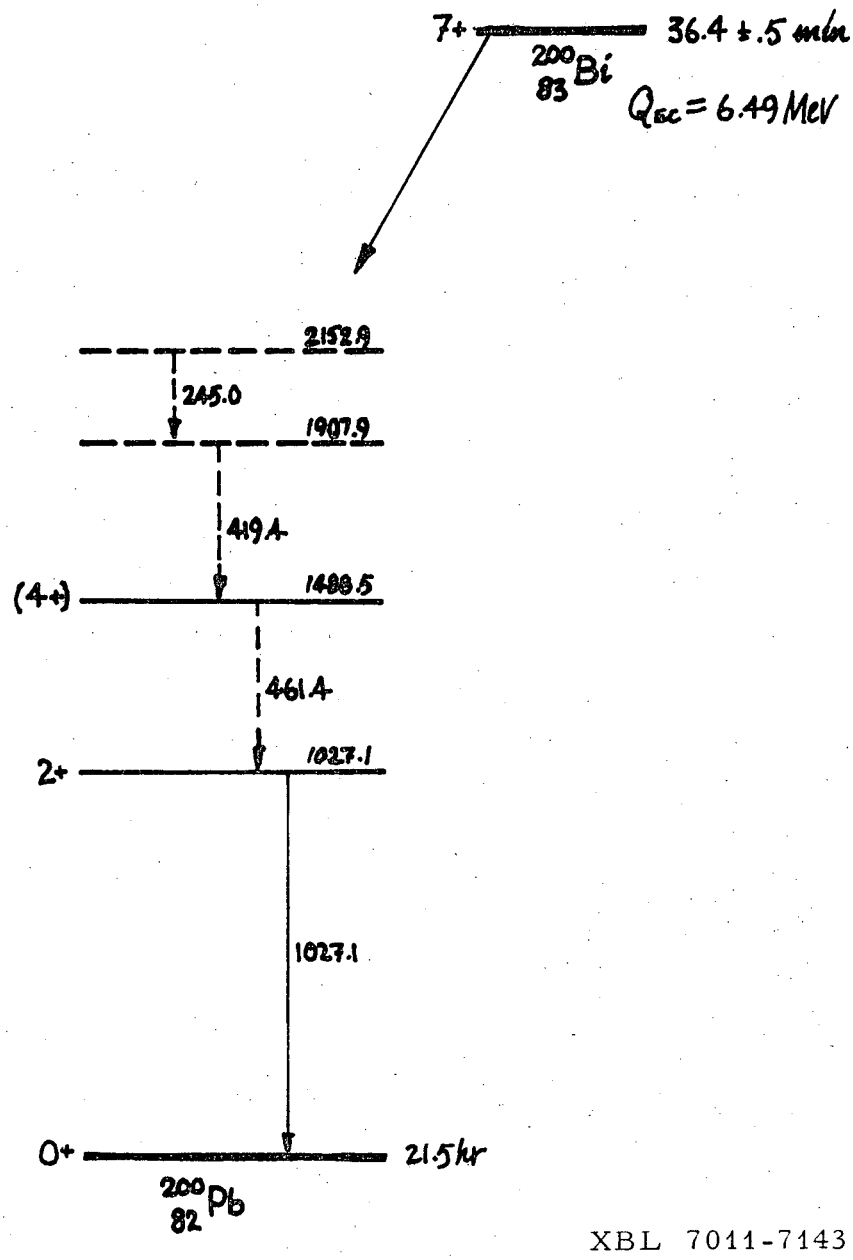

Fig. VI-4. Tentative decay scheme of ^{200}Bi.

Table VI-5 lists the relative intensities of these transitions and the decay scheme proposed in Fig. VI-5 is consistent with these intensities. Its features are identical to the scheme proposed for ^{200}Bi.

The half-life determined in these gamma measurements was used to establish the limiting value for the alpha branching ratio of ^{198}Bi reported in Chapter II.

Table VI-5. Energies and intensities of gamma transitions assigned to ^{198}Bi decay.

Energy (keV)	Relative intensity
140.5 ± 0.3	7
195.9 ± 0.6	62
317.3 ± 0.4	21
562.0 ± 0.5	75
1063.6 ± 0.4	100

5. Discussion

The data obtained from the decay of the even-mass bismuth isotopes can be summarized by looking at the excitation energy of the various spin states of the lead daughters as a function of neutron number. These results are plotted in Fig. VI-6.

All the levels appear to behave quite regularly. This regularity suggests a spin-parity assignment of 5^- for the 1821.5-keV level in ^{198}Pb (N = 116) and provides support for the ordering of the 195.9- and 562.0-keV transitions shown in Fig. VI-5. A spin assignment of either 4^+ or 5^- for the 1907.9-keV level in ^{200}Pb is also indicated.

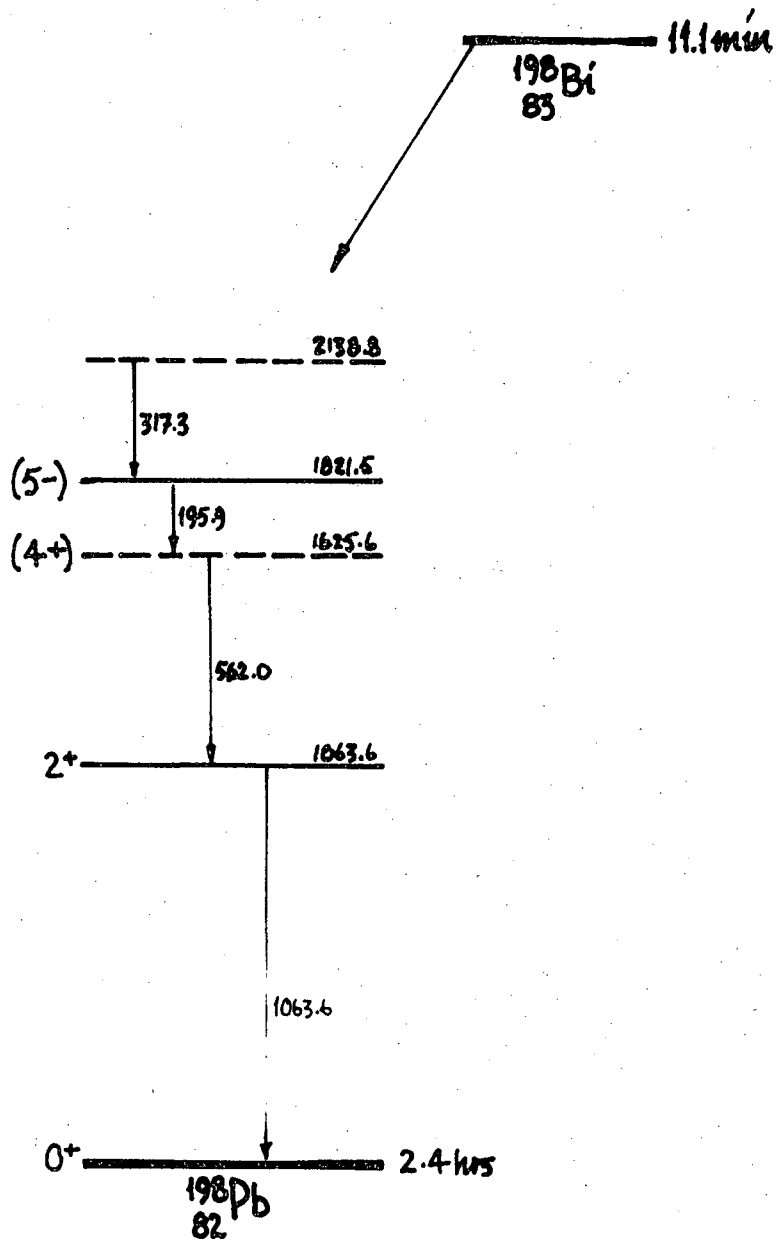

XBL 7011-7144

Fig. VI-5. Tentative decay scheme proposed for ^{198}Bi.

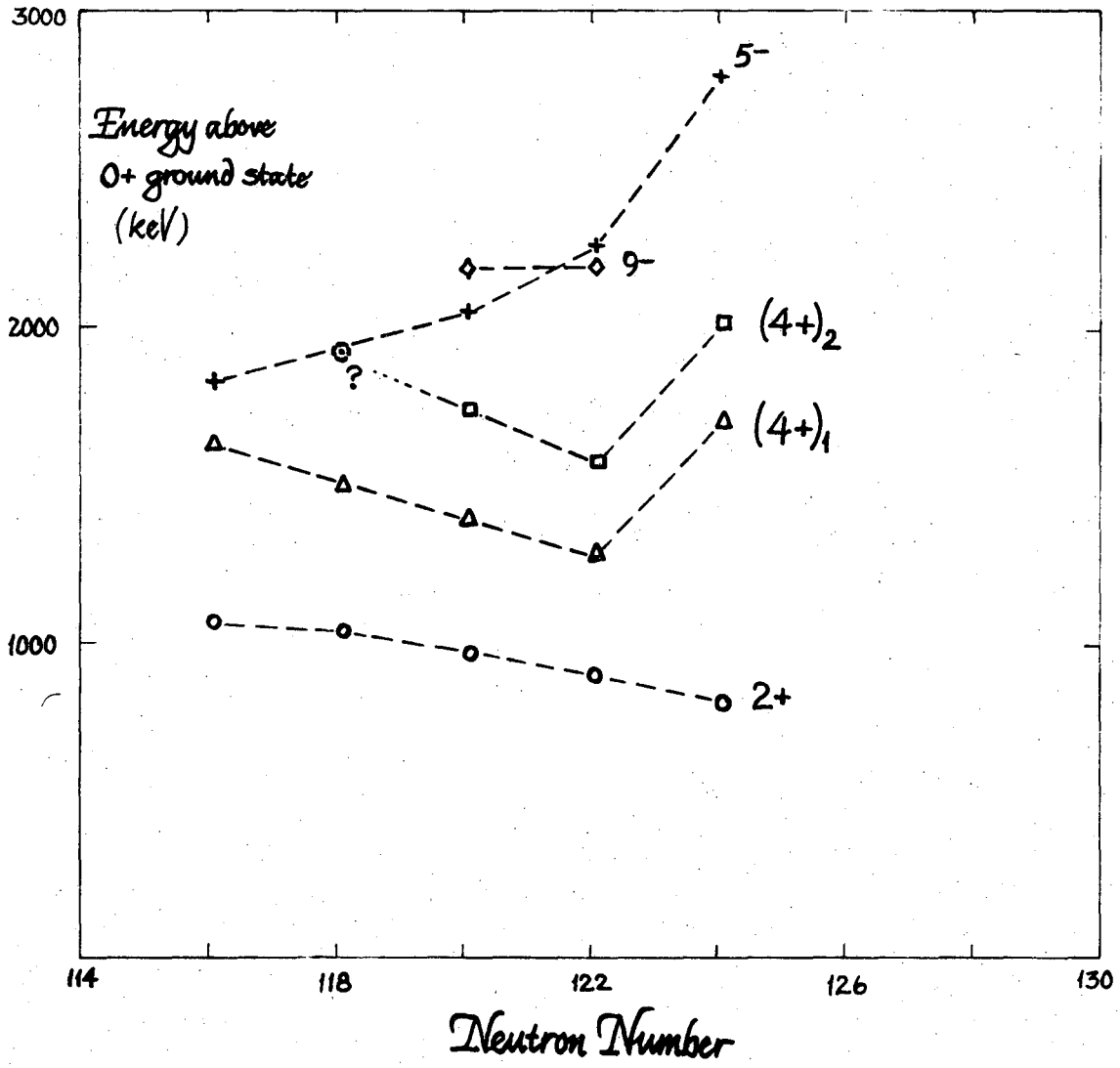

XBL 7011-7145

Fig. VI-6. Experimentally observed excited states in even-even lead isotopes.

The decay of the ^{202}Bi and ^{204}Bi isotopes also appears to proceed primarily to a 5^- state in the daughter Pb nucleus. ^{206}Bi has previously been observed to decay to two high-lying 5^- states in ^{206}Pb. (Led67) This level is probably the spin-5 state of the configuration $\nu(p_{1/2})^{-2}(f_{5/2})^{-(1+2n)}(i_{13/2})^{-1}$, where $n = 0$ for ^{204}Pb and $n = 1$ for ^{202}Pb.

The decay from the bismuth ground states (6^+ for ^{206}Bi and ^{204}Bi; 5^+ for ^{202}Bi) then would involve conversion of the odd $h_{9/2}$ proton to an $i_{13/2}$ neutron. The experimental log ft values (~7), however, are much too small for such a second forbidden transition which would be expected to proceed very slowly. However, the favoring of the 5^- states could be explained by a small admixture of $\pi(i_{13/2})^1$ in the ground state wave function of the bismuth isotopes. Then the conversion of an $i_{13/2}$ proton to an $i_{13/2}$ neutron would be allowed. Because the admixture is small the log ft values could be large for a favored transition.

It is questionable whether the same explanation would apply to ^{200}Pb and ^{198}Pb. With 8 and 10 neutron holes, respectively, the single-particle model may no longer be adequate. Detailed theoretical calculations will undoubtedly be extremely difficult due to the inherent complexities, but they will certainly be invaluable in understanding the observed experimental results.

B. ^{201}Bi

The predominant gamma line observed to decay with the half-life of ^{201}Bi is the 628.2-keV transition depopulating the 61-sec isomeric state ^{201m}Pb. Several other lines were also observed to decay with the same half-life (best value 1.77 ± 0.04 hr) and follow the same excitation function. They are duly listed in Table VI-6.

Table VI-6. Energies and intensities of gamma transitions assigned to ^{201}Bi decay.

Energy (keV)	Relative intensity
628.2 ± 0.3	100
901.5 ± 0.5	40
935.7 ± 0.4	38
1013.8 ± 0.7	27
(1325.5 ± 1.0)[a]	32

[a]Probable assignment.

The Q value for ^{201}Bi electron-capture decay is estimated as 4.20 MeV.(Mat65) The measured spin-parity of the ground state is $9/2^-$. (Lin59) Since ^{201m}Pb is probably a $13/2^+$ level, one would expect very little direct decay to this state; the population of the isomeric state must be accounted for by feeding from higher-lying states. Since so much energy is available for electron capture, the observed high-energy gamma rays could well be transitions feeding the isomeric state.

The decay scheme cannot be constructed without further experiments. A much stronger source is desirable; this could be attained by producing the bismuth directly, e.g., in a Pt(^{11}B, xn) Bi reaction. Coincidence studies are needed to determine the transitions responsible for the observed population of the 628-keV isomeric level.

VII. CONCLUSIONS

Among the more significant aspects of this work is the amount of spectroscopic information that can be derived directly from the analysis of complex many-component spectra. Nuclear decay properties of many isotopes of astatine, polonium, and bismuth have been ascertained without recourse to tedious chemical separation. Rigorous chemistry was not allowed by the short half-lives prevalent in the lower-mass region. The development of high-resolution solid state detectors, coupled with computer capabilities now available, enable a rapid accumulation and analysis of experimental data. In addition, the computer programs developed in this work should prove useful in extracting both qualitative and quantitative information from a wide variety of experimental spectra. The application of these techniques to analytical determinations should prove to be very profitable.

Considerable information has been added to the knowledge of decay schemes of neutron-deficient nuclei in the mass region A = 198 to 206. Many of the observed energy levels can be explained by the single-particle shell model, while a fuller understanding of the more complicated decay schemes must await more sophisticated theoretical treatment.

Decay schemes of the even-mass astatine isotopes, A = 202 to 206 have been constructed. Energies of the excited states observed in their Po daughter nuclei show systematic variations with neutron number, a property anticipated for the first few excited levels in

such even-even nuclei. Furthermore, evidence was obtained, from alpha measurements, for the existence of an isomeric state of ^{202}At--2.6-min ^{202m}At. The decay of the two odd-mass At isotopes studied, ^{205}At and ^{203}At, is characterized by a direct feeding of at least one $9/2^-$ level in the polonium daughter, followed by an intense gamma transition to the Po ground state.

The polonium isotopes exhibit extremely interesting decay patterns. Perhaps most surprising is the substantial amount of direct decay from the odd-mass Po nuclei to positive-parity levels in their Bi daughters. The most plausible explanation for these levels is core excitation, i.e., a hole in the Z = 82 proton shell. Tentative decay schemes were also proposed for ^{204}Po and ^{202}Po. Because of the complexity of their decays due to the large density of available states in their odd-odd Bi daughter nuclei, more experiments are required before the decay can be completely determined.

^{200}Po- ^{203}Po alpha decay has been accurately determined. Alpha energy values and lifetimes measured for ^{200}Po-^{202}Po agree with other recently published values. In addition, an alpha group at 5.37 ± 0.15 MeV was assigned to ^{203}Po; a value of 0.0018 ± 0.0002 was determined for the ^{203}Po alpha-branching ratio.

The level energies of the even-even Pb nuclei, determined from the electron-capture decay of their even-mass Bi parents, again show the expected regularities as their neutron number increases.

After a thorough search, no alpha groups could be assigned to ^{198}Bi decay; this resulted in a limiting value of ≤ 0.0020 for its alpha-branching ratio. However, several gamma lines were assigned to $^{198}Bi \rightarrow {}^{198}Pb$ decay, and an accurate half-life was determined: $t_{1/2} = 11.1 \pm 0.4$ min.

Much has been explained about the observed decay of these neutron-deficient astatine, polonium, and bismuth isotopes, but as is common in work of this nature, much remains to be explained. Perhaps this work can serve as a basis for continued study of these nuclei.

Coincidence studies are still needed for the lower-mass isotopes. Additional conversion-electron measurements to enable multipolarity assignments for all observed gamma transitions will clarify many of the remaining ambiguities in the decay schemes. A study of the gamma spectrum in the high-energy region of ^{205}At and ^{206}At decay should be particularly fruitful. The results obtained for ^{204}Po and ^{202}Po decay whet a desire to unravel more of the complexity of levels present. We have contributed necessary experimental information. The ultimate goal is, of course, a complete experimental and theoretical description encompassing all these neutron-deficient isotopes of At, Po, and Bi.

"Great is the art of beginning,
but greater the art is of ending."

Longfellow

ACKNOWLEDGMENTS

I wish to thank my research director, Professor Isadore Perlman, for his guidance and patience throughout the course of this work.

I am grateful to Dr. Frank Asaro who suggested this research and who provided day-to-day assistance.

I am indebted to Duane Mosier for providing an insight into the realm of electronics and for many discussions, concerning this work and the world in general. He and Ed Arnold not only maintained the electronics equipment but were always willing to assist with problems that arose in moments of stress. A. E. "Bud" Larsh and Al Wydler provided able help and encouragement to keep the grid chamber operating.

I would also like to express my appreciation to Mr. Albert Ghiorso for his helpful suggestions and aid in scheduling bombardments, often on short notice. I also thank the HILAC operating crew, particularly Chet Hatch, for efforts often beyond the call of duty.

The measurements on the short-lived nuclides would not have been possible without the assistance of the Health Chemistry staff, both for monitoring and for transportation. Special thanks are due Bette Shipley for her track-record speed in removing targets after bombardment.

The greatest amount of appreciation is reserved for my family: For my husband, Ned, who encouraged, supported, pushed and helped throughout the entire endeavor; who gave invaluable assistance

in the development of the computer programs and who, in the last two hectic months, drew the figures and at times also served as chief cook and bottle washer;

For my son, Jeff, whose outlook on life kept the entire work in perspective;

And for my parents in return for their early direction and continued interest.

This work was done under the auspices of the U. S. Atomic Energy Commission.

REFERENCES

(Alp69) M. Alpsten and G. Astner, Nucl. Phys. A134, 407 (1969).

(An65) J. An (Master's Thesis), University of California Lawrence Radiation Laboratory Report UCRL-16324, 1965 (unpublished).

(Arb57) E. Arbman, Nucl. Phys. 3, 625 (1957).

(Arb58) E. Arbman, J. Burde, and T. R. Gerholm, Arkiv Fysik 13, 501 (1958).

(Ast70) G. Astner and M. Alpsten, Nucl. Phys. A140, 643 (1970).

(Att59a) H. Atterling and W. Forsling, Arkiv Fysik 15, 81 (1959); W. Forsling and T. Alväger, Arkiv Fysik 19, 353 (1961).

(Att59b) H. Atterling, W. Forsling, and B. Aström, Arkiv Fysik 15, 279 (1959).

(Axe61) S. Axensten and C. M. Olsmats, Arkiv Fysik 19, 461 (1961); included in I. Lindgren, Table of Nuclear Spins and Moments, in Alpha-, Beta- and Gamma-Ray Spectroscopy, ed. by K. Siegbahn (North Holland, Amsterdam, 1965), Vol. II, p. 1621.

(Ber69) I. Bergström, C. J. Herrlander, and P. Thieberger, Phys. Rev. 181, 1642 (1969).

(Bra70) A. M. Bradley and M. R. Meder, Phys. Rev. C1, 1723 (1970).

(Bru64) C. Brun and M. Lefort, J. Inorg. Nucl. Chem. 26, 1633 (1964).

(Cam67) D. Camp, University of California Lawrence Radiation Laboratory Report, UCRL-50156, March 1967 (unpublished).

(Dav59) W. C. Davidon, Variable Metric Method for Minimization, ANL-5990, 1959; E Beals, VARMIT, Lawrence Radiation Laboratory Memo BKY-ZO (unpublished).

(Doe68) R. Doebler, Michigan State University Nuclear Chemistry Annual Report, 1968, p. 17.

(Ers62) J. R. Erskine, W. W. Buechner, and H. A. Enge, Phys. Rev. 128, 720 (1962).

(For61) W. Forsling, T. Alväger, L. W. Holm, O. Melin, J. Uhler, and B. Aström, Arkiv Fysik 19, 83 (1961).

(Fri56) A. R. Fritsch (Ph. D. Thesis), University of California Lawrence Radiation Laboratory Report UCRL-3452, 1956 (unpublished); A. R. Fritsch and J. M. Hollander, J. Inorg. Nucl. Chem. 6, 165 (1958).

(Gle62) N. Glendenning, University of California Lawrence Radiation Laboratory Report UCRL-10095, March 1962; Phys. Rev. 127, 923 (1962); N. Glendenning and K. Harada, Nucl. Phys. 72, 481 (1965).

(Har62) C. K. Hargrove and W. M. Martin, Can. J. Phys. 40, 964 (1962).

(Her56) C. J. Herrlander, R. Stockendal, J. A. McDonell, and I. Bergström, Nucl. Phys. 1, 643 (1956).

(Hof58) R. W. Hoff and J. M. Hollander, Phys. Rev. 109, 447 (1958).

(Hof63) R. W. Hoff, F. Asaro, and I. Perlman, J. Inorg. Nucl. Chem. 25, 1303 (1963).

(Hop69) P. K. Hopke, R. A. Naumann, and E. H. Spejewski, Princeton-Pennsylvania Accelerator Report PPAR 15, 1969.

(Hop70) P. K. Hopke, R. A. Naumann and E. H. Spejewski, Nucl. Phys. A149, 63 (1970).

(Kar51) D. G. Karracker and D. H. Templeton, Phys. Rev. 81, 510 (1951).

(Kim63) Y. E. Kim (Ph. D. Thesis) University of California Lawrence Radiation Laboratory Report UCRL-10865, June 1963; Y. E. Kim and J. Rasmussen, Nucl. Phys. 47, 184 (1963).

(Kim58) K. Kimura and T. Ishimori, Proceedings of the Second United Nations Internal Conference on the Peaceful Uses of Atomic Energy, Geneva, 28, 151, P/1322 (1958).

(Lat60) R. M. Latimer, G. Gordon, and T. D. Thomas, University of California Lawrence Radiation Laboratory Report UCRL-9217, 1960, J. Inorg. Nucl. Chem. 17, 1 (1961).

(LeB67a) Y. LeBeyec and M. Lefort, Arkiv Fysik 36, 183 (1967); C. Brun, Y. LeBeyec, and M. Lefort, Phys. Letters 16, 286 (1965); C. Brun, Y. LeBeyec, and M. Lefort, Compt. Rend. 261, 1667 (1965).

(LeB67b) Y. LeBeyec and M. Lefort, Nucl. Phys. A99, 131 (1967).

(Led67) C. M. Lederer, J. M. Hollander, and I. Perlman, Table of Isotopes (John Wiley & Sons, Inc., New York, 1967).

(Lin59) I. Lindgren and C. M. Johansson, Arkiv Fysik 15, 445 (1959); S. Axensten, C. M. Johansson, and I. Lindgren, Arkiv Fysik 15, 463 (1959).

(Lin57) W. T. Link, Ph.D. Thesis, McGill University, 1957 (unpublished).

(Mat65) J. H. E. Mattauch, W. Thiele, and A. H. Wapstra, Nucl. Phys. 67, 1 (1965).

(May55) M. G. Mayer and J. H. D. Jensen, Elementary Theory of Nuclear Shell Structure (John Wiley & Sons, Inc., New York, 1955).

(McD56) J. A. McDonell and I. Bergström, Arkiv Fysik 11, 105A (1956).

(McD57) J. A. McDonell, R. Stockendal, C. Herrlander, and I. Bergström, Nucl. Phys. 3, 513 (1957).

(Mei65) L. P. Meissner, Lawrence Radiation Laboratory Memo C2 BKY ZERO, 1965 (unpublished).

(NAS62) Application of Computers to Nuclear and Radiochemistry, NAS-NS-3107 (1962).

(Neu50) H. M. Neumann and I. Perlman, Phys. Rev. 78, 191 (1950).

(Nor60) L. C. Northcliffe, Phys. Rev. 120, 1744 (1960).

(Nov58) T. Novakov, R. Stockendal, M. Schmorak, and B. Johansson, Arkiv Fysik 14, 85 (1958).

(Per62) I. Perlman, F. Asaro, A. Ghiorso, A. Larsh, and R. Latimer, University of California Lawrence Radiation Laboratory Report UCRL-10094, 1962; Phys. Rev. 127, 917 (1962).

(Pru67) S. G. Prussin and J. M. Hollander, University of California Radiation Laboratory Report UCRL-17843, 1967; Nucl. Phys. A110, 176 (1968).

(Pry52) M. H. L. Pryce, Proc. Phys. Soc. (London) A65, 773 (1952).

(Rou68) J. Routti and S. Prussin, University of California Lawrence Radiation Laboratory Report UCRL-17672, 1968.

(Rou69) J. Routti, University of California Lawrence Radiation Laboratory Report UCRL-19452, October 1969.

(Sii64) A. Siivola, P. Kauranen, B. Jung, and J. Svedburg, Nucl. Phys. 52, 449 (1964).

(Sii67) A. Siivola, Nucl. Phys. A101, 129 (1967).

(Sli65) L. A. Sliv and I. M. Band, Tables of Internal Conversion Coefficients, in Alpha-, Beta-, and Gamma-Ray Spectroscopy, ed. by K. Siegbahn (North Holland, Amsterdam, 1965), Vol. II, p. 1639.

(Sto58) R. Stockendal, T. Novakov, B. Johansson, and M. Schmorak, Arkiv Fysik 14, 65 (1958).

(Sto60a) R. Stockendal, Arkiv Fysik 17, 553 (1960).

(Sto60b) R. Stockendal, Arkiv Fysik 17, 579 (1960).

(Sto56) A. W. Stoner (Ph. D. Thesis), University of California Lawrence Radiation Laboratory Report UCRL-3471, 1956 (unpublished).

(Tem47) See for example: D. H. Templeton, J. J. Howland, and I. Perlman, Phys. Rev. 72, 758 (1947); S. Rosenblum and H. Tyrén, Compt. Rend. 239, 1205 (1954).

(Tho62) T. D. Thomas, G. Gordon, R. Latimer, and G. Seaborg, Phys. Rev. 126, 1805 (1962).

(Tho63) P. E. Thoresen, F. Asaro, and I. Perlman, University of California Lawrence Radiation Laboratory Report UCRL-11148, 1963; J. Inorg. Nucl. Chem. 26, 1341 (1964).

(Tho66) P. Thoresen, University of California Lawrence Radiation Laboratory Report UCRL-17255, Jan. 1966.

(Tie67) E. Tielsch-Cassel, Nucl. Phys. A100, 425 (1967); E. Tielsch, Phys. Letters 17, 273 (1965).

(Tre66) W. Tretyl and K. Valli, University of California Lawrence Radiation Laboratory Report UCRL-17194, Oct. 1966; Nucl. Phys. A197, 405 (1967).

(Tre68) W. J. Tretyl, E. Hyde, and T. Yamazaki, University of California Lawrence Radiation Laboratory Report

UCRL-17529, April 1968; Nucl. Phys. A117, 481 (1968).

(Wah57) S. Wahlborn, Nucl. Phys. 3, 644 (1957).

(Wer56) G. K. Wertheim and R. V. Pound, Phys. Rev. 102, 185 (1956).

(Wil69) J. B. Wilhelmy (Ph.D. Thesis), University of California Lawrence Radiation Laboratory Report, UCRL-18978, 1969 (unpublished).

(Yam70) T. Yamazaki, Phys. Rev. C1, 290 (1970).

LEGAL NOTICE

This report was prepared as an account of Government sponsored work. Neither the United States, nor the Commission, nor any person acting on behalf of the Commission:

A. Makes any warranty or representation, expressed or implied, with respect to the accuracy, completeness, or usefulness of the information contained in this report, or that the use of any information, apparatus, method, or process disclosed in this report may not infringe privately owned rights; or

B. Assumes any liabilities with respect to the use of, or for damages resulting from the use of any information, apparatus, method, or process disclosed in this report.

As used in the above, "person acting on behalf of the Commission" includes any employee or contractor of the Commission, or employee of such contractor, to the extent that such employee or contractor of the Commission, or employee of such contractor prepares, disseminates, or provides access to, any information pursuant to his employment or contract with the Commission, or his employment with such contractor.

TECHNICAL INFORMATION DIVISION
LAWRENCE RADIATION LABORATORY
UNIVERSITY OF CALIFORNIA
BERKELEY, CALIFORNIA 94720